JOURNAL OF THE AMERICAN

ROCKET

SOCIETY

A journal devoted to rocket technology and the jet propulsion sciences

VOLUME 21 NOVEMBER, 1951 NUMBER 6

STACKS

Resistance to Thermal Shock . . . . . C. M. Cheng 147

Strengths of Several Steels for Rocket Chambers Subjected to High Rates of Heating . . . . . F. L. Noland 154

Aspects of Combustion Stability in Liquid Propellant Rocket Motors. Part I: Fundamentals. Low Frequency Instability with Monopropellants . . . . . L. Crocco 163

Chemical Kinetics and Rocket Nozzle Design . . . . . F. J. Krieger 179

Letters to the Editor 185

Jet Propulsion News 186

American Rocket Society News 190

Technical Literature Digest 193

1951 ARS ANNUAL CONVENTION ATLANTIC CITY, N. J. NOV. 28–30

JOURNAL OF THE AMERICAN
ROCKET
SOCIETY

Office: *Engineering Societies Building*
29 West 39th Street, New York 18, N. Y.

EDITORIAL BOARD

D. ALTMAN
California Institute of Technology

L. CROCCO
Princeton University

P. DUWEZ
California Institute of Technology

R. D. GECKLER
Aerojet Engineering Corporation

C. A. GONGWER
Aerojet Engineering Corporation

C. A. MEYER
Westinghouse Electric Corporation

P. F. WINTERNITZ
Reaction Motors, Inc.

K. WOHL
University of Delaware

M. J. ZUCROW
Purdue University

EDITOR-IN-CHIEF

MARTIN SUMMERFIELD

ASSOCIATE EDITORS

C. F. WARNER—*Jet Propulsion News*
A. F. BOCHENEK—*ARS News*
H. S. SEIFERT—*Literature Digest*

MANAGING EDITOR

A. F. BOCHENEK

ADVISORS ON PUBLICATION POLICY

L. G. DUNN
Director, Jet Propulsion Laboratory
California Institute of Technology

T. C. FETHERSTON
General Publicity Department
Union Carbide and Carbon Corporation

R. E. GIBSON
Director, Applied Physics Laboratory
Johns Hopkins University

LOVELL LAWRENCE, JR.
Engineering Consultant

D. L. PUTT
Major General, U.S. Air Force
Acting Deputy Chief of Staff
for Development

T. VON KÁRMÁN
Chairman, Scientific Advisory Board
U.S. Air Force

W. E. ZISCH
General Manager
Aerojet Engineering Corporation

Scope of the Journal

The Journal of the American Rocket Society is devoted to the advancement of the field of jet propulsion through the publication of original papers disclosing new knowledge and new developments. The term "jet propulsion" as used herein is understood to embrace all engines that develop thrust by rearward discharge of a jet through a nozzle or duct, and thus includes systems utilizing atmospheric air and underwater systems, as well as rocket engines. The Journal is open to contributions, either fundamental or applied, dealing with specialized aspects of jet and rocket propulsion, such as fuels and propellants, combustion, heat transfer, high temperature materials, mechanical design analyses, flight mechanics of jet-propelled vehicles, astronautics, and so forth. The Journal endeavors, also, to keep its subscribers informed of the affairs of the Society and of outstanding events in the rocket and jet propulsion field.

Submission of Manuscripts

Manuscripts should be submitted in duplicate to the Editor-in-Chief, Martin Summerfield, Department of Aeronautical Engineering, Princeton University, Princeton, N. J. See instructions on the inside back cover.

Security Clearance

Manuscripts must be accompanied by written assurance as to security clearance in the event the subject matter of the manuscript is considered to lie in a classified area. Alternatively, written assurance that clearance is unnecessary should be submitted. Full responsibility for obtaining authoritative clearance rests with the author.

Limitation of Responsibility

Statements and opinions expressed in the Journal are to be understood as the individual expressions of the authors and do not necessarily reflect the views of the Editors or the Society.

Copyright

Copyright, 1951, by the American Rocket Society, Inc. Permission for reprinting material in the Journal will be granted only upon application to the Secretary of the Society.

Subscription Rates

One year (six bi-monthly issues)	$7.50
Foreign countries, including Canada	add .50
Single copies	1.25
Back numbers	1.50

Subscriptions and orders for single copies should be addressed to the Secretary of the Society.

Change of Address

Notices of change of address should be sent to the Secretary of the Society at least 30 days prior to the date of publication.

Explanation of Numbering of Issues

The September 1951 issue is the first of a new series of expanded scope and contents. This series is numbered on an annual volume basis, beginning each year with the January issue as Number 1. Correspondingly, the September issue is Number 5, and since 1951 is the 21st year of publication the new series starts with Volume 21 Number 5. This replaces Number 86 of the previous series.

Advertisements

Information on advertising rates is obtainable from the Secretary of the Society.

Published Bimonthly by the American Rocket Society, Inc.

Journal of the American Rocket Society, published bimonthly by the American Rocket Society at 20th and Northampton Streets, Easton, Pa., U. S. A. The Editorial Office is located at the Engineering Societies Building, 29 West 39th Street, New York 18, N. Y. Price $1.25 per copy; $7.50 per year. Entered as second-class matter at the Post Office at Easton, Pa., under the Act of March 3, 1879.

Completely Revised!

DATA ON HIGH-TEMPERATURE ALLOYS

This new edition of "HAYNES Alloys for High-Temperature Service" summarizes all the available data on 10 super-alloys. Besides physical and mechanical properties of two newly developed alloys — HAYNES alloys Nos. 25 and 36 — the booklet now includes additional data on all 10 alloys.

There are tables and charts giving data on creep-rupture, stress-rupture, thermal expansion, stress-elongation, hardness, and impact properties, in addition to chemical composition and short-time tensile properties. The booklet also contains information on age-hardening and procedures for fabricating the wrought forms of the alloys.

Every engineer and metallurgist who designs or specifies equipment for service at elevated temperatures should have a copy of this book. Design engineers, particularly, will find it a useful guide in the selection of alloys to meet the exacting requirements of high-temperature service.

Fill in the handy coupon below if you wish a copy of this useful book. If you have the old edition, be sure to replace it immediately, so that you will have all the latest information available on the HAYNES high-temperature alloys.

HAYNES Trade-Mark *Alloys*

Haynes Stellite Company
A Division of
Union Carbide and Carbon Corporation
UCC

USE THIS HANDY COUPON

Haynes Stellite Company, 725 S. Lindsay Street, Kokomo, Indiana

Please send me, without obligation, a copy of "HAYNES Alloys for High-Temperature Service."

NAME_____

COMPANY_____

ADDRESS_____

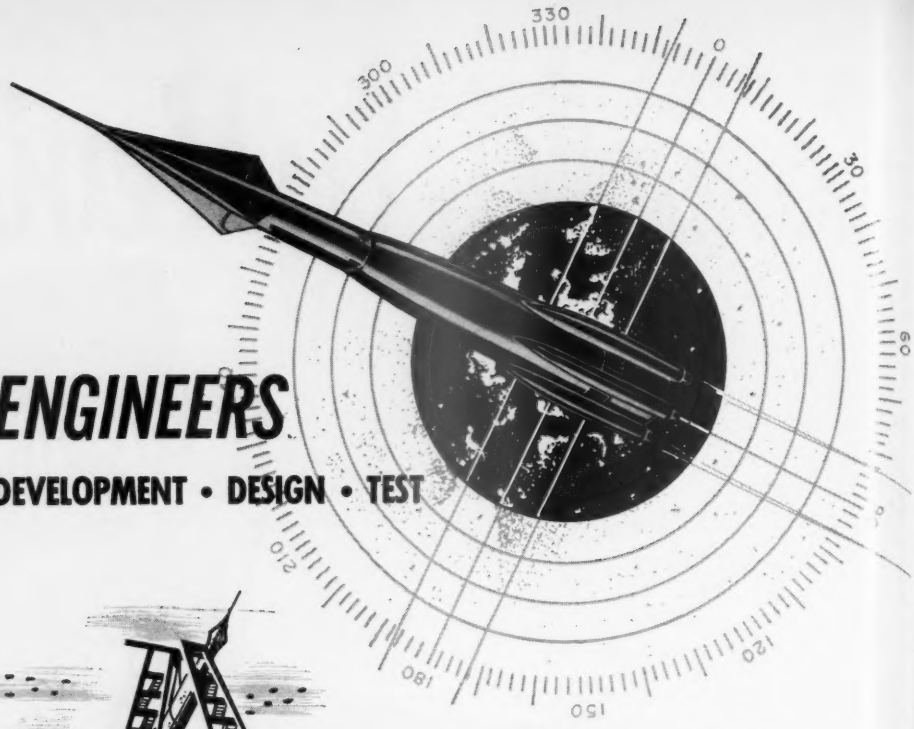

ROCKET ENGINEERS

RESEARCH • DEVELOPMENT • DESIGN • TEST

A long range program of research and development in guided missiles has created unlimited opportunities in all phases of rocket engineering.

Engineers with advanced degrees are needed for positions in Combustion Research and Physical Chemistry.

Engineers with or without advanced degrees are needed as:

RESEARCH ENGINEERS . . . for studies in heat transfer and Thermodynamics

DESIGN ENGINEERS . . . for design phases of liquid rocket power plants, thrust chambers, gas turbine pumps

FIELD ENGINEERS . . . for coordination of activities at field test sites

TEST ENGINEERS . . . for development and production testing of liquid rocket power plants and their components

Openings also for Design Draftsmen and Technicians

Send complete resume to: **Manager, Engineering Personnel**

COMPLETE ROCKET TESTING FACILITIES

BELL *Aircraft* CORPORATION

P. O. BOX 1, BUFFALO 5, NEW YORK

NOVEMBER, 1951
VOLUME 21 NUMBER 6

JOURNAL OF THE AMERICAN ROCKET SOCIETY

Editor-in-Chief
MARTIN SUMMERFIELD

Resistance to Thermal Shock

By C. M. CHENG[1]

California Institute of Technology, Pasadena, Calif.

The purpose of this investigation is to demonstrate that the resistance of ceramic and ceramal materials to thermal shock can be determined by analyzing the nonsteady thermal stresses in the material. First the nonuniform temperature distribution is computed by using the heat conduction equation. This temperature distribution is then used to compute the thermal stress. The material parameters which enter into the calculations are the coefficients of thermal conduction and of thermal expansion, the ultimate strength, Young's modulus, and Poisson's ratio of the material. These quantities together with the heating conditions then specify the resistance to thermal shock. The theory is verified by comparing the results with NACA test data.

RESISTANCE to thermal shock is the strength of the material against failure during rapid heating or cooling. The current interest in high temperature designs using ceramic and ceramal materials, which are relatively weak in thermal shock in comparison with metals, necessitates a closer examination of this composite property. To help the search for better materials, it is important to determine the physical and mechanical properties of the material which contribute to high thermal shock resistance. W. G. Lidman and A. R. Bobrowsky (1)[2] argued that the resistance to thermal shock is proportional to the value of $\sigma_0 k/\alpha E$, where k is the coefficient of heat conduction of the material, σ_0 the ultimate strength, α the coefficient of linear thermal expansion, and E, Young's modulus of elasticity. It is the purpose of this paper to give a more complete theory of resistance to thermal shock, together with a comparison with experimental data.

The failure of material is the result of high stress. In rapid heating or cooling, the stress is generated by the nonuniform temperature and hence nonuniform expansion. Then, the problem of resistance to thermal shock is really the problem of computing the thermal stress under such conditions. In order to correlate the theory with experiment, the particular case analyzed is that of a plate heated or cooled rapidly. For this simple shape, the computation is quite easy. In fact, the problem of thermal stress in a plate is already known (2), while the temperature distributions in the plate have also been calculated before (3). The specific task of this discussion is then to bring these elements together and properly interpret the results for a clear understanding of the problem of thermal shock.

Received June 15, 1951. This paper is based on part of a thesis submitted for partial fulfillment of Ph.D. in Mechanical Engineering, under the supervision of H. S. Tsien, Robert H. Goddard Professor, Daniel and Florence Guggenheim Jet Propulsion Center, California Institute of Technology.

[1] Graduate Assistant in Mechanical Engineering.

[2] Numbers in parentheses refer to References at end of paper.

Thermal Stress in a Flat Plate

Consider a flat plate with a uniform thickness much smaller than its lateral dimensions. Then if cooling and heating of the plate take place through heat transfer at the surfaces, the temperature of the material is different at different distances to the plate surface, but for the greater part of the plate the temperature is independent of the location in the plane of the plate. If the median plane of the plate is taken as the x, y plane (Fig. 1), then the temperature T is a function of z only. Let σ_x, σ_y, σ_z and e_x, e_y, e_z be the normal stresses and

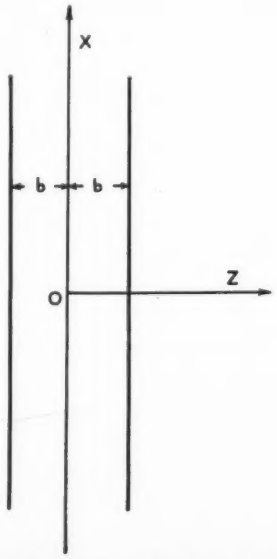

FIG. 1 DIAGRAM OF PLATE WITH BOTH SIDES UNIFORMLY HEATED, b HALF THICKNESS

normal strains in the x, y and z directions, respectively. The shearing stresses and shearing strains obviously vanish in this problem. The relations between the stresses and strains are

$$\left.\begin{aligned} e_x &= \frac{1}{E}\{\sigma_x - \nu(\sigma_y + \sigma_z)\} + e_T \\ e_y &= \frac{1}{E}\{\sigma_y - \nu(\sigma_z + \sigma_x)\} + e_T \\ e_z &= \frac{1}{E}\{\sigma_z - \nu(\sigma_x + \sigma_y)\} + e_T \end{aligned}\right\} \quad \ldots\ldots\ldots\ldots [1]$$

where e_T is the thermal strain due to thermal expansion, and E and ν are Young's modulus and Poisson's ratio. E and ν may be functions of temperature. Due to the lack of shearing stresses and applied surface forces, σ_z is identically zero by the equilibrium of forces in the z direction.

Now treat the case where the temperature is symmetrical with respect to the median plane of the plate. Then the only deformation the plate can undergo is a uniform lateral expansion. Therefore, $e_x = e_y$ and both are constants. Then $\sigma_x = \sigma_y$. Assume that the plate is not restrained at the edges, then the net tensile force at the edges must vanish or, $\int_{-b}^{b} \sigma_z \, dz = 0$, where b is the half-thickness of the plate. By using these relations, it can be easily deduced that

$$\left.\begin{aligned} e_x = e_y &= \frac{\displaystyle\int_{-b}^{b} \frac{Ee_T}{1-\nu}\, dz}{\displaystyle\int_{-b}^{b} \frac{E}{1-\nu}\, dz} \\ e_z &= -\frac{\displaystyle\int_{-b}^{b} \frac{Ee_T}{\nu}\, dz}{\displaystyle\int_{-b}^{b} \frac{E}{\nu}\, dz} \end{aligned}\right\} \quad \ldots\ldots\ldots\ldots [2]$$

and hence

$$\sigma_x = \sigma_y = \frac{E}{1-\nu}\left(\frac{\displaystyle\int_{-b}^{b} \frac{Ee_T}{1-\nu}\, dz}{\displaystyle\int_{-b}^{b} \frac{E}{1-\nu}\, dz} - e_T\right) \quad \ldots\ldots\ldots [3]$$

These equations show that given temperature distribution in the plate, the stress and strain at any point can be easily calculated, provided E, ν, e_T are known functions of temperature. If E, ν are constants and take $e_T = \alpha T$, where T is the change in temperature from the initially uniform state and α the constant coefficient of thermal expansion, Equation [3] reduces to

$$\sigma_x = \sigma_y = \frac{E\alpha}{1-\nu}\left(\frac{1}{2b}\int_{-b}^{b} T\, dz - T\right) \quad \ldots\ldots\ldots [4]$$

By introducing the dimensionless parameters

$$\xi = \frac{z}{b}, \qquad T^* = \frac{T}{T_0}, \qquad \bar{T}^* = \frac{1}{2}\int_{-1}^{1} T^*\, d\xi$$

$$\sigma^* = \frac{\sigma_x(1-\nu)}{\alpha E T_0}$$

where T_0 is any convenient reference temperature, Equation [4] simplifies to

$$\sigma^* = \bar{T}^* - T^* \quad \ldots\ldots\ldots\ldots [5]$$

Hence the reduced stress is equal to the difference between the average reduced temperature and the local reduced temperature.

For the more general case, where the temperature in the plate is not symmetric with respect to the median plane but still independent of x and y, one need only make the change

$$e_x = e_y = e + \beta z \quad \ldots\ldots\ldots\ldots [6]$$

where e and β are two constants so far undetermined, while the conditions $\sigma_x = \sigma_y$ and $\sigma_z = 0$ remain true. That a linear variation of e_x across the thickness is correct follows from the symmetric consideration imposed by the assumptions on the uniformity of temperature with respect to x and y, and the absence of external constraints. In addition to conditions of vanishing average tensile stress across the thickness of the plate, there

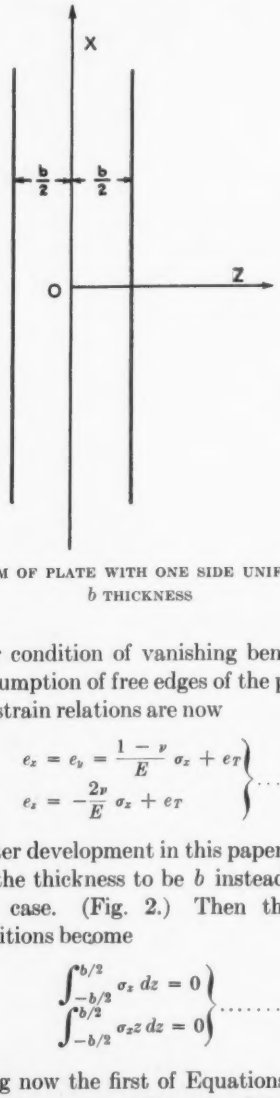

FIG 2 DIAGRAM OF PLATE WITH ONE SIDE UNIFORMLY HEATED
b THICKNESS

is the further condition of vanishing bending moment due to the assumption of free edges of the plate.

The stress-strain relations are now

$$\left.\begin{aligned} e_x = e_y &= \frac{1-\nu}{E}\,\sigma_x + e_T \\ e_z &= -\frac{2\nu}{E}\,\sigma_x + e_T \end{aligned}\right\} \quad \ldots\ldots\ldots\ldots [7]$$

In view of later development in this paper, it is convenient to take the thickness to be b instead of $2b$, as in the previous case. (Fig. 2.) Then the force and moment conditions become

$$\left.\begin{aligned} \int_{-b/2}^{b/2} \sigma_x\, dz &= 0 \\ \int_{-b/2}^{b/2} \sigma_x z\, dz &= 0 \end{aligned}\right\} \quad \ldots\ldots\ldots\ldots [8]$$

By integrating now the first of Equations [7] with respect to z, and, by means of Equation [8], the following equations for the two unknown e and β are obtained,

$$\left.\begin{aligned} e\int_{-b/2}^{b/2}\frac{E}{1-\nu}\,dz+\beta\int_{-b/2}^{b/2}\frac{Ez}{1-\nu}\,dz&=\int_{-b/2}^{b/2}\frac{Ee_T}{1-\nu}\,dz\\ e\int_{-b/2}^{b/2}\frac{Ez}{1-\nu}\,dz+\beta\int_{-b/2}^{b/2}\frac{Ez^2}{1-\nu}\,dz&=\int_{-b/2}^{b/2}\frac{Ee_Tz}{1-\nu}\,dz\end{aligned}\right\}\quad\ldots[9]$$

Here again, e and β and hence e_x, e_y, σ_x, σ_y, and e_z are determined when the temperature distribution is known, and when E, ν, and e_T are known functions of temperature. If $e_T = \alpha T$, and if E, ν, and α are constant, the following equation for the reduced stress is readily obtained.

$$\sigma^* = \bar{T}^* + 12\xi\int_{-1/2}^{1/2} T^*\xi\,d\xi - T^* \quad\ldots[10]$$

where, as before,

$$\xi = \frac{z}{b}, \qquad T^* = \frac{T}{T_0}, \ \bar{T}^* = \int_{-1/2}^{1/2} T^*\,d\xi$$

$$\sigma^* = \frac{\sigma_x(1-\nu)}{\alpha E T_0}$$

Since for this case the thickness of the plate is b, $-(b/2) \leq z \leq (b/2)$. When T is symmetric with respect to z, $\int_{-1/2}^{1/2} T^*\xi\,d\xi = 0$, then Equation [10] reduces to Equation [5].

Actually, to compute the thermal stress in a plate one needs to know the temperature distribution. For this purpose, consider two special cases: As the first case, take a plate heated or cooled uniformly on both sides by a constant heat source. As the second case, consider a plate uniformly heated or cooled on one side, and insulated on the other. As far as temperature distribution is concerned, only the second case needs to be computed, since at the median plane of the plate in the first case there is no heat transfer due to the symmetry of the temperature distribution and the median plane can be considered as insulated. This is the reason that the thickness in the symmetric case is taken to be $2b$ and the thickness in the second case is taken to be b.

Transient Temperature Distribution

Proceed now to the calculation of the temperature distribution in an infinite plate with one side uniformly heated or cooled and the other side insulated. Take b as the constant thickness, and x and y axis of a Cartesian co-ordinate system in the middle plane. For small strain, i.e., when the shape and size of the plate are only slightly changed by thermal strain, the ordinary heat-conduction equation may be used. If k is the coefficient of heat conduction, h the surface conductivity at $z = -b/2$, c the specific heat per unit volume, and if k, h, and c are constants, the heat conduction equation is

$$k\frac{\partial^2 T}{\partial z^2} = c\frac{\partial T}{\partial t}$$

The boundary conditions are

$$k\frac{\partial T}{\partial z} = h(T - T_0), \text{ at } z = -\frac{b}{2}$$

$$\frac{\partial T}{\partial z} = 0, \text{ at } z = \frac{b}{2}$$

where T_0 = constant is now taken as the temperature of the heat source. Initially the plate is considered to be at uniform temperature $T = 0$. The above equations may be written in dimensionless form if one introduces

$$\left.\begin{aligned} T^* &= \frac{T}{T_0}, \qquad \xi = \frac{z}{b}\\ f &= \frac{kt}{cb^2}, \qquad R = \frac{k}{hb}\end{aligned}\right\}\quad\ldots\ldots[11]$$

where R is the so-called resistance ratio, and f the Fourier number. Thus

$$\left.\begin{aligned} \frac{\partial^2 T^*}{\partial \xi^2} &= \frac{\partial T^*}{\partial f}\\ \text{and}\\ R\,\frac{\partial T^*}{\partial \xi} &= 1 - T^*, \text{ at } \xi = -\frac{1}{2}\\ \text{and}\\ \frac{\partial T^*}{\partial \xi} &= 0, \text{ at } \xi = \frac{1}{2}\\ T^* &= 0, \text{ at } f = 0\end{aligned}\right\}\quad\ldots\ldots[12]$$

The solution to the above equation is well known (3). It is written down here for reference:

$$\left.\begin{aligned} T^* &= 1 - \sum_{k=0}^{\infty}\frac{2e^{-\eta_k^2 f}}{\eta_k}\,\frac{\cos\eta_k(1/2-\xi)}{(1+R+R^2\eta_k^2)\sin\eta_k}\\ \bar{T}^* &= 1 - \sum_{k=0}^{\infty}\frac{2e^{-\eta_k^2 f}}{\eta_k^2}\,\frac{1}{1+R+R^2\eta_k^2}\\ \int_{-1/2}^{1/2} T^*\xi\,d\xi &= -\sum_{k=0}^{\infty}\frac{2e^{-\eta_k^2 f}}{\eta_k^2}\,\frac{1-\cos\eta_k-\frac{\eta_k}{2}\sin\eta_k}{(1+R+R^2\eta_k^2)\sin\eta_k}\end{aligned}\right\}\quad[13]$$

where η_k are roots of the transcendental equation

$$R\eta_k \tan\eta_k = 1 \quad\ldots\ldots[14]$$

For small values of f, Equations [13] may be expressed asymptotically as (4)

$$\left.\begin{aligned} T^* &= erfc\left(\frac{1/2+\xi}{2\sqrt{f}}\right) + erfc\left(\frac{3/2-\xi}{2\sqrt{f}}\right) - e^{1/R(1/2+\xi)+(f/R^2)}\times\\ &\quad erfc\left\{\frac{1/2+\xi}{2\sqrt{f}} + \frac{\sqrt{f}}{R}\right\} - e^{1/R(3/2-\xi)+(f/R^2)}\times\\ &\quad erfc\left\{\frac{3/2-\xi}{2\sqrt{f}} + \frac{\sqrt{f}}{R}\right\} + 0\left(f^{1/2}e^{-(1/4f)}\right)\\ \bar{T}^* &= \frac{2f^{1/2}}{\sqrt{\pi}} - R + Re^{f/R^2}\,erfc\left(\frac{\sqrt{f}}{R}\right) + 0\left(f^{1/2}e^{-(1/4f)}\right)\\ \int_{-1/2}^{1/2} T^*\xi\,d\xi &= -\frac{1}{2}\bar{T}^* + R + f - \frac{2R^2f^{1/2}}{\sqrt{\pi}} -\\ &\quad R^2e^{f/R^2}\,erfc\left(\frac{\sqrt{f}}{R}\right) + 0\left(f^{1/2}e^{-(1/4f)}\right)\end{aligned}\right\}\quad[15]$$

where $erf(u)$ is the complimentary error function, defined as

$$erfc(u) = 1 - erf(u) = \frac{2}{\sqrt{\pi}}\int_u^{\infty} e^{-s^2}\,ds$$

Computation of Thermal Stresses

For the plate with both sides heated it follows from

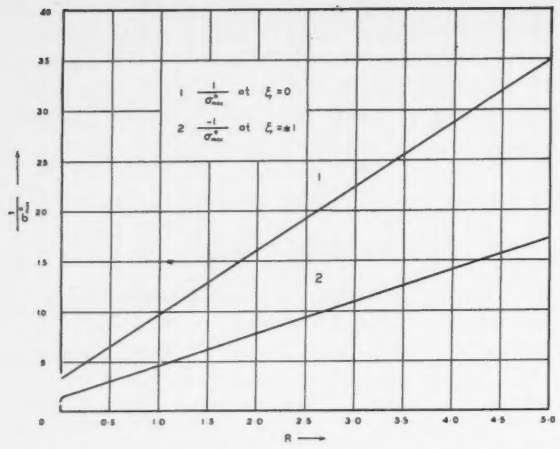

FIG. 3 MAXIMUM THERMAL STRESS IN A LARGE PLATE WITH BOTH SIDES UNIFORMLY HEATED. AT $\xi = 0$, TENSILE STRESS IN HEATING AND COMPRESSIVE STRESS IN COOLING. AT $\xi = \pm 1$, TENSILE STRESS IN COOLING AND COMPRESSIVE STRESS IN HEATING

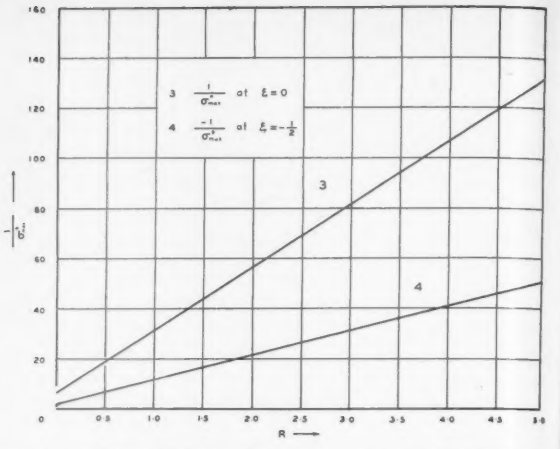

FIG. 4 MAXIMUM THERMAL STRESS IN A LARGE PLATE WITH ONE SIDE UNIFORMLY HEATED. AT $\xi = 0$, TENSILE STRESS IN HEATING AND COMPRESSIVE STRESS IN COOLING. AT $\xi = -1/2$, TENSILE STRESS IN COOLING AND COMPRESSIVE STRESS IN HEATING

Equations [5], [13], and [15] that

$$\sigma^* = \sum_{k=0}^{\infty} \frac{2e^{-\eta_k^2 f}}{\eta_k} \frac{1}{1 + R + R^2\eta_k^2} \left(\frac{\cos \eta_k \xi}{\sin \eta_k} - \frac{1}{\eta_k} \right) \quad [16]$$

$$\sigma^* = \frac{2f^{1/2}}{\sqrt{\pi}} - R + Re^{f/R^2} \operatorname{erfc}\left(\frac{\sqrt{f}}{R}\right) - \operatorname{erfc}\left(\frac{1+\xi}{\sqrt{f}}\right) - \operatorname{erfc}\left(\frac{1-\xi}{\sqrt{f}}\right) + e^{1/R(1+\xi)+(f/R^2)} \operatorname{erfc}\left(\frac{1+\xi}{2\sqrt{f}} + \frac{\sqrt{f}}{R}\right) + e^{1/R(1-\xi)+(f/R^2)} \operatorname{erfc}\left(\frac{1-\xi}{\sqrt{f}} + \frac{\sqrt{f}}{R}\right) + 0(f^{1/4} e^{(1/4f)}) \quad [17]$$

where now $-1 \leq \xi \leq 1$. It is to be noted that, since

$$\sigma^* = \overline{T}^* - T^*$$

T^* being symmetric and monotonic to either side of the z axis, maximum stress must occur at $\xi = \pm 1$ and $\xi = 0$. In the case of heating, i.e., $T \geq 0$, σ^* at $\xi = \pm 1$ will be a compression and that at $\xi = 0$, a tension. The converse is true during cooling. Consequently in the following numerical computation, stresses are computed only at $\xi = -1$, and $\xi = 0$.

Maximum tensile and compressive stresses in the plate are computed according to Equations [16] and [17], for various values of R. The result is plotted in Figs. 3 and 4. In the following paragraphs the approximate formulas for maximum stresses at $\xi = \pm 1$ and $\xi = 0$ for very small and very large values of R are given.

By Equations [16] and [17], at $\xi = \pm 1$,

$$\sigma^* = \sum_{k=0}^{\infty} \frac{2e^{-\eta_k^2 f}}{1 + R + R^2\eta_k^2} \left(R - \frac{1}{\eta_k^2} \right) \quad [18]$$

$$\sigma^* = \frac{2f^{1/2}}{\sqrt{\pi}} + (1 + R) \left\{ e^{f/R^2} \operatorname{erfc}\left(\frac{\sqrt{f}}{R}\right) - 1 \right\} + 0\left(f^{1/2} e^{-(1/4f)}\right) \quad [19]$$

When $R = 0$, σ^* obviously reaches its maximum at $f = 0$. Hence it is expected that for very small R, Equation [19] should be adequate for computational purposes. To determine maximum σ^*, set

$$\frac{\partial \sigma^*}{\partial f} = 0$$

Equation [19] then gives

$$\frac{1}{1 + R} = \sqrt{\pi} e^{f/R^2} \frac{f^{1/2}}{R} \operatorname{erfc} \frac{\sqrt{f}}{R} \quad [20]$$

Hence, given $\sqrt{f}/R$, one can compute R and hence determine f. The applicability of Equation [20] is of course limited to small values of f since it is an asymptotic solution. For four-decimal point accuracy, f is limited to values below 0.1. Corresponding to this value of f, $R \sim 0.32$. It can be seen from the structure of Equation [20] that, as R decreases to zero, $\sqrt{f}/R$ must increase to infinity, although f itself decreases. In fact,

$$\operatorname{erfc} \frac{\sqrt{f}}{R} = \frac{1}{\sqrt{\pi}} \frac{R}{f^{1/2}} e^{-(f/R^2)} \left[1 - \frac{1}{2}\left(\frac{R}{f^{1/2}}\right)^2 + \frac{3}{4}\left(\frac{R}{f^{1/2}}\right)^4 + 0\left(\frac{R^6}{f^3}\right) \right]$$

To this order of approximation

$$f = \frac{3R^2}{1 - \left(1 - \frac{12R}{1 + R}\right)^{1/2}} \quad [21]$$

It can be shown that when $R < 0.005$, the above formula is adequate for four-place accuracy in f. When f is known, it is but a simple matter to calculate σ^*. Accordingly as $R \to 0$,

$$\sigma_{max}{}^* = -1 + \sqrt{\frac{8}{\pi}} R^{1/2} \quad [22]$$

On the other hand, when $R \to \infty$, f also increases as R increases. Hence, one may use Equation [18], the first two terms of which give accurate answers up to four significant figures, when f is larger than 0.10. After a similar analysis as outlined previously, one obtains for maximum σ^* at $\xi = \pm 1$,

$$\sigma_{max}^* = -\frac{2\left(\frac{1}{\eta_0^2} - R\right)}{1 + R + R^2\eta_0^2}\, e^{-\eta_0^2 f}\left(1 - \frac{\eta_0^2}{\eta_1^2}\right)$$

where η_0, η_1 are the first two roots of $R\eta \tan \eta = 1$, and

$$f = \frac{1}{\eta_1^2 - \eta_0^2} \log\left[\frac{1 + R + R^2\eta_0^2}{1 + R + R^2\eta_1^2}\,\frac{R\eta_1^2 - 1}{1 - R\eta_0^2}\right]$$

Now, for large values of R,

$$\left.\begin{aligned} \eta_0 &= R^{-1/2} - \frac{1}{6}R^{-3/2} - \frac{11}{360}R^{-5/2} + 0(R^{-7/2}) \\ \eta_1 &= \pi + \frac{1}{\pi}R^{-1} - \frac{1}{\pi^3}R^{-2} - \frac{\pi^2 - 6}{3\pi^5}R^{-3} + 0(R^{-4}) \end{aligned}\right\} \quad [23]$$

By making use of these results, one obtains

$$\sigma_{max}^* = -\frac{1}{3R}\left[1 + \frac{1}{\pi^2 R}\log 6R + \left(\frac{2}{15} + \frac{1}{\pi^2}\right)\frac{1}{R}\right]^{-1} \quad [24]$$

or roughly,

$$\sigma_{max}^* = -\frac{1}{3R} \quad [24a]$$

This last result may be used when $R > 10$, to yield answers of two significant figures. It can be shown that when $R \geq 1$, Equation [24] already gives sufficiently accurate answers up to two significant figures.

At the point $\xi = 0$, preliminary calculations show that when $R = 0$, $f = 0.102$, for maximum σ^*. Hence the Fourier series solution [16] may be used for small as well as large values of R, when numerical solutions are not carried beyond four significant figures. While Equations [23] correspond to large values of R, one must use, for small values of R,

$$\left.\begin{aligned} \eta_0 &= \frac{\pi}{2}(1 + R) + 0(R^2) \\ \eta_1 &= \frac{3\pi}{2}(1 + R) + 0(R^2) \end{aligned}\right\} \quad [25]$$

Accordingly, for σ_{max}^* at $\xi = 0$, the following relations hold,

$$\sigma_{max}^* = \frac{1}{6R}\left(1 + \frac{1}{\pi^2 R}\log 12R + \frac{\pi^2 + 3}{3\pi^2}\frac{1}{R}\right) \quad [26]$$

or, roughly

$$\sigma_{max}^* \sim \frac{1}{6R} \quad \text{as } R \to \infty \quad [26a]$$

and

$$\sigma_{max}^* \sim \frac{32}{9\pi^2}\frac{(\pi - 2)^{3/2}}{(3\pi + 2)^{1/2}}\left(1 - \frac{6\pi + 5}{\pi - 2}R\right) \text{ as } R \to \infty \quad [27]$$

Equation [26] may be used when $R \geq 3$ for two significant figures. Comparison between Equations [22], [24], [26], and [27] shows that the ratio of maximum stresses on the surface to that at the center is about 2 to 1 when $R \to \infty$, and is about 10 to 3 when $R \to 0$.

For the plate with one side heated and the other side insulated, the maximum stresses are computed for $\xi = -1/2$ and $\xi = 0$. The results are plotted on Figs. 3 and 4. It should be noted that in the present case the maximum stresses at $\xi = -1/2$ or $\xi = 0$ may not be the absolute maximum stresses in the whole plate for given R. However, this deviation is not considered to be important and the computed maximum stresses are representative.

For comparison with the previous case, the following result is given for σ_{max}^* at $\xi = -1/2$ when R is very small,

$$\sigma_{max}^* = -1 + \sqrt{\frac{32}{\pi}}R^{1/2} \quad [28]$$

Due to the difference in the definition in the thickness of the plate, for the same plate, R in this case is only one-half of the R in the previous case. Equation [28] then shows that the thermal stress at the surface is smaller when only one side of a plate is heated, as is to be expected, since bending of the plate constitutes a relief of the thermal stress.

Application to the Evaluation of Thermal Shock Resistivity of Certain Ceramic and Ceramal Materials

An experimental method (1 and 5), currently used by NACA for the evaluation of the thermal shock properties of ceramic and ceramal materials, is conducted in the following way: A specimen 2 in. in diam and 1/4 in. in thickness is subjected to repeated cycles of heating and cooling until fracture occurs. Heating is performed in a furnace of controlled temperature, and cooling in an air stream at about room temperature. The specimen was first subjected to 25 temperature cycles with a furnace temperature of 1800 F. If it

TABLE 1

Material	Physical properties: α (60–1100 F), in./in. F	k, Btu/(hr) (ft²) (F/in.)	E, psi	Tensile strength, psi	Thermal shock evaluation (cycles completed): 1800 F	2000 F	2200 F	2400 F
Ceramal (80% TiC, 20% CO)	5.0×10^{-6}	247	5.5×10^7	33,000 (1800 F) 11,000 (2200 F)	25	25	25	25
Titanium carbide (TiC)	4.1×10^{-6}	240	5.5×10^7	17,200 (1800 F)	25	25	25	21
Beryllium oxide (BeO)	5.28×10^{-6}	233	4.28×10^7	6,200 (1800 F)	25	3	...	...
Zircon ($ZrSiO_4$)	2.24×10^{-6}	11.6	2.4×10^7	8,700 (1800 F)	1	...	...	...
Magnesium oxide (MgO)	6.94×10^{-6}	14.5 (1832 F) 17.7 (2192 F) 40.8 (2012 F)	1.24×10^7	3,100 (1800 F)	1/2	...	...	...
94% zirconium dioxide + 6% calcium oxide (CaO)	4.95×10^{-6}	6.4 (2192 F)	2.5×10^7	6,750	...	...	...	...

survived this treatment, 25 cycles were repeated in succession with furnace temperature at 2000 F, 2200 F, and 2400 F, except when failure occurred. The results obtained at the NACA Lewis Flight Propulsion Laboratory, are collected in Table I.

Test results showed that all specimens failed by tension during cooling, with the exception of stabilized zirconium dioxide, which failed by shear. Hence, only tensile strengths are given in Table I. The tensile strength for stabilized zirconium given in the table is considered close to the shear strength.

W. G. Lidman and A. R. Bobrowsky reported (1) that the increase of thermal shock strength was accompanied by an increase in the ratio $k\sigma_0/\alpha E$, where σ_0 is the fracture tensile strength of the material under consideration. This correlation was qualitative and, in so far as the parameter $k\sigma_0/\alpha E$ is not dimensionless, has only limited applications. However, the previous results on the calculation of maximum stress in a plate can be used to determine a more satisfactory correlation between the thermal shock test results and the physical parameters of the material.

The deciding factor whether a brittle material fails or does not fail is clearly the ratio of the failure strength to the actual stress. If the ratio exceeds one, it will fail, and vice versa. Moreover, general fatigue tests show that when a specimen is repeatedly stressed through cycles, the number of cycles that the specimen can survive bears a statistical relation to this ratio. This relation, however, may vary from material to material and becomes less definite when the stress cycles are operated close to the failure strength. Applied to the phenomena of thermal stresses, these considerations should still be true, if all changes in physical and mechanical properties due to change of temperature are properly taken care of. Hence, one still can take this ratio as the criterion for thermal shock evaluations, and write

$$S = \frac{\sigma_0}{\sigma} \quad \ldots\ldots\ldots\ldots\ldots\ldots [29]$$

where σ now stands for the maximum thermal stress actually reached in the specimen. When S is less than unity, one can predict with certainty that the specimen will fail. S can be called the thermal shock resistivity.

To find the maximum stress in the circulate plate tested by NACA, the results of the previous section for a plate heated on both sides can be applied with the following assumptions: (1) The plate is infinite in extent, and constant in thickness; (2) the physical parameters E, ν, α, k, c, and h are constant; (3) the plate is heated (or cooled) uniformly on both sides by the same heat source (or sink). The time duration is such that at the end of each temperature cycle, a uniform temperature is re-established in the plate; and (4) small strain. Applied to the present problem, assumptions 4 and 3 are justified by the very nature of the experiment. Assumption 2 is made on account of the fact that little information is available on the variation of E, ν, α, k, c, and h with respect to temperature. Assumption 1 seems warranted in view of the uncertainty introduced by assumption 2 in addition to the fact that the test specimen was reasonably thin.

The theoretical results in the previous section computed for a plate heated or cooled on both sides may be expressed as

$$\sigma = \frac{\alpha E T_0}{1-\nu}\,\sigma_{\max}{}^* \quad \ldots\ldots\ldots\ldots\ldots\ldots [30]$$

where σ is the maximum stress at $Z = \pm b$. These points are chosen simply because at these points, maximum stresses occur both during cooling and heating. By the definition of S, Equation [29],

$$S = \frac{(1-\nu)\sigma_0}{\alpha E T_0}\,\frac{1}{\sigma_{\max}{}^*} \quad \ldots\ldots\ldots\ldots\ldots\ldots [31]$$

Hence S depends only on R and another dimensionless parameter $\dfrac{(1-\nu)\sigma_0}{\alpha E T_0}$. The dependence of S on R is not in general linear, as shown in Fig. 3. However, as $\sigma_{\max}{}^* \sim \dfrac{1}{3R}$, when R becomes sufficiently large, say $R > 10$, it is seen that S is then proportional to R or k/hb. Thus, when plates of the same thickness are tested in identical ways, one has

$$S \sim \frac{(1-\nu)\sigma_0 k}{\alpha E}$$

for large values of R. This is the relation used by Lidman and Bobrowsky. As noted before, this relation is sufficiently accurate for two significant figure computations when $R > 10$.

To compare the test results given in Table 1 with the theoretical thermal shock resistivity, h is taken to be the same for all specimens, since they were tested under identical conditions. The value $h = 50$ Btu/F ft^2 hr gives a satisfactory correlation. The room temperature and ν are taken as 60 F and $1/3$, respectively. In the following table, the thermal shock resistivity theoretically evaluated is compared with the test results.

In Table 2, except for ceramal, data given in Table 1 only have been used, together with Fig. 3 and Equation [31]. For ceramal, at 2000 F, σ_0 is taken to be 22,000 psi, which is the mean value of the two tensile strengths at 1800 F and 2200 F. Where two different values for k are given, two values for S are evaluated. The reason that the tensile strength at high temperature is used instead of the tensile strength at low temperature becomes clear, if one recalls that none of the specimens failed by compression during the test, and that the maximum stress occurs always on the surface.

The assertion, that whether the specimen will or will not survive any thermal cycle will depend on the value of S, is satisfactorily confirmed by the correlation between experimental results and computations based on the simplified theory. The values of S for titanium

TABLE 2

Material	Thermal shock evaluation	Furnace temperature —Room temperature 60 F— 1800 F	2000 F	2200 F	2400 F
Ceramal (80% TiC, 20% CO)	Exp.	25	25	25	25
	S	5.5	3.3	1.5	...
Titanium carbide	Exp.	25	25	25	21
	S	3.4	3.0	2.7	2.5
Beryllium oxide	Exp.	25	3	...	...
	S	1.17	1.05	...	...
Zircon	Exp.	1			
	S	0.45			
		0.54			
Magnesium oxide	Exp.	1/2			
	S	0.14			
		0.28			
94% zirconium dioxide + 6% calcium oxide	Exp.	0			
	S	0.10			

carbide at 2000 F, 2200 F, and 2400 F are probably too high, since in the calculation the ultimate tensile strength at 1800 F is used instead of its exact values at these high temperatures, owing to the lack of data. The same comment goes for S at 2000 F, calculated for beryllium oxide.

Concluding Remarks

On the strength of this correlation with experiments presented in the previous section, one may conclude that for the type of experiment on thermal shocks described, the question of immediate failure upon application of a temperature gradient can be satisfactorily answered by calculating the thermal shock resistivity S according to the present simple theory. When S is smaller than unity, one can be quite sure that the specimen will suffer immediate failure.

The question as to how many cycles a specimen can undergo before failure eventually occurs, remains open. The NACA test procedure described above cannot be used as the basis of such an analysis, since the thermal cycles were stopped as soon as 25 cycles were completed without failure. Yet, from the practical point of view this question is of greater interest than that of immediate failure. Ceramic and ceramal materials are used generally for machine parts that have only a limited life. Hence, in the study of the relationship between the number of cycles N and thermal shock resistivity, the primary interest is in low or mediumly high values of N, in contrast to the usual fatigue tests on metals. Perhaps an empirical relation between S and N of the following type,

$$N = e^{m(S-1)}, \qquad S > 1$$

may be constructed, where m is a positive number to be determined experimentally. This sort of relationship, of course, can be used only in a statistical sense. A great deal of deviation is to be expected when S is close to unity.

It may also be pointed out that the thermal shock resistance is by no means an intrinsic property of a material. Thermal shock resistance depends rather strongly on the manner in which heat is supplied and the form of the specimen, as seen from the influence of b and h on S, according to the simple theory described. This fact limits greatly the usefulness of thermal shock experiments carried out on special specimens and under special conditions, to no more than an evaluation of the comparative merits of various materials against thermal shock. Such a test cannot predict the performance of any particular design subjected to specified heating or cooling conditions. For any specific design, the thermal stress induced in the material by the nonuniform and unsteady heating and cooling must be first determined. Then with the known strength of the material under repeated stress, the performance of the design can be ascertained. This is the rational theory of thermal shock resistance. It is the primary purpose of this paper to demonstrate what fundamental physical parameters are essential to the construction of a rational theory by which the thermal shock phenomenon may be analyzed for any given material of any shape and under any service condition.

References

1 "Correlation of Physical Properties of Ceramic Materials with Resistance to Fracture by Thermal Shock," by W. G. Lidman and A. R. Bobrowsky, NACA Technical Note No. 1918, 1949.

2 "Theory of Elasticity," by S. Timoshenko, 1934, McGraw-Hill Publishing Co., Inc., New York, N. Y., pp. 203–212.

3 "Heat Transmission," by W. H. McAdams, 1942, McGraw-Hill Publishing Co., Inc., New York, N. Y., pp. 32–35.

4 "Operational Methods in Applied Mathematics," by H. S. Carslaw and J. C. Jaeger, 1948, Oxford Press, London, pp. 271–279.

5 "Initial Investigation of Carbide-Type Ceramal of 80 Per Cent Titanium Carbide Plus 20 Per Cent Cobalt for Use as Gas-Turbine-Blade Material," by C. A. Hoffman, G. M. Ault, and J. J. Gangler, NACA Technical Note No. 1836, 1949.

Notice to Members of ARS:

Are Your Membership Fees Up to Date?

BECAUSE of the increased cost of production of the Journal, it will be necessary to remove the names of all dues-delinquent members from the JOURNAL mailing list. What is the status of your dues?

Strengths of Several Steels for Rocket Chambers Subjected to High Rates of Heating

By R. L. NOLAND

Aerojet Engineering Corporation, Azusa, Calif.

This paper presents a summary of the results of a series of tests conducted to determine the tensile strengths of various types of steels when subjected to rates of heating comparable to those encountered by the metal parts of solid propellant rocket motors. The results of these tests indicate that time at temperature has a very definite effect upon the high temperature strength characteristics of the types of steels investigated under this program. These data indicate that the high temperature strength properties based on relatively high temperature long-exposure periods, approximately 15 minutes, are conservative for design purposes when the exposure times do not exceed 5 seconds.

THE design engineer is continually attempting to improve the efficiency of rocket motors and at the same time accomplish a reduction in cost. One of the basic requirements necessary for achievement of these goals is a good working knowledge of the various materials employed in fabricating the inert parts of a rocket motor. Accordingly, in an effort to aid the design engineer in accomplishing his objectives, a material evaluation program was conducted, and the results of this program are presented in this paper. The data presented are mainly for short-duration units and were obtained from tests conducted at Aerojet Engineering Corporation, Azusa, Calif., and the Battelle Memorial Institute, Columbus, Ohio. In the Aerojet tests the high temperature strength characteristics of various steels were determined under short-duration heating conditions similar to those encountered by the metal parts in solid propellant booster motors. The typical temperature gradient through the chamber wall at the end of propellant burning was duplicated in the test specimen. In the Battelle Memorial Institute tests the test specimen was uniformly heated through its cross section. Emphasis in the two programs was placed on the determination of an approximate strength-temperature relationship for a large number of materials.

Received June 11, 1951.

[1] Principal design engineer, Solid Engine Department. Member ARS.

Aerojet Test Apparatus

Fig. 1 is a schematic sketch of an apparatus which was designed and fabricated at Aerojet for the purpose of evaluating the strength of various steels when subjected to heating conditions which are encountered in solid propellant rocket engines. This test apparatus consists of a gas generating chamber where a solid propellant charge is burned; a test cylinder where the material being studied is stressed and heated at a rapid rate; and a nozzle section through which the generated gases are allowed to escape. This design was selected after considerable thought because of the flexibility it offers in solid propellant rocket materials testing work. By suitable selection of the propellant charge and annu

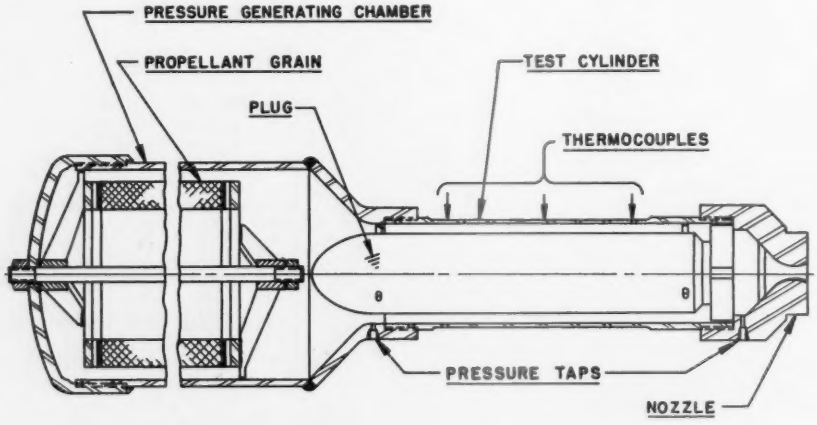

FIG. 1 SKETCH OF MATERIAL EVALUATION TESTING APPARATUS

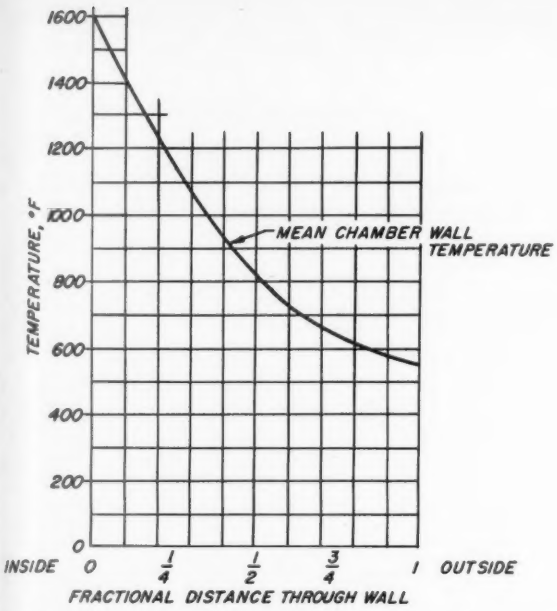

FIG. 2 THERMAL GRADIENT THROUGH THE CHAMBER WALL AT THE END OF PROPELLANT BURNING FOR TYPICAL AEROJET BOOSTER UNIT

lar gas passage dimensions for a test series, heating conditions imposed upon the test sample (the small cylinder in Fig. 1) can be held constant over a wide range of applied stress to the material, or heating conditions can be widely varied at a constant stress.

Heating Conditions for the Test Cylinder

It was desired to subject the test cylinder to heating conditions which are approximately the same as those encountered in solid propellant rocket engines. The chamber wall of a solid propellant rocket motor is subjected to a very high rate of transmission of heat from the products of combustion, resulting in a thermal gradient through the wall at the cessation of burning similar to that shown in Fig. 2. The analytical procedure followed in determining the heat transfer conditions that exist in a solid propellant rocket engine is as follows (1)[2].

1 The temperature at any position in the chamber wall at a given time increment is a function of two dimensionless parameters. They are:

$$at/L_w^2 = \text{Fourier modulus} \quad [1]$$

$$h_G L_w/K_w = \text{Biot modulus} \quad [2]$$

where

a = thermal diffusivity of the chamber material; ft^2hr^{-1}
k_w = thermal conductivity of the chamber material Btu $ft^{-2}hr^{-1}(°F/ft)^{-1}$
t = time, hr
L_w = thickness of chamber wall, ft
h_G = heat transfer coefficient, Btu $ft^{-2}hr^{-1}\ °F^{-1}$

2 The Fourier modulus is simply a measure of elapsed time, and the Biot modulus is a measure of the rate of heat transfer, both being in dimensionless form. The temperature at a given position in the chamber wall may be written in the dimensionless form:

$$\frac{T_G - T_x}{T_G - T_i} = \text{unconsumed temperature difference at position } x \text{ in the chamber wall}$$

T_G = temperature of the gas in °F
T_i = initial temperature of the chamber wall in °F

3 The dependence of the unconsumed temperature difference upon the Fourier and Biot moduli is very complicated when expressed analytically; therefore, graphs are used to show the relationship among the three parameters. For each position in the chamber wall, a separate graph is required. These graphs are used to determine the space mean, inside, and outside temperatures of the chamber wall.

Aerojet Test Procedure

Upon completion of fabrication of the test cylinder, measurements of wall thickness, circumference, and hardness were made at three positions along the chamber. At each position four wall thickness measurements were made, each at an angle of 90 deg to each other. A special tool was designed and fabricated for the purpose of obtaining accurate circumferential measurements. By making circumferential measurements before and after each test, it is possible to determine the amount of permanent set taken by the test cylinder. It must be remembered that these measurements are based on a gage length of approximately 14.4 in. (the circumference of the chamber) and, as a result, the effects of localized "necking down" of the chamber wall are minimized.

Temperature data were obtained during testing by attaching thermocouples to the outside surfaces of the test cylinders at the three positions along the chamber where wall thickness and circumferential measurements had been made. The thermocouples were attached to

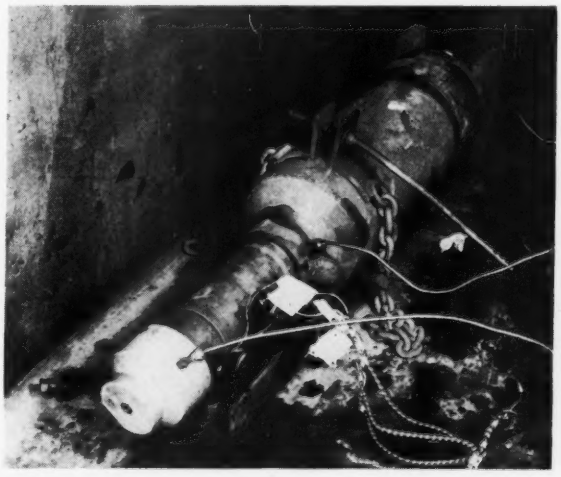

FIG. 3 MATERIAL EVALUATION TEST APPARATUS

[2] Numbers in parentheses refer to Biblography at end of paper.

the chamber by resistance welding, eliminating the need for a foreign material which may affect the recorded temperature measurements.

During operation, pressure measurements were taken at the entrance and exit ends of the test cylinder. A photograph of the test apparatus in the firing bay ready for test is shown in Fig. 3.

In order to obtain reliable strength-temperature data, it is desirable that the maximum pressure generated in the test unit occur at the end of propellant burning when the temperature is at a maximum. In Fig. 4 it can be seen that the maximum pressure occurs at the end of propellant burning. The recorded pressure-time curve for an actual test with conditions similar to those used in the theoretical calculation is also shown in Fig. 4.

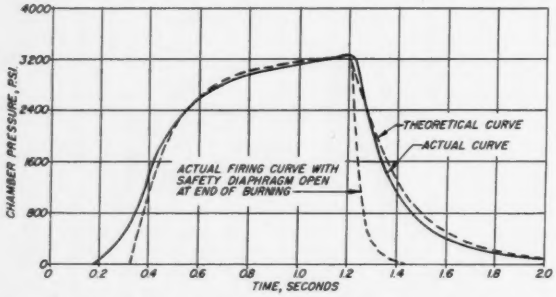

FIG. 4 THEORETICAL AND ACTUAL PRESSURE TIME CURVES FOR THE MATERIAL EVALUATION TEST APPARATUS

The strength-temperature relationship of the materials evaluated was determined by maintaining constant heating conditions and increasing the pressure progressively until rupture or excessive deformation occurred. This procedure was repeated at each heating condition until the strength-versus-temperature relationship was determined. After the strength-versus-temperature curve for the AISI-A4130 material had been determined, it was possible, by comparing the cold strength of a new material with that of the A4130, to predict an approximate relationship between strength and temperature for the new material. As a result, it was possible to obtain chamber rupture, or substantial deformation, at each heating condition without conducting a large number of tests.

To determine whether a change in the structure of the various materials had occurred during testing, some of the chambers were sectioned and metallographically analyzed.

Aerojet Test Results

A total of 69 material evaluation tests were conducted with various types of steels. The materials tested and the number of tests conducted with each material are as follows (the chemical composition for each of the steels is presented in Table 1):

1 AISI-A4130 steel heat-treated to an ultimate tensile strength of approximately 150,000 psi—19 tests.

2 Refire tests of chambers previously tested in (1)—four tests.

3 AISI-A4130 steel heat-treated to an ultimate strength of approximately 190,000 psi—six tests.

4 AISI-A4130 steel in the normalized condition—five tests.

5 NE 8630 steel heat-treated to an ultimate strength of approximately 150,000 psi—seven tests.

6 Boron-treated AISI-1035 steel, heat-treated to an ultimate strength of approximately 170,000 psi—seven tests.

7 J-55 steel (National Tube Company material designation) in the normalized condition—six tests.

8 AISI 3140 steel, heat-treated to an ultimate tensile strength of approximately 170,000 psi—four tests.

9 AISI C1015 steel, as purchased in the cold-drawn condition—five tests.

10 Same as (9) above except that a 0.75-in. wide band of 0.125-in. thick mild steel was intermittently welded around the center of each chamber—two tests.

11 AISI 2330 steel heat-treated to an ultimate tensile strength of approximately 150,000 spi—four tests.

A typical set of test data is presented in Table 2. Graphical representations for the A4130 steel, heat-treated to 150,000 and 190,000 psi, and the N.E. 8630 steel test data, are shown in Figs. 5 through 7, respectively, in order to demonstrate typical test data. Fig. 8 presents curves of the ultimate strength versus temperature for all of the steels investigated in this program. For the 150,000-A4130 steel it will be noted that a large number of ruptures were not obtained, but there were sufficient near failures to establish the ultimate strength versus temperature curve. For instance, for practical purposes a 2.77 per cent permanent defor-

TABLE 1 CHEMICAL COMPOSITION STEELS TESTED IN THE MATERIAL EVALUATION TESTS

Material	Carbon	Manganese	Phosphorus	Sulphur	Silicon	Nickel	Chromium	Vanadium	Molybdenum	Others
AISI A4130	0.31	0.55	0.03	0.01	0.26	...	0.95	...	0.21	...
N.E. 8630	0.29	0.82	0.02	0.02	0.29	0.45	0.42	...	0.18	...
AISI C1015	0.11	0.49	0.015	0.03	0.11	...	...	...	...	...
AISI 3140	0.39	0.73	Neg.	Neg.	...	1.20	0.67	...	...	...
AISI 2330	0.34	0.78	0.02	0.02	...	3.32	...	...	...	...
Modified AISI 1035	0.38	0.88	0.02	0.03	0.21	0.13	0.04	0.02	0.07	0.002 Boron
J-55	0.46	1.03	0.02	0.03	0.33	...	...	...	...	...

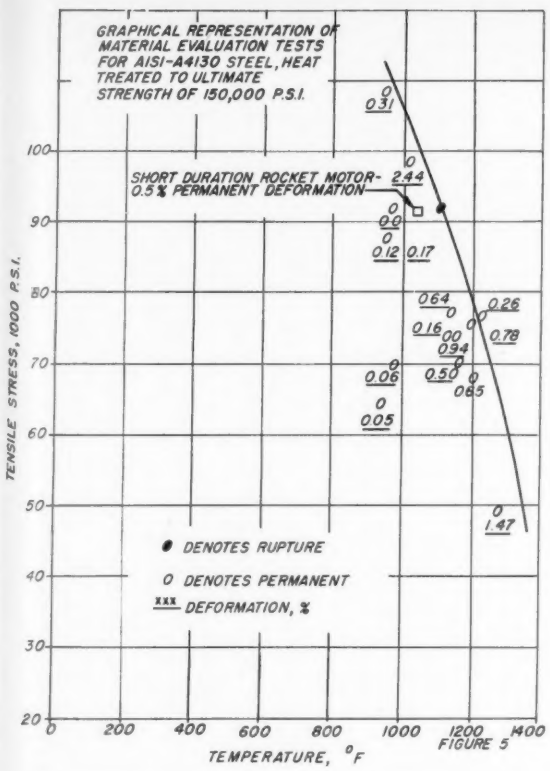
GRAPHICAL REPRESENTATION OF MATERIAL EVALUATION TESTS FOR AISI-A4130 STEEL, HEAT TREATED TO ULTIMATE STRENGTH OF 150,000 P.S.I.
SHORT DURATION ROCKET MOTOR- 0.5 % PERMANENT DEFORMATION
TENSILE STRESS, 1000 P.S.I.
TEMPERATURE, °F
DENOTES RUPTURE
DENOTES PERMANENT
DEFORMATION, %
FIGURE 5

FIG. 5 GRAPHICAL REPRESENTATION OF MATERIAL EVALUATION TESTS FOR AISI-A4130, HEAT-TREATED TO ULTIMATE STRENGTH OF 150,000 PSI

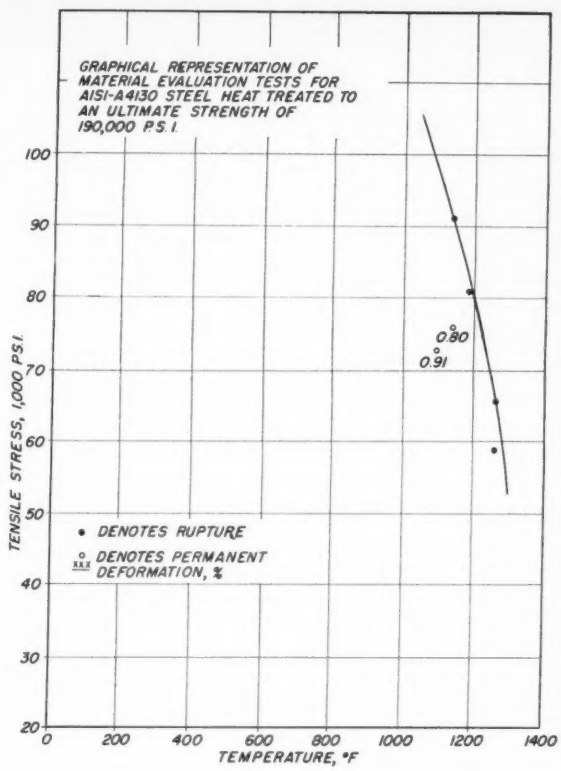
GRAPHICAL REPRESENTATION OF MATERIAL EVALUATION TESTS FOR AISI-A4130 STEEL HEAT TREATED TO AN ULTIMATE STRENGTH OF 190,000 P.S.I.
TENSILE STRESS, 1,000 PSI
TEMPERATURE, °F
DENOTES RUPTURE
DENOTES PERMANENT DEFORMATION, %

FIG. 6 GRAPHICAL REPRESENTATION OF MATERIAL EVALUATION TESTS FOR AISI-A4130 STEEL HEAT-TREATED TO AN ULTIMATE STRENGTH OF 190,000 PSI

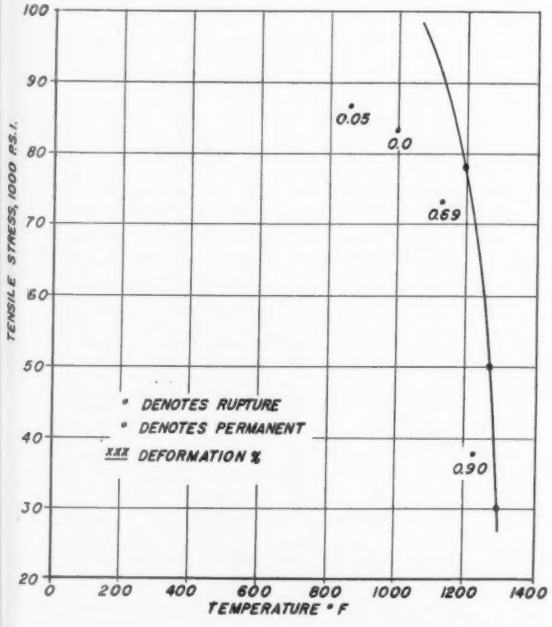

FIG. 7 GRAPHICAL REPRESENTATION OF MATERIAL EVALUATION TESTS FOR N.E. 8630 STEEL HEAT-TREATED TO AN ULTIMATE STRENGTH OF 150,000 PSI

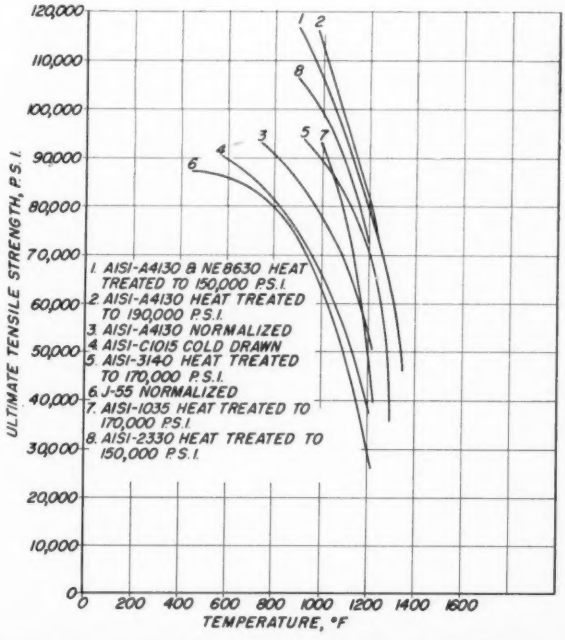
ULTIMATE TENSILE STRENGTH, P.S.I.
TEMPERATURE, °F
1. AISI-A4130 & NE8630 HEAT TREATED TO 150,000 P.S.I.
2. AISI-A4130 HEAT TREATED TO 190,000 P.S.I.
3. AISI-A4130 NORMALIZED
4. AISI-C1015 COLD DRAWN
5. AISI-3140 HEAT TREATED TO 170,000 P.S.I.
6. J-55 NORMALIZED
7. AISI-1035 HEAT TREATED TO 170,000 P.S.I.
8. AISI-2330 HEAT TREATED TO 150,000 P.S.I.

FIG. 8 MATERIAL EVALUATION TEST RESULTS FOR VARIOUS STEELS—ULTIMATE TENSILE STRENGTH VERSUS TEMPERATURE

TABLE 2 SUMMARY OF EXPERIMENTAL DATA, CHAMBER MATERIAL EVALUATION TESTS

Test No.[a]	22	16	27	29	47	36	43	44	50	51	53	56
Chamber material	AISI A4130	AISI A4130	AISI A4130	AISI A4130	NE 8630	NE 8630	NE 8630	NE 8630	NE 8630	NE 8630	NE 8630	1035
Initial strengh (Rockwell), psi × 10^{-3}	128	153	153	153	141	142	141	144	145	147	143	171
Final strength (Rockwell), psi × 10^{-3}	123	153	153	...	...	...	141	115	140	144	...	136
Applied stress, psi × 10^{-3}	57	108	98	137	30	78	74	38	86	84	50	55
Space-mean temperature, °F	930	950	1020	600	1300	1200	1140	1240	880	1000	1270	1070
Permanent deformation, %[b]	0.0	0.31	2.77	R	R	R	0.69	0.09	0.05	0.0	R	0.30
Maximum pressure, psi	2560	4600	4220	5920	2000	3300	3320	1660	3730	3750	2160	2630
Wall thickness, in.	0.100	0.096	0.096	0.096	0.094	0.093	0.098	0.095	0.098	0.098	0.094	0.091
Inside diameter, in.	4.36	4.36	4.36	4.36	4.36	4.36	4.36	4.36	4.36	4.36	4.36	4.18
Plug diameter, in.	...	4.00	4.00	...	4.0	...	3.7	4.0	3.32	3.32	4.0	3.32
Rate of temperature rise, °F sec^{-1}	980	2100	1950	900	1270	1300	1100	1400	820	1070	1210	1100
Outside wall temperature at maximum pressure, °F	720	660	550	440	1125	1080	980	1050	750	805	1115	940
Average pressure, psia	...	2762	2813	...	1714	...	2517	1442	2791	2920	...	2140
Chamber no.	6	16	16	16	23	39	25	24	31	32	35	56

[a] Test Series 45SC. [b] R denotes rupture.

mation, as obtained in Test No. 27, may be considered as closely approximating the ultimate strength of the material. The curves present approximately the nominal values of ultimate tensile strength versus temperature and should be satisfactory for design purposes in which the designs are based on the yield strength rather than the ultimate strength. It is customary in the case of steels to assume that the yield strength is equal to 0.8 of the ultimate strength. A good correlation between the allowable and applied stresses is obtained in comparing these data with those obtained in actual applications. This is clearly shown in Fig. 5, where the stress-temperature point for a short-duration rocket motor has been plotted. This unit, which had an original ultimate tensile strength of 150,000 psi, was stressed to approximately 90,000 psi, had a mean chamber wall temperature of 1040 F, and was permanently deformed to 0.5 per cent.

AISI-A4130 Steel, Heat-Treated to an Ultimate Tensile Strength of Approximately 150,000 Psi

For comparative purposes, Fig. 9 shows the ultimate strength versus temperature curves for the 150,000-A4130 steel based on the following data:

1 The material evaluation tests.

2 The Battelle Memorial Institute tests (see page 161).

3 Steel mill tests, in which the test specimens were heated to the test temperature for approximately 15 minutes prior to testing. The strength versus temperature relationship formerly used at Aerojet was based on these data.

4 The recommended tensile strength versus temperature curve for the purpose of the design of rocket motors is included in Fig. 9. The strength values shown on the design curve are 80 per cent of the ultimate strength based on the material evaluation tests.

In Fig. 9 it will be noted that a good correlation is obtained between the material evaluation data and the Battelle Memorial Institute data. As discussed on page 161 of this paper, the specimen is uniformly heated through its cross section in the Battelle Memorial Institute tests, whereas in the material evaluation tests there is a temperature gradient through the chamber wall at the end of propellant burning. These data indicate that for AISI-A4130 steel, quenched and tempered to an ultimate tensile strength of 150,000 psi, the temperature gradient through the chamber wall may be used as a criterion for determining the strength of the chamber at the end of propellant burning.

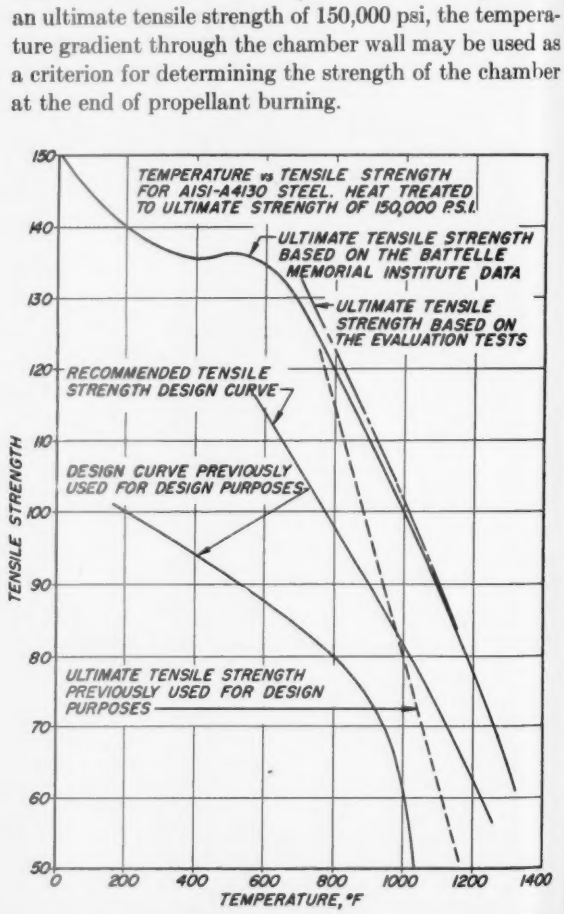

FIG. 9 TEMPERATURE VERSUS TENSILE STRENGTH FOR AISI-A4130 STEEL HEAT-TREATED TO ULTIMATE STRENGTH OF 150,000 PSI

A comparison of the material evaluation data and that previously used for design purposes (see Fig. 9) indicates that time at temperature has an appreciable effect upon the high-temperature-strength properties of the steel. In the material evaluation tests the specimens were heated for less than two seconds, whereas the other data are based on "long time" heating of the test specimens. The difference in strength properties obtained by the two methods of test is probably due to the extent to which the grain structure of the steel is altered prior to, or during, testing. For the "long period" tests a structural change probably occurs prior to test, whereas the material evaluation tests were conducted in such short periods of time that it was not possible for a grain structure change to occur. A 150,000-A4130 chamber was quenched with water approximately five sec after completion of propellant burning, and a metallographic examination of the steel following the test indicated that no structural change had occurred even though it was at a temperature of 1180 F for at least five sec prior to quenching. However, on a basis of the other tests, it is known that if the mean temperature exceeds approximately 950 F (the original tempering temperature of the chamber) for an appreciable time and the chamber is allowed to cool slowly, a structural change of the steel occurs. This indicates that time at temperature is an important factor in altering the structure of the steel. If the mean temperature of the chamber wall remains below the original tempering temperature, the strength of the chamber wall is not affected, with the exception of a slight amount of alteration that might occur at the inner surface of the chamber.

AISI-A4130 Steel, Heat-Treated to an Ultimate Tensile Strength of Approximately 190,000 Psi

In Fig. 8 it will be noted that at temperatures above 1000 F there is little difference between the strengths of the A4130 steel heat-treated to 150,000 psi and 190,000 psi. As a result, it may be concluded that there is little advantage in using the higher strength steel in applications when the mean chamber wall temperature exceeds 1000 F. The greatest advantage of the 190,000-A4130 steel[3] is to be gained by maintaining its mean chamber wall temperature at values below 1000 F. It may be advantageous to use the higher strength steel if the metal part is to be subjected to repeated firings, because after test it retains a higher ultimate strength than the lower strength steel.

AISI-A4130 Steel in the Normalized Condition

The data in Fig. 8 indicate that the strength of the A4130 steel in the normalized condition does not decrease as rapidly with increasing temperatures as the quenched and tempered steels. Because the quenched and tempered steels lose strength so rapidly at the high temperatures, the data tend to indicate that the normalized steel will function as satisfactorily as the quenched and tempered steels at temperatures above 1400 F.

Cold-Drawn AISI 1015 Steel

Fig. 8 indicates that C1015 steel is good only for applications at high temperatures where low magnitudes of stress are involved. However, if the temperature of the steel is maintained below 600 F, it can be used effectively.

J-55 Steel

The J-55 steel in the normalized condition has temperature-strength properties very similar to those of the C1015 steel (see Fig. 8). One possible advantage of this steel over the C1015 steel may be that it can be welded continuously and then renormalized and have its original strength properties restored.

N.E. 8630, Heat-Treated to an Ultimate Tensile Strength of Approximately 150,000 Psi

The results of the tests conducted with this steel indicate that its strength-temperature relationship is almost identical to that of the 150,000-A4130 steel.

AISI 2330 Steel, Heat-Treated to an Ultimate Tensile Strength of Approximately 150,000 Psi

The results of the material evaluation tests conducted with this material indicate that it has strength properties equal to approximately 95 per cent of those for the 150,000-A4130 steel at temperatures above 1000 F.

AISI 3140 Steel, Heat-Treated to an Ultimate Tensile Strength of Approximately 170,000 Psi

The results of the material evaluation tests conducted with this material indicate that in the temperature range of 1100–1200 F the AISI 3140 material has strength properties equal to approximately 88 per cent of those of the 150,000-A4130 steel.

Boron-Treated AISI 1035 Steel, Heat-Treated to an Ultimate Strength of Approximately 170,000 Psi

This material was originally purchased as AISI 1035 steel, and chemical and physical tests conducted by Aerojet indicated that it conformed to the specifications for AISI 1035 steel. However, when this steel was oil-quenched and then tempered at a temperature of 1000 F, it had a Rockwell "C" hardness of approximately 37. Because normal AISI 1035 steel has a Rockwell "C" hardness of approximately 30 following an oil quench (2), a more thorough chemical analysis of the steel was con-

[3] 190,000-A4130 will henceforth be used as an abbreviated form of referring to AISI-A4130 steel heat-treated to an ultimate tensile strength of approximately 190,000 psi.

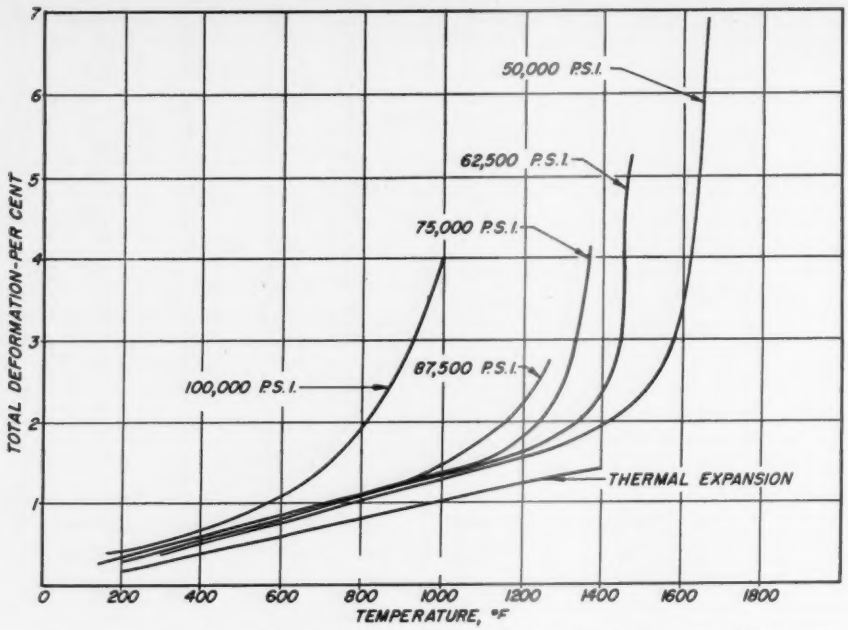

FIG. 10 TEMPERATURE VERSUS DEFORMATION FOR UNILOY 19–9 DL STAINLESS STEEL, 1200 F STRESS RELIEVED. HEATING RATE—430 F PER SEC

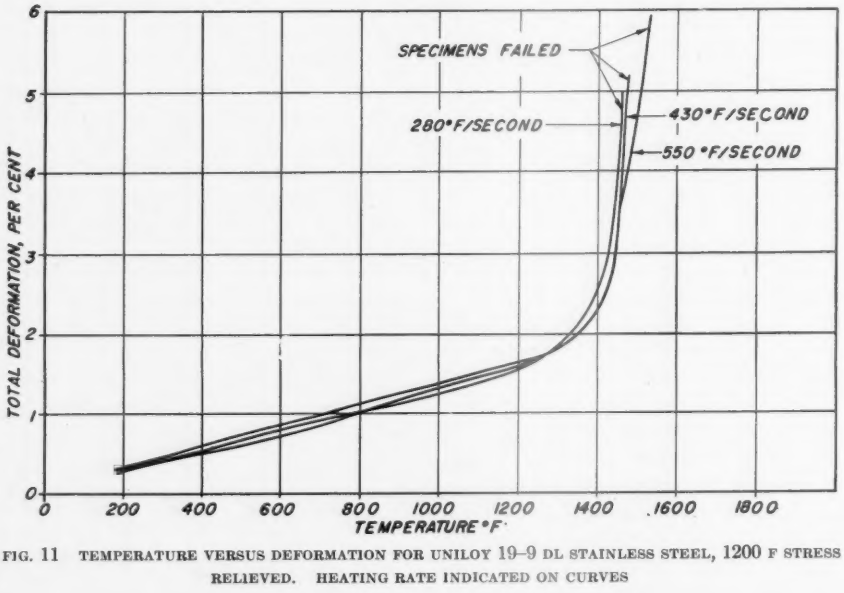

FIG. 11 TEMPERATURE VERSUS DEFORMATION FOR UNILOY 19–9 DL STAINLESS STEEL, 1200 F STRESS RELIEVED. HEATING RATE INDICATED ON CURVES

ducted to determine whether sufficient residual constituents were present to give the steel its high hardenability qualities. The residual constituents, such as nickel, molybdenum, chromium, and copper found in the steel, are not in sufficient quantity to give the steel its high hardenability characteristics. However, as presented in the *Transactions* of the American Society for Metals, Vol. 37, 1946, it is known that very small quantities of boron (approximately 0.0025 per cent) have an appreciable effect upon the hardenability characteristics of a plain carbon steel (3). As a result, a spectrographic analysis of the steel was conducted, and it was found that it contained approximately 0.002 per cent boron. Consequently, it was possible to include a boron-treated steel in this evaluating program. The results of this study are indicative of the potential use of plain carbon steels treated with boron, because the hardenability characteristics of the steel studied in this program were slightly superior to those of AISI-A4130 steel. It is realized that this may not be a true boron steel, where the boron is added to the metal under carefully controlled processing techniques.

This boron-treated AISI 1035 steel is approximately 85 per cent as strong as the 150,000-A4130 steel at temperatures above 1000 F. The boron-treated steel appears to lose strength with increase in temperature more rapidly than the A4130 steel. Because of the high strength characteristics of this material at temperatures below 900 F, it would be advantageous to utilize this steel in applications in which the temperature did not exceed 900 F.

Battelle Memorial Institute Test Results

Tensile tests with high rate of rise in temperature were conducted by Battelle Memorial Institute in order to obtain a comparison between specimens uniformly heated and those with temperature gradients through their cross sections. In addition to obtaining temperature-strength data by this method of testing, it is possible to obtain the variation of modulus of elasticity with changes in temperature and stress. These data are invaluable for use in thermal stress problems.

A brief description of the test setup employed by Battelle follows:

1 The test section of the specimen is $^1/_2$ in. wide and approximately 8 in. long. The over-all length of each specimen is approximately 17 in., and the width at the ends where the specimen is clamped during test is 2 inches.

2 Heating is obtained by passing a high current through the specimen from an electric arc welding transformer. It is possible to vary the rate of rise in temperature from 10 F/sec to 1300 F/sec.

3 Two test specimens clamped together are tested simultaneously. The rise in temperature is measured with thermocouples clamped between the two specimens.

4 The tensile load is applied to the specimen by means of a dead load through a 9:1-ratio lever arm. The test equipment does not allow for a rate of change in the applied load, and, as a result, it is necessary to conduct the tests under constant loading conditions.

Tests were conducted with Uniloy 19–9DL stainless steel and AISI-A4130 steel, quenched and tempered to an ultimate strength of approximately 150,000 psi.

Uniloy 19–9DL Stainless Steel

The results of tests conducted with the 19–9DL stainless steel specimens in a 1200 F stress-relieved condition are shown in Figs. 10 and 11. The figures are reproductions of the curves forwarded to Aerojet from the Battelle Memorial Institute. The termination of each curve indicates where failure of the specimen occurred. In Fig. 11 it will be noted that a variation in the rate of temperature rise from 280 F/sec to 550 F/sec has little effect upon the tensile strength properties of the material.

By use of the data from Fig. 10 and assuming that there is no strain at zero stress, it is possible to plot con-

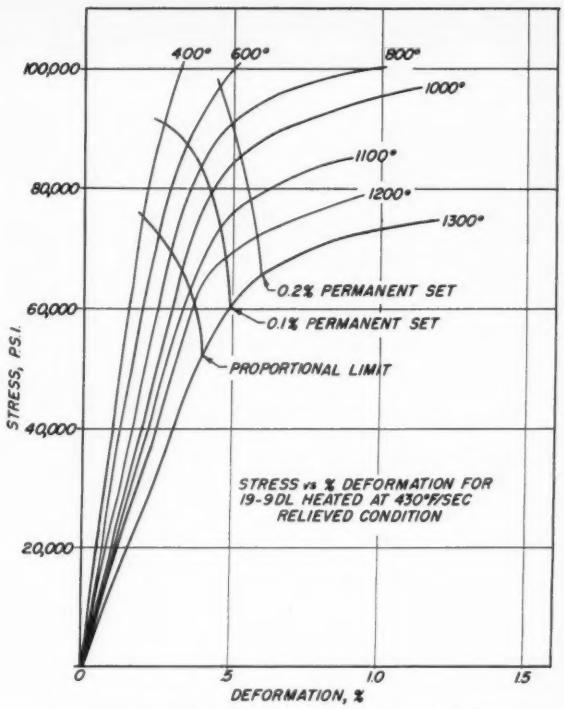

FIG. 12 STRESS VERSUS PER CENT DEFORMATION FOR 19–9 DL HEATED AT 430 F PER SEC—RELIEVED CONDITION

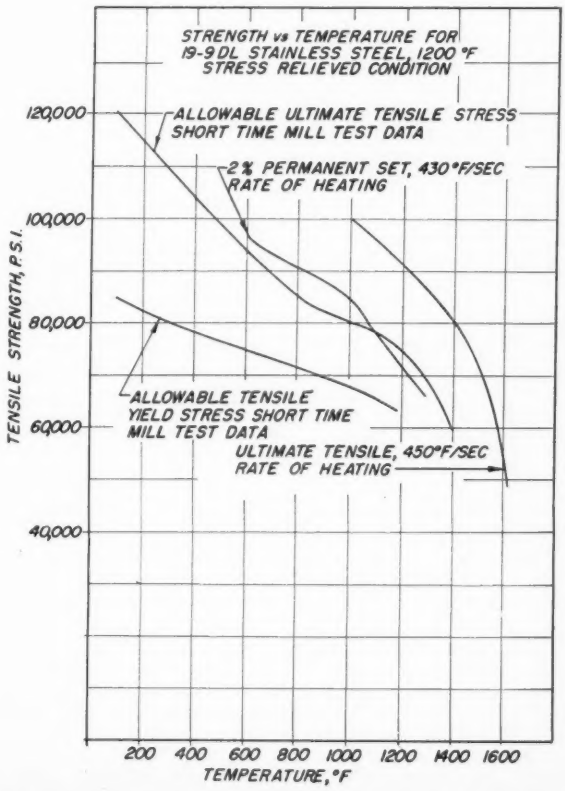

FIG. 13 STRENGTH VERSUS TEMPERATURE FOR 19–9 DL STAINLESS STEEL, 1200 F STRESS RELIEVED CONDITION

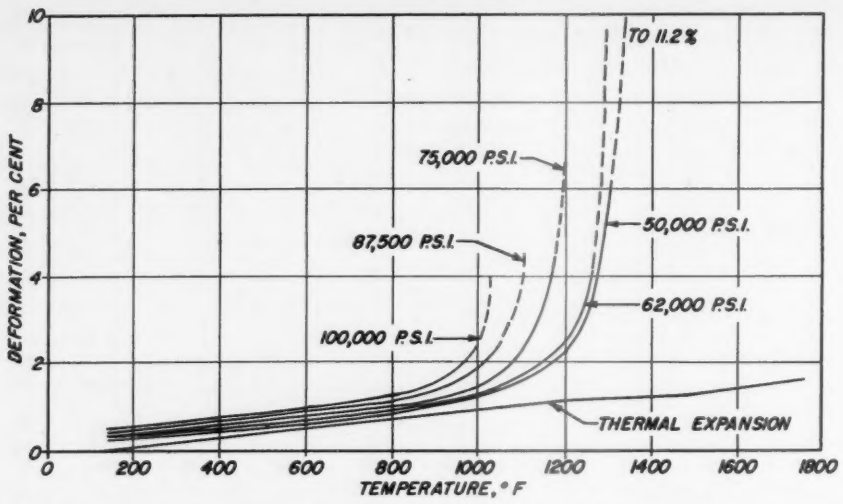

FIG. 14 TEMPERATURE VERSUS DEFORMATION CURVES FOR QUENCHED AND TEMPERED AISI-A4130 STEEL SHEET (TENSILE STRENGTH 150,000–160,000 PSI). HEATING RATE 500 F PER SEC. ALL TESTS RUPTURED AT APPROXIMATE DEFORMATIONS SHOWN

stant temperature curves of applied stress versus per cent deformation as shown in Fig. 12. These curves represent a conservative average of the plotted points and are considered to be only approximate because of the lack of sufficient data. However, if it is assumed that these are valid stress-strain curves, it is possible to ascertain values of tensile strength versus temperature. These data are graphically represented in Fig. 13. Fig. 13 also includes curves of the yield (0.2 per cent permanent-set method) and ultimate tensile strengths based on short-time mill test data for comparative purposes. These data indicate that for very short periods of heating the 19–9DL stainless steel has considerably higher tensile strength than is shown by the short-time mill test data.

By comparing these data with those obtained for the A4130 steel, as shown in Fig. 9, it will be observed that the 19–9DL stainless steel, in the 1200 F stress-relieved condition, appears to be superior to the AISI-A4130 steel, quenched and tempered to an ultimate tensile strength of 150,000 psi. However, with the A4130 steel, it is possible to obtain a weld strength which is equal to, or greater than, the strength of the parent metal. When the 19–9DL stainless steel is welded, the areas adjacent to the weld lose considerable strength. Accordingly, in many applications the A4130 steel will actually be superior to the 19–9DL stainless steel.

AISI-A4130 Steel, Heat-Treated to an Ultimate Tensile Strength of 150,000 Psi

The graphical representation of the data on deformation versus temperature received from Battelle Memorial Institute is shown in Fig. 14. The ultimate strength versus temperature based on these data is shown in Fig. 9. By comparing these data with the data obtained with the test cylinders, it will be observed that the temperature gradient through the cross section of the specimen does not have a great effect upon the strength properties of the material. This is for AISI-A4130 steel with an approximate ultimate tensile strength of 150,000 psi. The temperature gradient may have an appreciable effect upon the strength of other materials, for it is a function of the relationship among stress, strain, and temperature.

Bibliography

1 "Heat Transmission," by William H. McAdams, 1942, McGraw Hill Book Company, Inc., New York, N. Y., 2nd edition.

2 "Modern Steels and Their Properties," Bethlehem Steel Corporation, Bethlehem, Pa., Handbook 268, Copyright 1949.

3 "Factors Affecting the Hardenability of Boron-Treated Steels," by R. A. Grange and T. M. Garvey, *Transactions*, American Society for Metals, vol. 37, 1946, pp. 136–174.

Have you made your reservations for the Annual Convention at Atlantic City?

Aspects of Combustion Stability in Liquid Propellant Rocket Motors

Part I: Fundamentals. Low Frequency Instability With Monopropellants

By L. CROCCO[1]

Daniel and Florence Guggenheim Jet Propulsion Center, Princeton University, Princeton, N. J.

Existing theories are able to explain part of the observed effects of low-frequency unstable combustion with the assumption of a constant time lag between the propellants injection and their transformation into hot gases. A discussion shows that the time lag cannot be constant if the pressure oscillates, but must be correlated to the pressure history during the time lag itself. A reasonable formula is suggested to represent this correlation, and this formula is applied to the determination of the critical conditions. It is first shown that instability can arise even for constant rate of injection. Secondly, it is shown how the variation of the injection rate affects the critical conditions for monopropellant feeding systems of constant rate or constant pressure type, having given characteristics of inertia and elasticity. Finally, the influence of nonuniform values of the time lag for different portions of the injected propellant is discussed. The bipropellant case and the case of high frequency instability will be discussed in Part II, to be published in next issue of the "Journal of the American Rocket Society."

Nomenclature

Combustion Chamber

t	= time
τ	= instantaneous value of the time lag
$\bar{\tau}$	= value of the time lag in steady operation
n, m	= pressure exponents of pressure dependence of the processes taking place during the time lag
p	= instantaneous pressure in the combustion chamber
$\bar{p}$	= pressure in the combustion chamber in steady operation
φ	= $(p - \bar{p})/\bar{p}$ = fractional variation of pressure in the combustion chamber
$\dot{m}_i, \dot{m}_b, \dot{m}_e$	= instantaneous rate of injection, burning and ejection of propellants
$\bar{m}$	= common value of these in steady operation
μ	= $(\dot{m}_i - \bar{m})/\bar{m}$; $\mu_b = (\dot{m}_b - \bar{m})/\bar{m}$ = fractional variation of injection and burning rate
M_g	= instantaneous mass of gases in the combustion chamber
$\bar{M}_g$	= same in steady operation
θ_g	= $M_g/\bar{m}$ = gas residence time in steady operation
θ	= $\theta_g + \bar{\tau}$ = total residence time of propellants in steady operation
a^*, L^*	= characteristic velocity and length of the rocket
R, γ	= gas constant and adiabatic index of combustion gases
T_g, ρ_g	= absolute temperature and density of combustion gases
$z = t/\theta_g$; δ	= $\bar{\tau}/\theta_g$ = reduced time and reduced time lag
α	= $\lambda + i\omega$ = root of the characteristic equation with the reduced time as the independent variable
λ	= reduced amplification coefficient
ω	= reduced angular frequency
Ω	= angular frequency
T	= period of oscillations
Subscript$_*$	= critical conditions of incipient instability

Monopropellant Feeding System

p_1	= instantaneous pressure at that place in the feeding line where the capacitance representing the elasticity is located.
$\bar{p}_1$	= same in steady operation
Δp	= $\bar{p}_1 - \bar{p}$ = injector pressure drop in steady operation
ψ	= $(p_1 - \bar{p}_1)/2\Delta p$ = relative variation of p_1
p_0	= regulated gas pressure for constant pressure supply
A_i, A_t	= area of the injector ports and of the cross section of the feeding line
v_i, v_t	= velocity of the fluid in A_i and A_t
ρ	= density of the propellant
C	= variable volume of the capacitance introduced in the feeding system to represent its elasticity
χ	= dC/dp = compressibility coefficient
M_t	= mass of propellant in the line
l	= length of the line
ξ	= fractional length for the constant pressure supply
E	= $2\rho\chi\Delta p/\bar{m}\theta_g$ = elasticity parameter of the line
J	= $l\bar{m}/2\Delta p A_t\theta_g$ = inertia parameter of the line
P	= $\bar{p}/2\Delta p$ = pressure drop parameter
$\dot{m}_1, \mu_1$	= instantaneous mass flow and its fractional variation upstream of the capacitance

Nonuniform Time Lag

$f(0 < f < 1)$	= location of a given fraction of propellant in the jet from the injector
$\tau(f)$	= time lag corresponding to the fraction considered
$\delta(f)$	= corresponding reduced time lag
δ_m	= average reduced time lag
$\epsilon(f)$	= $\delta(f) - \delta_m$ = variation from the average
ϵ_0, ϵ_1	= extreme values of $\epsilon(f)$

Received July 3, 1951.

[1] Robert H. Goddard Professor. Member ARS.

1 Introduction

THE pressure in the combustion chamber of a rocket motor is determined by the balance between the mass flow of propellants into the chamber from the feeding system and the mass flow of gases ejected from the combustion chamber through the nozzle. If the feeding system has the desired properties of stability, that is, is able to provide under constant operating conditions a constant flow of propellants through the injector ports, then, since the exhaust through the nozzle is also constant for constant operating conditions, the pressure in the combustion chamber would have to stay perfectly constant as long as no voluntary change is introduced in the operating parameters. Direct measurement of the pressure shows that this constant pressure is never exactly obtained, and that even when the combustion looks smooth, small, high-frequency fluctuations of the pressure are always present. But what is more interesting for the practical engineer is the case of rough combustion, when the pressure fluctuations are of large amplitude and can produce unfavorable effects on the operation of the rocket and eventually on its life.

It is only in recent years that the observations on rough combustion have been co-ordinated and a distinction made between low-frequency oscillations (chugging: generally below 100 cycles per second) and high-frequency oscillations (screaming: many hundreds of cycles per second). Also, a theory has been advanced and studied quantitatively (1, 2, 3)[2] which appears to explain satisfactorily some of the observed phenomena of the low-frequency instability.

The purpose of this paper is to extend the discussion of the existing theory, and to introduce the consideration of a new factor of instability which not only may affect considerably the results in the low-frequency case, but which affords an explanation of the high-frequency instability.

2 The Time Lag: Physical Facts

The key to the existing theory resides in the consideration that the processes which are responsible for the transformation of the propellants into high temperature gases require a certain time. That the existence of this time lag is a possible reason for instability can be qualitatively seen as follows: If the development of high-temperature gases follows immediately the injection of the propellants, an accidental increase in the chamber pressure would result in, on one side, an increase in gas flow from the rocket, and on the other side, a decrease in propellant flow to the rocket chamber (if the feeding system is sensitive to pressure variations) and an immediate decrease in burning rate, so that the accidental over-pressure would drop to zero with time, and a self-excited oscillation would not be possible. But if, on the contrary, the burning does not immediately follow the injection, then a self-excited oscillation can exist because a reduction in mass flow due to an excess in chamber pressure results in a decreased burning rate at a later time, when, provided the time lag and the period of the oscillations are in a certain relation, there is a pressure defect.

The physical and chemical processes taking place during the time lag are quite complicated and, in any case, are not sufficiently known, so that a quantitative treatment is impossible today. Nevertheless, some qualitative information can be obtained from the following considerations:

(*a*) Let us consider first the simpler case of a monopropellant. As soon as the liquid leaves the injector in the form of one or many jets, the combined actions of the relative velocity with respect to the gases and of the capillarity break the jets into droplets. The rapidity and the fineness of the resulting atomization depend substantially on the type of injector and on the density of the gases, and generally increase with the latter, so that for a given injector an increase in chamber pressure has the effect of producing faster and finer atomization. Once the droplets are formed they move through a mass of hot gases, produced downstream by the previously burned propellant and recirculated backwards by eddies. This recirculation is always present in a rocket chamber and is believed to be an essential part of the mechanism of combustion. Its intensity will depend substantially on the type and distribution of the injectors, but, except for eventual periodical variations in the flow pattern, can be considered to be constant for a given injector system. The relative motion of the droplets with respect to the high-temperature gases will produce heating and partial vaporization of the droplets, and the rapidity of this process increases with the temperature difference (which is fixed) and with the density of the gases. Also, it will increase with decreasing size of the droplets. For both reasons we see that an increase in pressure produces a faster heating of the droplets. So far, the process is only physical. The rest, which involves chemical transformations, can take place in two different ways. Following the first in the heated body of the droplet (and eventually of the formed vapor) some exothermic reactions begin to develop at a rate that increases with the temperature, so that once they have started they are also accelerated, and in a very short time a complete transformation is obtained into the final high-temperature products. The rapidity of these reactions will also in some cases (especially when they take place in the vapor phase) increase with the pressure. The second way in which the transformation can happen is by a surface process, analogous to the deflagration of solid propellants, on the surface of the droplets.[3] Here

[2] Numbers in parentheses refer to the Bibliography at end of Part I.

[3] The evidence of such possibility for mixed bipropellants is afforded by recent experiments of Tait, Whittaker, and Williams (4).

again, as the rate of deflagration increases and the size of the droplets decreases with the pressure, the time necessary for the transformation in hot gases will decrease with the pressure. Finally, we can conclude that an increase in chamber pressure produces a decrease in the partial times required for the different processes to take place, and therefore a decrease of their sum, which represents the time lag.

(*b*) The bipropellant case is more involved because a necessary prerequisite for any combustion to take place is a certain degree of mixing of the two propellants. In this case, no matter how finely and quickly each one of the propellants has been atomized, heated, and vaporized, nothing can happen until it comes in contact with the other propellant. Now the rate of mixing depends essentially on the injection system, and also to a smaller extent on recirculation, but probably not on pressure. However, the conditions, droplet size, temperature, vaporization, and eventually chemical transformation, of the propellants when the mixing takes place depend considerably, as in the monopropellant case, on the chamber pressure; and therefore the rapidity of the following vapor-vapor reaction or vapor-liquid reaction will also be increased by an increase in pressure not only because of a direct effect on the kinetics of the reactions, but also because of the conditioning of the propellants before mixing. The consequence of these considerations is that also in the bipropellant case the total time lag will decrease when the pressure increases, though that part of the time lag that represents the mixing delay is unaffected by pressure. (An exception is afforded by two self-igniting propellants mixed in a nonatomized form and reacting in liquid-liquid phase, a case in which a pressure variation will have but negligible effect on the time lag.)

3 The Time Lag: Approximate Assumptions

From what has been said, it follows that if we track a small amount of monopropellant, or corresponding small amounts of the two propellants destined to be mixed and burned together, from the injection to the final conversion in hot gases, though no real discontinuity in the physicochemical processes exists, practically all of the chemical reactions, and the largest part of the temperature and volume increase, take place in a very short time near the end of the time lag. Therefore, the time lag can be approximately considered as the time after which the liquids are suddenly transformed into hot gases at the final temperature, and as the specific volume of the liquids is negligible with respect to that of the gases (even at large pressures), it is only at the end of the time lag that the introduction of the propellants will be felt in the balance of masses in the rocket chamber.

A second approximation consists in taking the same time lag for all the particles of propellants. This is not exactly true even in the simple case of the monopropellant, since the conditions of the particles are not uniform in all the spray; and it is certainly a very rough assumption in the bipropellant case since the mixing delay is fundamentally different for different particles injected simultaneously. In Section 9 we shall discuss the effect of the nonuniformity of the time lag. For the moment, however, let us accept the simple assumption of a uniform time lag, that is, all the particles injected simultaneously are burned simultaneously.

The actual determination of the time lag for a given combination of propellants, given designs of injecting system and rocket chamber, and given pressure level in the chamber, can be reached only experimentally. If, without changing the other conditions we alter the combustion pressure, the time lag, as it has been seen, must change, and the variation should also be determined experimentally. As such experimental information is not yet available, it is necessary to assume some plausible and simple law of variation. For instance, one could assume that the time lag is inversely proportional to the pressure or, more generally, to some power of the pressure, so that

$$\tau p^n = \bar{\tau}\bar{p}^n = \text{const}$$

where the superposed bar indicates some fixed reference condition. A more general formula could be

$$\tau = \tau_0 + \tau_1; \quad \bar{\tau} = \bar{\tau}_0 + \bar{\tau}_1, \qquad \tau_0 = \bar{\tau}_0 = \text{const}; \quad \tau_1 p^m = \bar{\tau}_1 \bar{p}^m = \text{const}$$

For small pressure variations it is possible to approximate both formulas with a linear relation, and the two become equivalent, with certain relations between the constants involved.

So far, the combustion pressure has been supposed to be constant during the operation, and only the effect of changing this pressure level has been considered. What if the pressure is oscillating? In this case the pressure will change during the time lag, and it is its integrated effect during the time lag which determines the time lag. For instance, if we schematize the monopropellant case as a heating of the droplets from the injection temperature to a fixed deflagration temperature followed by an instantaneous transformation in the final products, the time lag will be the time necessary to supply a definite amount of heat to the droplets; and if the heat transfer is taken proportional to the instantaneous value of the pressure to a certain exponent n, the time lag of those particles that reach the deflagration temperature at a time t will be given by the equation

$$\int_{t-\tau}^{t} p^n dt' = \bar{\tau}\bar{p}^n = \text{const} \qquad [3.1]$$

t' being the integration variable. We now assume that the same relation applies to the whole of the processes responsible for the time lag, so that Equation [3.1], or more generally

$$\tau = \tau_0 + \tau_1; \quad \tau = \bar{\tau}_0 + \bar{\tau}_1; \quad \tau_0 = \bar{\tau}_0 = \text{const};$$

$$\int_{t-\tau_1}^{t} p^m \, dt' = \bar{\tau}_1 \bar{p}^{-m} = \text{const} \qquad [3.2]$$

defines the time lag when the pressure is variable.

If p is constant, Equations [3.1] and [3.2] are reduced to the first relations we have written. But this time even for small variations of pressure the two equations remain fundamentally different. In fact, for a given time lag, Equation [3.1] assumes that the variation of the time lag depends on the pressure values during all the time lag; Equation [3.2] assumes an effect of the pressure values during only one part, τ_1, of the total time lag. From the discussion of Section 2, it would seem that a law of the type [3.1] should represent sufficiently well the behavior of a monopropellant; but for the bi-propellant case, the law [3.2] would be more representative of the actual phenomenon, τ_0 being related to the mixing delay, independent of the pressure variations. On the other hand we have explicitly observed that even the pressure values during the mixing delay can have an effect on the rest of the time lag because they contribute to the combustion in "conditioning" the propellants. To take this effect into account a more complicated formula than [3.1] or [3.2] would be required. But at this stage of the knowledge of these questions, it is felt that such a refinement would not be justified, and that only a general consideration of the effects of the time lag variation is required. For this reason, it was decided to discard even Equation [3.2], which involves three constants, and to select for the following developments the simpler Equation [3.1], which contains only two constants and allows easier mathematical treatments.

4 Equation of the Combustion Chamber

Before proceeding to the quantitative discussion of the combustion stability based on Equation [3.1], let us see the qualitative result of the variation of the time lag. Equation [3.1], or any other equation expressing the relation between time lag and pressure, shows that if the pressure is oscillatory, the time lag will also be an oscillating quantity around an average value. Now suppose for simplicity that the injection rate is constant. If the time lag is oscillating, it is immediately seen that when the time lag is decreasing the burning of the particles that were injected later will catch up with the burning of those injected earlier, and an increased rate of burning (with respect to the average) is the result. The opposite happens when the time lag is increasing. If now the increased or decreased rate of burning coincides with a pressure increase or decrease (which happens when the average time lag and the period of pressure oscillations are in a certain relation), then self-excited oscillations can exist and give rise to rough combustion, *even in the absence of any variation in the injection rate.*

Let us now write the equation expressing the mass balance in the combustion chamber. If the working pressure is rigorously constant and equal to $\bar{p}$, the time lag will be constantly equal to $\bar{\tau}$ and the injection rate at every instant will equal the burning rate and the exhaust rate. Let us call $\bar{m}$ this equilibrium flow rate. By the first approximate assumption on the time lag (Section 3), the propellants do not contribute to the chamber pressure until, after the time lag has elapsed, they are suddenly converted into gases at the final temperature. Neglecting the volume of the propellants during the time lag, these gases fill all the volume of the combustion chamber. The mass $\bar{M}_g$ of hot gases contained in the chamber at constant pressure $\bar{p}$ can then be computed. Now suppose a deviation from the equilibrium conditions, and assume that the pressure variations are sufficiently slow so that at every instant the pressure is uniform throughout the combustion chamber and equal to $p(t)$. If the temperature in the chamber is supposed independent of the pressure variations,[4] then the new values of the mass M_g and of the exhaust rate $\dot{m}_e$ will simply vary proportionally with p:

$$\frac{\dot{m}_e(t)}{\bar{\dot{m}}} = \frac{p(t)}{\bar{p}} = \frac{M_g(t)}{\bar{M}_g} \qquad [4.1]$$

If the burning rate in the interval of time dt is called $\dot{m}_b(t)$, the injection rate $\dot{m}_i(t)$, and if the time lag is $\tau(t)$, the mass burning during the interval dt must be equal to the mass injected during the interval $d(t - \tau)$, so that

$$\dot{m}_b\, dt = \dot{m}_i^{(\tau)}\, d(t - \tau), \text{ with } \dot{m}_b = \dot{m}_b(t);\ \dot{m}_i^{(\tau)} = \dot{m}_i(t - \tau) \qquad [4.2]$$

(For brevity of writing we have here made the convention that the superscript $^{(\tau)}$ means that the corresponding quantity has to be evaluated at time $t - \tau_1$). Now the balance of mass in the chamber is

$$\dot{m}_b\, dt = \dot{m}_e\, dt + d\, M_g$$

which can be written, using Equation [4.2]:

$$\frac{dM_g}{dt} + \dot{m}_e = \dot{m}_b = \left(1 - \frac{d\tau}{dt}\right)\dot{m}_i^{(\tau)} \qquad [4.3]$$

This can be put in nondimensional form dividing by $\bar{\dot{m}}$, using Equation [4.1] and introducing the fractional variations of pressure, injection rate, and burning rate with respect to the equilibrium values:

$$\varphi = \frac{p - \bar{p}}{\bar{p}};\quad \mu = \frac{\dot{m}_i - \bar{\dot{m}}}{\bar{\dot{m}}};\quad \mu_b = \frac{\dot{m}_b - \bar{\dot{m}}}{\bar{\dot{m}}} \qquad [4.4]$$

so that the mass balance equation becomes

$$\frac{\bar{M}_g}{\bar{\dot{m}}}\frac{d\varphi}{dt} + \varphi + 1 = \mu_b + 1 = \left(1 - \frac{d\tau}{dt}\right)(\mu^{(\tau)} + 1) \qquad [4.5]$$

Observe that $\bar{M}_g/\bar{\dot{m}}$ is nothing else than the gas residence time θ_g in the combustion chamber in equilibrium conditions. As the residence time before the transformation into hot gases is equal to the time lag, the total residence time of the propellants in the combustion chamber in steady operation is

$$\theta_t = \bar{\tau} + \theta_g \qquad [4.6]$$

The quantity θ_g has an essential role in the problems of combustion stability, which was disregarded by Gunder and Friant (1), but taken into account by Yachter

[4] The effects of pressure oscillations on the temperature will be considered in Section 11 to appear in the next issue.

(2) and especially by Summerfield (3) who used the expression

$$\theta_g = \frac{L^* c^*}{RT_g} = f^2(\gamma)\frac{L^*}{c^*}$$

in terms of the characteristic length and velocity and of the temperature of the product of combustion or the adiabatic index γ.

θ_g can be used to obtain a reduced time and a reduced time lag:

$$z = \frac{t}{\theta_g}, \qquad \delta = \frac{\bar{\tau}}{\theta_g} \ldots\ldots\ldots\ldots\ldots\ldots [4.7]$$

Coming back to Equation [4.5], let us find an explicit expression for $d\tau/dt$. Differentiating Equation [3.1] with respect to t, and assuming that p is a function only of the integration variable t' and not of the instantaneous value of τ (an assumption to be checked finally), we obtain

$$[p(t)]^n - [p(t-\tau)]^n \left(1 - \frac{d\tau}{dt}\right) = 0$$

that is, by Equation [4.4],

$$1 - \frac{d\tau}{dt} = \left[\frac{1+\varphi}{1+\varphi^{(\tau)}}\right]^n \cong 1 + n(\varphi - \varphi^{(\tau)}) \ldots [4.8]$$

where we have again used the superscript convention of Equation [4.2], the last step being allowed if we consider only small values of φ, and consequently small relative differences between τ and $\bar{\tau}$.

If this expression is introduced in Equation [4.5] and we assume that μ also is a small quantity, so that we can neglect the product $\mu\varphi$, the result is the equation

$$\frac{d\varphi}{dz} + \varphi = \mu_b = \mu^{(\delta)} + n(\varphi - \varphi^{(\delta)}) \ldots\ldots\ldots [4.9]$$

between the two variables φ (fractional variation of pressure), μ (fractional variation of injection rate), and the reduced time, z (Equation [4.7]), with the convention $\mu^{(\delta)} = \mu\ (z - \delta)$, and the same for $\varphi^{(\delta)}$.

Equation [4.9] is the fundamental equation of the combustion chamber. We see now that the time lag appears in this equation only through δ, which is related to the equilibrium value of the time lag; this means that φ and therefore p are independent of the instantaneous values of the time lag, so that the assumption introduced in the derivation of Equation [4.8] is justified (this is, however, only true for small values of φ).

5 Constant Injection Rate and Intrinsic Instability

The simplest case to which Equation [4.9] can be applied is when the injection rate is made independent of the pressure variations. This can be obtained using volumetric pumps or some other device (5) provided the compressibility of the propellants, or the elasticity of the tubing, or the presence of bubbles does not introduce an appreciable variation of volume downstream of the device. In this case μ is zero at every instant and Equation [4.9] is reduced to

$$\frac{d\varphi}{dz} + (1-n)\varphi + n\varphi^{(\delta)} = 0 \ldots\ldots\ldots\ldots [5.1]$$

This is not simply an ordinary differential equation, since it contains the values of the variable φ at two different instants;[5] with the consequence that, while to determine the solution of a first-order linear equation we need only a boundary condition at $z = 0$ (for instance, the value of φ); in the present case we need to know the values of φ in the complete interval of time from $z = -\delta$ to $z = 0$.

In order to find particular solutions of Equation [5.1], let us try the exponential $\varphi = \exp(\alpha z)$. Making the actual substitution we find that if the coefficient α satisfies the transcendental equation

$$\alpha + 1 - n + ne^{-\alpha\delta} = 0 \ldots\ldots\ldots\ldots [5.2]$$

then $\exp(\alpha z)$ is a solution of Equation [5.1]. If α is a real quantity, the discussion of Equation [5.2] gives the following results. For a fixed value of n, if δ is smaller than a certain δ_1 (which depends on n), there are two roots $\alpha < 0$. On the other hand, if $n > 1$ and $\delta >$ than a certain δ_2 (depending on n), there are two roots $\alpha > 0$. In the first case the exponential dies out with the time, but in the second case φ will increase exponentially with time, and the solution is unstable. We see that the prerequisites for this type of aperiodic instability are $n > 1$, $\delta > \delta_2$, so that if $n \leq 1$ (as appears to be likely) the exponential solutions, when they exist, are always stable. When $n = 0$, $\alpha = -1$ represents the trivial case in which there is no influence of the time lag.

Let us consider now the more interesting case of complex $\alpha = \lambda + i\omega$. Upon substitution, Equation (5.2) splits into the two real equations

$$\left.\begin{aligned} \lambda + 1 - n + ne^{-\lambda\delta}\cos\omega\delta &= 0 \\ \omega - ne^{-\lambda\delta}\sin\omega\delta &= 0 \end{aligned}\right\} \ldots\ldots\ldots [5.3]$$

Suppose we know a couple of values λ, ω satisfying Equation [5.3] for given n, δ. Then also the couple λ, $-\omega$ satisfies the equation, which means that any linear combination of the two conjugate quantities $\exp(\alpha z)$ and $\exp(\bar{\alpha} z)$, or—remaining in the real field—any linear combination of $e^{\lambda z}\sin(\omega z)$ and $e^{\lambda z}\cos(\omega z)$ satisfies the equation. This combination represents a real oscillatory solution φ with arbitrary phase, oscillating with a reduced angular frequency ω with respect to the reduced time z, or an angular frequency $\Omega = \omega/\theta_g$ with respect to t. The period is $T = 2\pi/\Omega$ and the frequency, the inverse of this quantity. The quantity $\omega\delta$ which appears in Equation [5.3] has the following simple interpretation; because of Equation [4.7]:

$$\frac{\omega\delta}{2\pi} = \frac{\Omega\bar{\tau}}{2\pi} = \frac{\bar{\tau}}{T} \ldots\ldots\ldots\ldots [5.4]$$

so that $\omega\delta$, measured in revolutions, represents the ratio between the time lag and the period of the oscillations.

[5] This kind of equation is sometimes designated as hysterodifferential equation. The discussion of a particular case is contained in (6); some methods of solution are discussed in (1).

The amplitude of the oscillation varies with time following the factor $\exp(\lambda z)$; if $\lambda < 0$, the amplitude decreases and the solution is stable; if $\lambda > 0$, the amplitude increases exponentially and the solution is unstable. The neutral case, $\lambda = 0$ represents, therefore, the limiting case between stable and unstable solutions, when the amplitude remains constant.

From the two Equations [5.3], we find

$$\lambda\delta + (1 - n)\delta = -\frac{\omega\delta}{\tan \omega\delta}$$

Introducing the value of $\lambda\delta$ obtained from this into the second Equation [5.3], we have the following equation:

$$f(\delta, n) = n\delta e^{(1-n)\delta} = \frac{\omega\delta}{\sin \omega\delta} e^{-\frac{\omega\delta}{\tan \omega\delta}} = h(\omega\delta)$$

which can be solved graphically, for any n, δ, plotting $h(\omega\delta)$, as we have done on the right side of Fig. 1, and cutting the curves with a horizontal line of ordinate $f(\delta, n)$. This quantity is shown as a function of δ on the left side of Fig. 1 for three different values of n. The value of λ can then be found using, for instance, the second Equation [5.3]:

$$e^{\lambda\delta} = n\delta \frac{\sin \omega\delta}{\omega\delta} = \frac{n\delta}{k(\omega\delta)}$$

The function $k(\omega\delta)$ is plotted on the right-hand side of Fig. 1, and $n\delta$ is shown on the left-hand side. We see that the solution is stable, neutral, or unstable if $n\delta \lessgtr k(\omega\delta)$. The examination of Fig. 1 shows that for every couple of values n, δ there is an infinite number of roots $\omega\delta$, corresponding to an infinite series of increasing ω, the first root being contained between 0 and π, the second between 2π and 3π, etc. There is less than one-half oscillation in the duration of the time lag for the first, or fundamental, mode; but more than one for all the other higher frequency modes. For small δ or large n, the first root can become imaginary, but the higher frequency modes exist always.

Considering first the case $n = 1$, we see that as $f(1, \delta)$ coincides with $n\delta = \delta$ the solution will be stable, neutral or unstable if $k \gtrless h = \delta$. The solution is therefore stable when $\omega\delta$ is contained in the first quadrant, unstable when it is in the second quadrant. Hence, the fundamental mode is stable or unstable if $\delta \lessgtr \delta_* = \frac{\pi}{2}$, the first higher frequency mode is stable or unstable if $\delta \lessgtr 5\frac{\pi}{2}$, etc. When δ increases from small values the first solution to become unstable is the fundamental mode. When this one is unstable, the fact that the others are still stable or already unstable has but little importance. We conclude that the examination of the behavior of the solutions for $0 < \omega\delta < \pi$ gives in this case all the required information about stability.

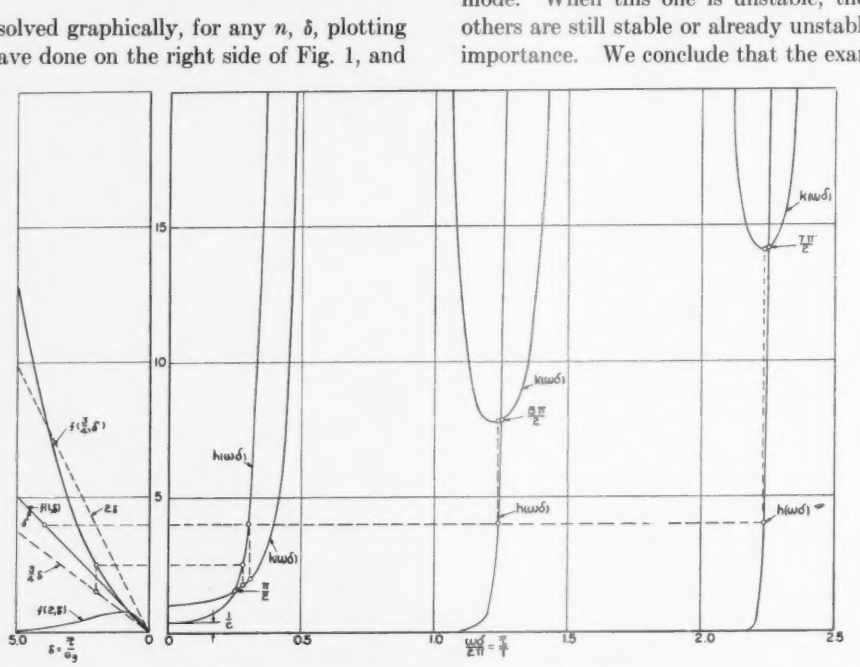

FIG. 1. GRAPHICAL SOLUTION OF EQUATION [5.3]

The case $n < 1$ is illustrated in Fig. 1 for $n = 0.75$. In this case, $n\delta < f(n, \delta)$, so that the stability can exist also when $h > k$, and the stability conditions are improved. Here again, for δ small, all the modes are stable; after a certain critical δ_* larger than for $n = 1$, the fundamental mode becomes unstable; and with increasing δ other successive modes become unstable; and the behavior for n not too small, is analogous to that previously discussed. The quantitative evaluation of δ_* will be deduced in the following.

Finally, when $n > 1$ (as in the case $n = 2$ of Fig. 1) $n\delta > f(n, \delta)$ and instability can exist with $h < k$; which means that the range of stability is reduced, and δ_* decreases with increasing n. The other qualitative conclusions are the same as before.

A general conclusion from this discussion is that there are always an infinite number of solutions of Equation [5.3] and therefore of Equation [5.1]. A linear combination of these solutions, with the eventual use of the exponential solutions corresponding to Equation [5.2] with real α, solves the problem of finding the solution of Equation [5.1] with a quite general shape of the prescribed initial distribution of $\varphi(z)$ between $-\delta$ and 0; and the corresponding solution is stable or unstable following if the reduced time lag δ is smaller or larger than a certain critical value δ_*.

The kind of instability discussed in this section can be denominated "intrinsic" since it depends only on the conditions inside the rocket combustion chamber, and not on variations of the injection rate. The value of δ_* and of the corresponding ω_* can be deduced directly from Equation [5.3], putting $\lambda = 0$. We obtain:

$$\left.\begin{aligned} \cos(\omega_*\delta_*) &= -\frac{1-n}{n}; \quad \omega_* = n\sin(\omega_*\delta_*) \\ &= \sqrt{n^2-(1-n)^2} = \sqrt{2n-1}; \\ \delta_* &= \frac{\cos^{-1}\left(-\dfrac{1-n}{n}\right)}{\sqrt{2n-1}} \\ &= \frac{1}{\sqrt{2n-1}}\left(\pi - \tan^{-1}\frac{\sqrt{2n-1}}{1-n}\right) \end{aligned}\right\} \quad [5.5]$$

The corresponding values are plotted against n in Fig. 2.

Real values are obtained only when $n > 0.5$, which means that below 0.5 the solutions are always stable. The intrinsic instability can therefore exist only if $n > 0.5$.

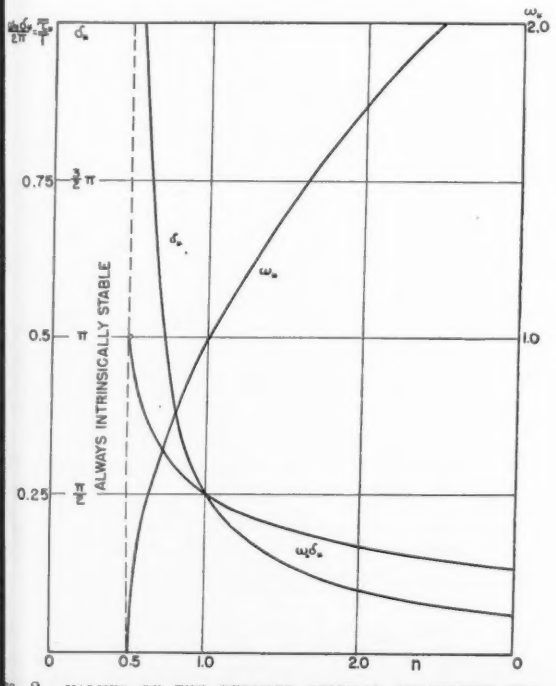

FIG. 2. VALUES OF THE REDUCED CRITICAL QUANTITIES FOR INTRINSIC INSTABILITY AT VARIOUS PRESSURE EXPONENT n

Let us finally observe that if, instead of Equation [3.1] we select Equation [3.2] to represent the pressure dependence of the time lag, the results are the same provided m replaces n and $\bar{\tau}_1$ replaces $\bar{\tau}$, that part τ_0 of the total time lag which does not vary with pressure being in this case without influence on the stability.

6 The Feeding System

The assumption of constant injection rate used in the preceding section does not correspond generally to the real operating conditions of a rocket motor. The oscillations of the chamber pressure are in fact responsible, with the ordinary feeding systems, for oscillations in the injection rate which have in turn an effect on the pressure oscillations. This may be true even when using devices designed to produce a constant mass flow, placed at a certain section of the tubing; since variations of the mass flow may still occur between this section and the injector if some intermediary part has an elastic behavior (gas or vapor bubbles, compressibility of the propellant, elasticity of the walls). We exclude from our analysis the case of a feeding system with centrifugal pumps, whose response to chamber pressure variations cannot be defined in a general way, especially when some kind of automatic control is used. In the last hypothesis, oscillations in the automatic control system can arise that may interfere with the operation of the combustion chamber, in which case the analysis becomes very involved.

To confine our considerations to simple and general cases, let us consider two types of feeding system: (*a*) A constant rate supply system, connected with the injector by lines of a certain length and with an elastic behavior; and (*b*) a constant pressure supply system, again connected with the injector by elastic lines. For the moment, we will consider a monopropellant system to avoid complications. In Section 10 (Part 2) we shall consider separately the effects of a bipropellant combination.

Case (*a*): Fig. 3 shows this type of feeding system schematically. When the flow is steady, neglecting the friction and other eventual losses,[6] we have

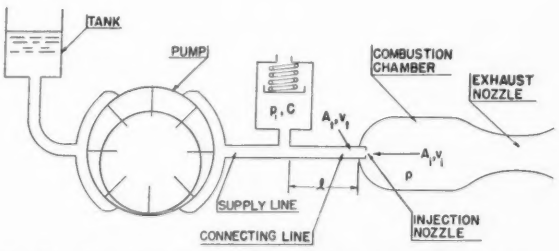

FIG. 3. SCHEMATIC REPRESENTATION OF A CONSTANT RATE FEEDING SYSTEM WITH ELASTICITY IN THE LINES

[6] These can be taken implicitly into account in this case and in some other cases by using instead of A_i an equivalent area, such that the Equation [6.1] is still satisfied.

$$\bar{p}_1 - \bar{p} = \Delta p = \frac{\bar{\dot{m}}^2}{2\rho A_i^2} \quad [6.1]$$

where A_i represents the area of the jets from the injector, that is, the orifice area corrected for the contraction coefficient. Under the pressure $\bar{p}_1$ the capacitance, C, takes a constant volume so that the mass flow is the same before and after the capacitance. When the flow is unsteady the pressure will vary and also the capacitance C; for small variations of pressure C will vary linearly with p_1, and we can define a coefficient

$$\chi = \frac{dC}{dp_1} \quad [6.2]$$

In the supply line, the mass flow is constantly $\bar{\dot{m}}$; the continuity equation then gives for the mass flow in the connecting line (injection rate):

$$\dot{m} - \bar{\dot{m}} = -\rho \frac{dC}{dt} = -\rho\chi \frac{dp_1}{dt} \quad [6.3]$$

Equating the work performed per unit time by the instantaneous pressure drop $p_1 - p$ to the rate of increase of the kinetic energy in the connecting line, plus the kinetic energy produced in the jets per unit time (neglecting the small variations of kinetic energy between the supply line and the connecting line, and in the capacitance itself) we obtain:

$$\frac{\dot{m}}{\rho}(p_1 - p) = \frac{1}{2}\dot{m}v_i^2 + \frac{M_l}{2}\frac{d(v_l^2)}{dt} \quad [6.4]$$

with

$$\dot{m} = \rho A_l v_l = \rho A_i v_i; \quad M_l = \rho l A_l; \quad [6.5]$$

where M_l represents the fluid mass in the connecting line.[7]

Equation [6.4] can be written

$$p_1 - p = \frac{\dot{m}^2}{2\rho A_i^2} + \frac{l}{A_l}\frac{d\dot{m}}{dt} \quad [6.6]$$

Subtracting Equation [6.1] from Equation [6.6] we obtain:

$$p_1 - \bar{p}_1 - (p - \bar{p}) = \frac{1}{\rho A_i^2}\frac{\dot{m}^2 - \bar{\dot{m}}^2}{2} + \frac{l}{A_l}\frac{d\dot{m}}{dt}$$
$$\cong \frac{\bar{\dot{m}}}{\rho A_i^2}(\dot{m} - \bar{\dot{m}}) + \frac{l}{A_l}\frac{d\dot{m}}{dt}$$

the last step being justified for small variations of mass flow. Dividing by $2\Delta p$; introducing the reduced time z (Equation [4.7]), the fractional variations defined by Equation [4.4], and the three quantities:

$$\psi = \frac{p_1 - \bar{p}_1}{2\Delta p}, \quad J = \frac{l\bar{m}}{2\Delta p\, A_l \theta_g}, \quad P = \frac{\bar{p}}{2\Delta p} \quad [6.7]$$

the preceding equation becomes:

$$\psi - P\varphi = \mu + J\frac{d\mu}{dz} \quad [6.8]$$

[7] When the connecting line is composed of pieces of different length and areas, and we select a representative area A_l, with the corresponding velocity v_l, M_l is defined by: $M_l(v_l^2/2) = \sum M_k (v_k^2/2)$; and l by the second Equation [6.5].

Using the same variables, Equation [6.3] becomes

$$\mu = -E\frac{d\psi}{dz} \quad [6.9]$$

where the elasticity parameter

$$E = \frac{2\rho\chi\Delta p}{\bar{\dot{m}}\,\theta_g} \quad [6.10]$$

includes all the effects of the elasticity of the system, and can be interpreted as the double of the ratio between the increase in volume of the system under the pressure Δp and the volume injected during the gas residence time.

Equations [6.8] and [6.9] are sufficient to describe the behavior of the feeding system in case (a). They depend only on the three constants, P, J, E. The meaning of E has just been discussed; the pressure drop parameter P has an immediate interpretation as a measure of the relative value of the pressure drop through the injector; and the inertia parameter J, which includes all the effects of the inertia of the propellant in the lines, can also be written:

$$J = \frac{\frac{1}{2}M_l v_l^2}{\Delta p \frac{\bar{m}}{\rho}\cdot\theta_g} = \frac{M_l}{\bar{\dot{m}}\theta_g}\left(\frac{v_l}{v_i}\right)^2$$

so that it represents the ratio between the kinetic energy of the propellant in the connecting line and the work performed by the pressure drop during the gas residence time, or (what is the same) the kinetic energy produced in the injected propellant during the gas residence time; everything being computed under steady conditions. This definition of J remains true for composite connecting lines.

Case (b): This type is shown schematically in Fig. 4. Again neglecting the friction in the lines and the

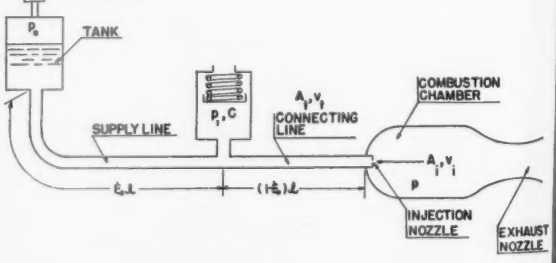

FIG. 4. SCHEMATIC REPRESENTATION OF A CONSTANT PRESSURE FEEDING SYSTEM WITH ELASTICITY IN THE LINES

variation of kinetic energy from the supply to the connecting line, as well as the kinetic energies in the capacitance and in the tank, we have in steady conditions:

$$\bar{\dot{m}}_1 = \bar{\dot{m}}; \quad p_0 - \bar{p}_1 = 0; \quad p_0 - \bar{p} = \frac{\bar{\dot{m}}^2}{2\rho A_i^2} = \Delta p \quad [6.11]$$

and in nonsteady flow the two equations, corresponding to Equation [6.6]:

$$p_0 - p_1 = \frac{\xi l}{A_t}\frac{d\dot{m}_1}{dt}; \quad p_1 - p = \frac{\dot{m}^2}{2\rho A_t^2} + \frac{(1-\xi)l}{A_t}\frac{d\dot{m}}{dt}, \ldots [6.12]$$

where $\dot{m}_1$ and $\dot{m}$ represent the mass flows in the supply and in the connecting line, whose difference satisfies to:

$$\dot{m}_1 - \dot{m} = \rho\chi\frac{dp_1}{dt} \ldots\ldots\ldots\ldots\ldots [6.13]$$

similar to Equation [6.3]; and where the pressure p_0 generated by a regulated gas pressure is assumed constant.

Subtracting Equations [6.11] from [6.12], dividing by $2\Delta p$, introducing the quantities defined by Equations [6.7] and [6.10] and the fractional variation of mass flow from the tank

$$\mu_1 = \frac{\dot{m}_1 - \bar{\dot{m}}}{\bar{\dot{m}}},$$

Equations [6.12] and [6.13] are transformed into

$$\left.\begin{aligned} \psi &= -\xi J\frac{d\mu_1}{dz};\\ \psi - P\varphi &= \mu + (1-\xi)J\frac{d\mu}{dz};\\ \mu_1 - \mu &= E\frac{d\psi}{dz} \end{aligned}\right\} \ldots\ldots\ldots\ldots\ldots [6.14]$$

which are sufficient to describe the behavior of the feeding system in case (*b*), and again contain only the three constants P, J, E whose meaning is the same as in case (*a*); plus the supplementary parameter ξ.

7 Limits of Stability with Constant Rate Supply (*Case (a)*)

Equations [4.9], [6.8], and [6.9] are sufficient for the description of the behavior of the three unknown functions $\varphi(z)$, $\mu(z)$, $\psi(z)$ when proper initial conditions are given. In fact, they could be reduced by elimination to a single third-order hystero-differential equation in, say, $\psi(z)$ alone, an equation that could be treated in a way similar to that of Section 5. Instead of actually carrying out the elimination, we can write the equation corresponding to Equation [5.2] by trying directly in the system a particular solution of the type:

$$\frac{\varphi}{A} = \frac{\mu}{B} = \frac{\psi}{C} = e^{\alpha z} \ldots\ldots\ldots\ldots\ldots [7.1]$$

α, A, B, C being complex constants. Eliminating the common factor $\exp(\alpha z)$, we see that Equation [7.1] represents a solution of our system if the three homogeneous, first-degree equations in A, B, C

$$\begin{aligned} (\alpha + 1 - n + ne^{-\alpha\delta})A - e^{-\alpha\delta}B &= 0\\ PA + (1 + J\alpha)B - C &= 0\\ B + E\alpha C &= 0 \end{aligned}$$

are simultaneously satisfied, which happens if, and only if, the determinant of the coefficients vanishes, that is, if

$$\begin{vmatrix} \alpha + 1 - n + ne^{-\alpha\delta} & -e^{-\alpha\delta} & 0\\ P & 1 + J\alpha & -1\\ 0 & 1 & E\alpha \end{vmatrix} = 0$$

Expanding the determinant we find that if α satisfies the equation

$$(1 + E\alpha + JE\alpha^2)(\alpha + 1 - n + ne^{-\alpha\delta}) + PE\alpha e^{-\alpha\delta} = 0 \quad \ldots. [7.2]$$

then Equation [7.1] represents a possible solution of the system. Equation [7.2] is reduced to Equation [5.2] when $E = 0$, and in general it can be discussed in the same way; also in this case real roots can exist, but the most interesting are the complex conjugate roots $\alpha = \lambda \pm i\omega$, which correspond to oscillatory solutions, stable or unstable following if $\lambda \lesseqgtr 0$. Again, an infinite number of roots are possible, corresponding to increasing frequencies and dampings; and again the solution corresponding to the first root will be the first to become unstable when δ increases from small values and reaches a value δ_*, ω taking a certain value ω_*. The determination of these critical values can be performed directly from Equation [7.2], upon substitution of $\alpha = i\omega_*$. We obtain:

$$\begin{aligned} &(1 - n + i\omega_*)(1 - JE\omega_*^2 + iE\omega_*) =\\ &\quad -[n(1 - JE\omega_*^2) + i(n + P)E\omega_*]e^{-i\omega_*\delta_*} \end{aligned}$$

Equating the moduli and the arguments of the two sides of this equation and considering that for the first root $\omega_*\delta_*$ must be $<2\pi$, we have

$$\left.\begin{aligned} &[(1-n)^2 + \omega_*^2][(1 - JE\omega_*^2)^2 + E^2\omega_*^2] =\\ &\qquad n^2(1 - JE\omega_*^2)^2 + (n + P)^2E^2\omega_*^2\\ &\tan^{-1}\frac{\omega_*}{1-n} + \tan^{-1}\frac{E\omega_*}{1 - JE\omega_*^2} =\\ &\qquad \pi + \tan^{-1}\frac{n+P}{n}\frac{E\omega_*}{1 - JE\omega_*^2} - \omega_*\delta_* \end{aligned}\right\} \ldots\ldots [7.3]$$

The first of these equations is a third-degree equation in ω_*^2; if ω_*^2 is deduced from here in terms of n, P, J, E, and introduced in the second Equation [7.3], this would give the value of δ_* in terms of the same four quantities, and we would obtain the critical value of the time lag and of the angular frequency for any given combination of the constants. But the solution of the system is simpler in the following way. Solve the first Equation [7.3] for $1 - JE\omega_*^2$:

$$\begin{aligned} 1 - JE\omega_*^2 &= \pm E\omega_*\sqrt{\frac{(n+P)^2 - \omega_*^2 - (1-n)^2}{\omega_*^2 + (1-n)^2 - n^2}} =\\ &\pm E\omega_* \cdot \frac{1}{\Phi} \quad \ldots [7.4] \end{aligned}$$

(Φ representing for brevity the inverse of the radical), and replace this value in the second Equation [7.3]; solving for δ_* we obtain:

$$\delta_* = \frac{1}{\omega_*}\left[\pi - \tan^{-1}\frac{\omega_*}{1-n} \pm \left(\tan^{-1}\frac{n+P}{n}\Phi - \tan^{-1}\Phi\right)\right] \ldots\ldots\ldots\ldots [7.5]$$

which shows that the relation between δ_* and ω_* depends only on the values of n and P, but not on J and E. Figs. 5, 6, 7 show this relation for $n = 0$, 0.5, and 1[8] computed from Equation [7.5] for various values of $\Delta p/\bar{p} = 1/2P$. On each curve there are two values of the ordinate for a given value of ω_*, corresponding to the two signs of Equation [7.5]. The reality of the radical Φ involves the inequality

[8] These values have been selected only as examples; the actual values of n have to be derived experimentally, and might be even larger than unity.

$$2n - 1 = n^2 - (1 - n)^2 < \omega_*^2 < (n + P)^2 - (1 - n)^2 = (P + 1)(2n + P - 1)$$

so that the curves are all contained between a minimum and a maximum of the abscissa. The minimum is different from zero only when $n > 0.5$; when $n \leq 0.5$ the curves extend up to the ordinate axis where the critical time lag goes to infinity. In the last case, a limitation exists also for P since, in order to have a positive value of the maximum ω_*^2, the inequality $P > 1 - 2n$ must be satisfied. When, on the contrary, $P \leq 1 - 2n$, no real value of ω_* and δ_* can be found, and the stability of the combustion is assured no matter what values δ, E, J take. When $n = 0$ this condition coincides with the result of (1) and (3) which show that for their particular feeding system, the combustion is always stable when $\Delta p/\bar{p} > 0.5$. We see now

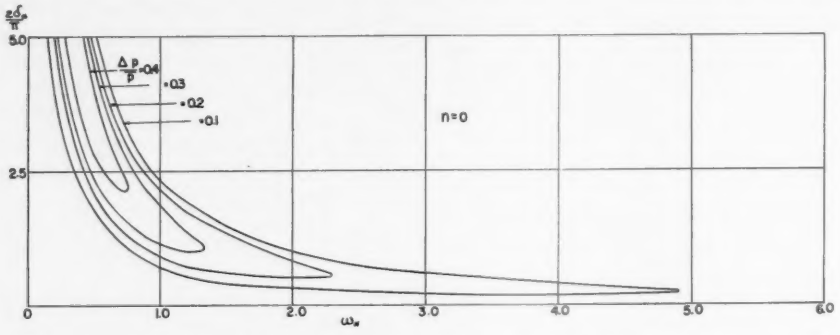

FIG. 5. GENERAL RELATION BETWEEN REDUCED CRITICAL TIME LAG AND REDUCED ANGULAR FREQUENCY FOR DIFFERENT RELATIVE PRESSURE DROPS WITH $n = 0$

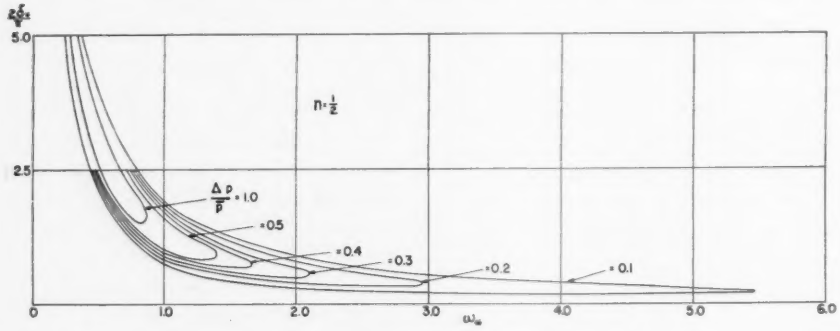

FIG. 6. GENERAL RELATION BETWEEN REDUCED CRITICAL TIME LAG AND REDUCED ANGULAR FREQUENCY FOR DIFFERENT RELATIVE PRESSURE DROPS WITH $n = 1/2$

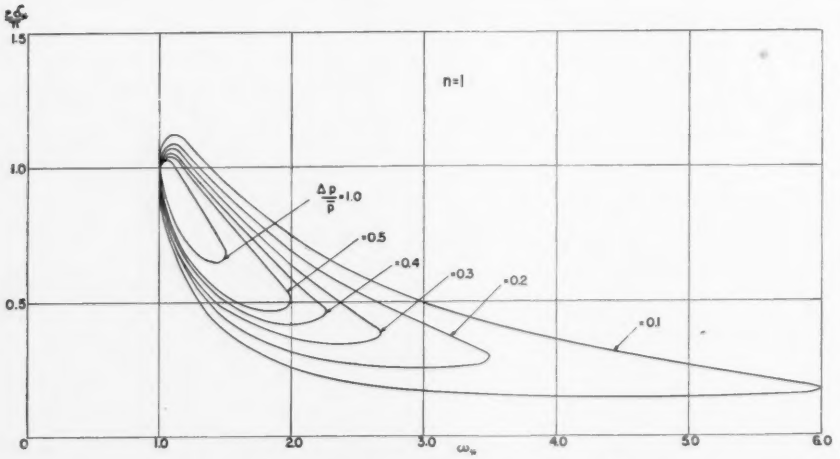

FIG. 7. GENERAL RELATION BETWEEN REDUCED CRITICAL TIME LAG AND REDUCED ANGULAR FREQUENCY FOR DIFFERENT RELATIVE PRESSURE DROPS WITH $n = 1$

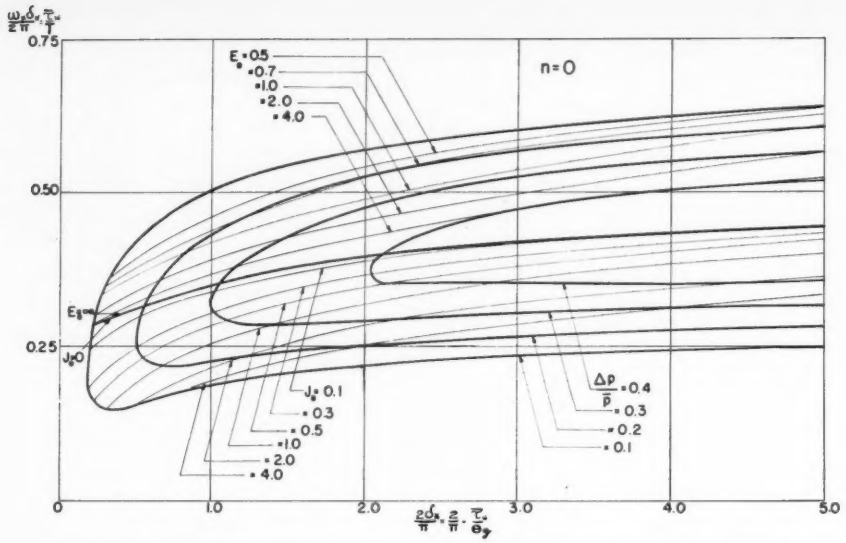

FIG. 8. GENERAL RELATION BETWEEN REDUCED CRITICAL TIME LAG AND RATIO TIME LAG/PERIOD OF OSCILLATIONS FOR DIFFERENT PRESSURE DROPS WITH $n = 0$. [VALUES E_0 OF THE ELASTICITY PARAMETER (FOR VANISHING INERTIA PARAMETER) FOR A CONSTANT RATE SUPPLY SYSTEM, AND VALUES J_0 OF THE INERTIA PARAMETER (FOR VANISHING ELASTICITY PARAMETER) FOR A CONSTANT PRESSURE SUPPLY SYSTEM]

that the possibility of assuring an unconditioned stability through an increase in Δp exists only when $n < 0.5$; and that the necessary increase in Δp becomes more and more important when n approaches 0.5; until for $n > 0.5$ even an infinite increase of Δp may not be sufficient to produce stability. Remembering the results of Section 5, we recognize that this happens when the operation can be intrinsically unstable, in which case it is not possible to obtain stability by changes in the parameters of the feeding system.

In Figs. 8, 9, and 10 we have plotted for $n = 0$, 0.5, 1 the values of $\omega_* \delta_* / 2\pi = \bar{\tau}_* / T_*$ against δ_*. Here again the curves $\Delta p/\bar{p} =$ constant are closed curves if $n > 0.5$; while they extend to infinite values of δ_* if $n \leq 0.5$. When $n > 0.5$ the points corresponding to the minimum value of ω_* (which makes $\Phi = 0$) have the co-ordinates

$$\left(\frac{\bar{\tau}_*}{T_*}\right)_{\Phi=0} = \frac{1}{2} - \frac{1}{2\pi} \tan^{-1} \sqrt{\left(\frac{n}{n-1}\right)^2 - 1};$$

$$(\delta_*)_{\Phi=0} = \frac{2\pi - \tan^{-1} \sqrt{\left(\frac{n}{n-1}\right)^2 - 1}}{\sqrt{2n-1}}$$

independent of P, and all the curves pass through the same point. When $n = 0.5$ this point goes to $\delta_* = \infty$, and becomes imaginary when $n < 0.5$.

For all values of n the co-ordinates of the points corresponding to the maximum value of ω_* (which makes $\Phi = \infty$) are

$$\left(\frac{\bar{\tau}_*}{T_*}\right)_{\Phi=\infty} = \frac{1}{2} - \frac{1}{2\pi} \tan^{-1} \sqrt{\left(\frac{n+P}{1-n}\right)^2 - 1};$$

$$(\delta_*)_{\Phi=\infty} = \frac{\pi - \tan^{-1} \sqrt{\left(\frac{n+P}{1-n}\right)^2 - 1}}{\sqrt{(n+P)^2 - (1-n)^2}}$$

The curve connecting these points for various P separates the values corresponding to the upper sign of Equations [7.4], [7.5] (above the curve) from those corresponding to the lower sign (below the curve). For $n = 1$ the curve becomes an horizontal line.

At every point of a given curve $\Delta p/\bar{p} =$ const, ω_* and Φ take definite values. The selected point represents the critical conditions with a given feeding system provided the values of E and J of this system satisfy Equation [7.4]. The simplest case is when the length of the connecting line is negligible and $J = 0$. Then, from Equation [7.4],

$$E_{J=0} = E_0 = \pm \frac{\Phi}{\omega_*} \quad \ldots\ldots\ldots\ldots\ldots\ldots [7.6]$$

But by its definition (Equation [6.10]), E must be positive, so that in this case only the upper portions of the curves have a physical meaning. The point $\Phi = 0$ corresponds therefore to $E_0 = 0$, and the line $\Phi = \infty$ to $E_0 = \infty$. Lines of equal E_0 have been drawn in Figs. 8, 9, and 10. When $n \leq 0.5$ the point $\Phi = 0$ is imaginary, which means that at $E_0 = 0$ the conditions are always stable (in accordance with the results of Section 5). In the case $n < 0.5$, Equation [7.6] shows that $E_0 = \infty$ both when $\Phi = \infty$ and when $\omega_* = 0$ ($\delta_* = \infty$) so that if we move in the clockwise direction on the curves of, for instance, Fig. 8 starting from the line $E_0 = \infty$, E_0 will first decrease, reach a minimum value $E_{0\min}$, and then increase again. The combustion is stable for all δ's when $E_0 < E_{0\min}$; as soon as $E_0 > E_{0\min}$ the combustion becomes suddenly unstable if δ is larger than the value of δ_* corresponding to $E_{0\min}$; for $E_0 > E_{0\min}$ there are on the curves two points corresponding to the same value of E_0. The one contained

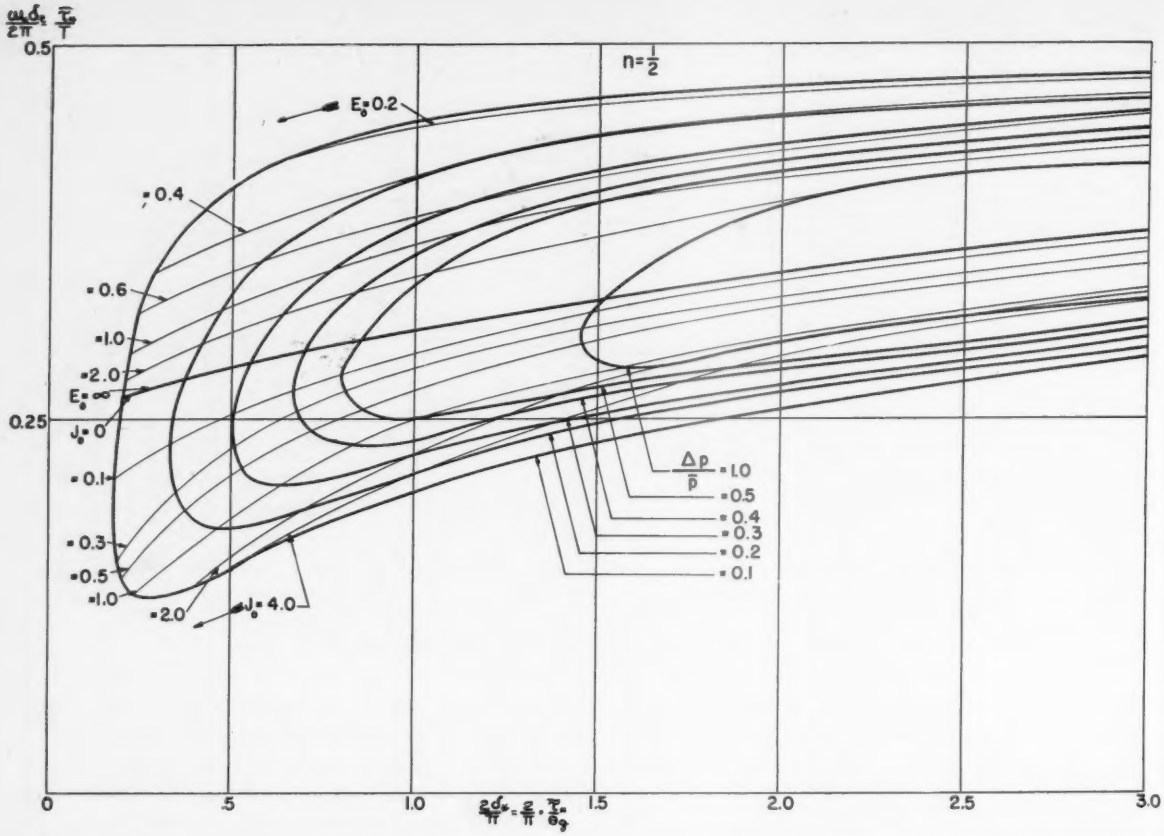

FIG. 9. GENERAL RELATION BETWEEN REDUCED CRITICAL TIME LAG AND RATIO TIME LAG/PERIOD OF OSCILLATIONS FOR DIFFERENT PRESSURE DROPS WITH $n = 1/2$

in the portion of the curve between $E_0 = \infty$ and $E_0 = E_{0\min}$ has the smaller δ_* and therefore is the first to become unstable, and the only one of practical importance. When n increases the value of δ_* at which $E_0 = E_{0\min}$ increases, until it reaches infinity when $n = 0.5$, still with a finite value of $E_0 = 1/\sqrt{P(P+1)}$; as soon as $n > 0.5$ the curves become closed and at the value of δ_* corresponding to $\Phi = 0$ (which decreases from infinity with increasing n) we have $E_0 = 0$. For $n > 0.5$, therefore, instability exists even with $E_0 = 0$ if δ is larger than the corresponding δ_*. From Fig. 10 we see that in this case for small values of E_0, δ_* increases slightly and the stability is improved; a further increase of E_0, however, makes δ_* drop again, and the system becomes less stable. This is true for all the values $n > 0.5$.

In the general case $J \neq 0$, Equation [7.4] can be written:

$$\frac{1}{E} = \frac{1}{E_0} + J\omega_*{}^2,$$

E_0 now being only the mathematical expression defined by Equation [7.6], without any physical correspondence, so that also negative values are allowed. The point $E = 0$ coincides with $E_0 = 0$ ($\Phi = 0$), when this point exists, that is when $n > 0.5$; on the other hand, when $n < 0.5$ and $\omega_* = 0 (\delta_* = \infty)$, E is still infinity like E_0, no matter what is the value of J. However, $E = \infty$ is also obtained, for all values of n, when

$$J = -\frac{1}{E_0\omega_*{}^2} \qquad [7.7]$$

and as J must be positive, it is obtained for negative E_0, below the line $E_0 = \infty$. For $n < 0.5$, between the two infinite values of E there is a minimum, smaller than $E_{0\min}$ but still positive, and again $E = 0$ gives certain stability. When E is larger than the minimum there are two corresponding values of δ_*, of which only the smaller has an actual interest. In the corresponding region when $n < 0.5$, and everywhere when $n > 0.5$, the effect of an increase of J is to displace the critical point in the counterclockwise direction on the curves of Figs. 8, 9, and 10; and therefore an increase or a decrease of δ_* (with a better or worse condition of stability) may follow, depending on the location of the point on the curve. However, the maximum and the minimum possible values of δ_* remain unchanged, and depend only on n and P.

8 Limits of Stability with Constant Pressure Supply (*Case (b)*)

This case is described by the four Equations [4.9], [6.14]. Here again, a process of elimination would lead to a single fourth-order hystero-differential equa-

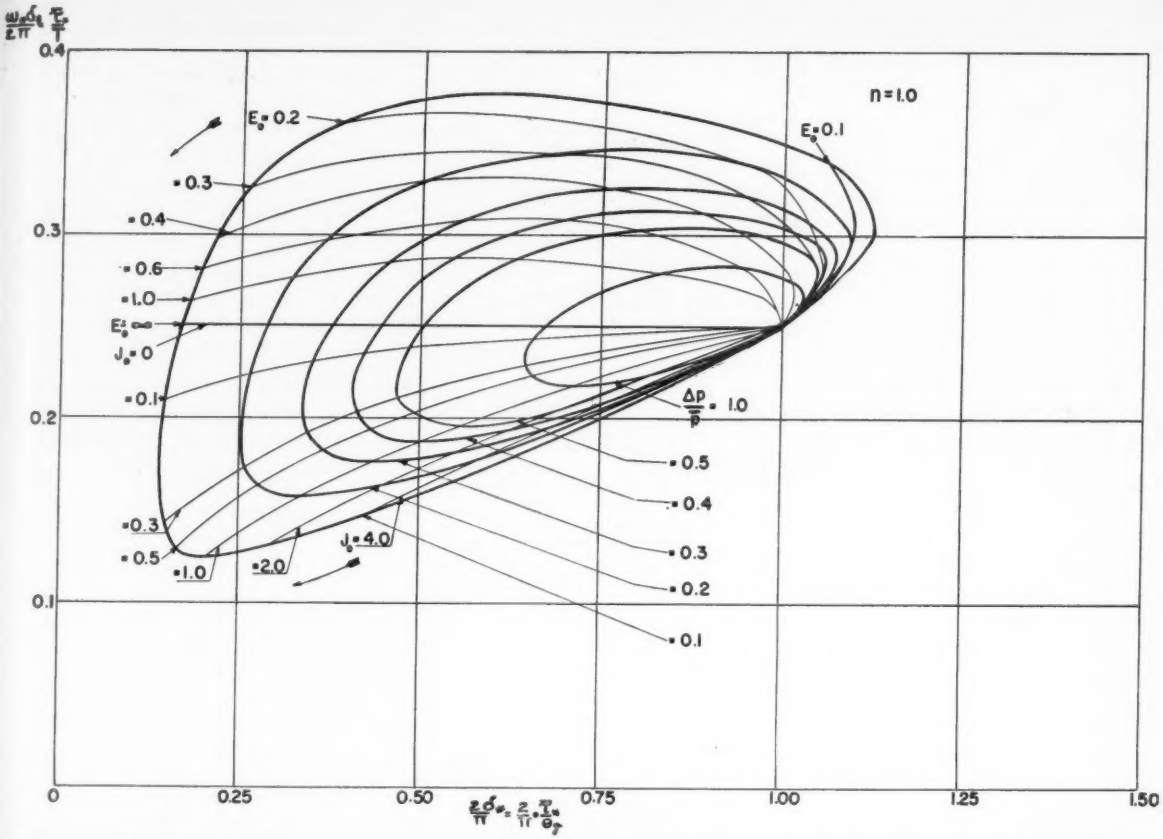

FIG. 10. GENERAL RELATION BETWEEN REDUCED CRITICAL TIME LAG AND RATIO TIME LAG/PERIOD OF OSCILLATIONS FOR DIFFERENT PRESSURE DROPS WITH $n = 1$

tion in, say, $\mu_1(z)$, which is reduced to a third-order equation when $\xi = 1$ or when $\xi = 0$. If the concentrated variable capacitance of Fig. 4 is assumed to represent the diffused elasticity of the line and the enclosed propellant, the proper location of it would be in the center of the line, that is, $\xi = 0.5$. However, we have not developed this case, and we have discussed only the case $\xi = 1$ because the corresponding formulas can be simply discussed using the treatment of Section 7 (the case $\xi = 0$ is a trivial case in which the elasticity has no effect at all on the system; and can be included in the $\xi = 1$ case assuming $E = 0$).

Using, with $\xi = 1$, the same technique of Section 7, we find that if the four unknown functions are assumed to vary proportionally to $\exp(\alpha z)$, α must be such that the determinant

$$\begin{vmatrix} \alpha + 1 - n + ne^{-\alpha\delta} & -e^{-\alpha\delta} & 0 & 0 \\ P & 1 & 0 & -1 \\ 0 & 1 & -1 & E\alpha \\ 0 & 0 & J\alpha & 1 \end{vmatrix}$$

has zero value.

Developing the determinant we obtain the equation

$$(1 + J\alpha + JE\alpha^2)(\alpha + 1 - n + ne^{-\alpha\delta}) + P(1 + JE\alpha^2)e^{-\alpha\delta} = 0$$

whose discussion is conducted in the same fashion as for Equations [5.2] and [7.2], and gives analogous results. If we are interested only in the limit of stability (when the fundamental mode becomes unstable) we substitute again $\alpha = i\omega_*$, and the preceding equation gives

$$(1 - n + i\omega_*)(1 - JE\omega_*^2 + iJ\omega_*) = -[(n + P)(1 - JE\omega_*^2) + inJ\omega_*]e^{-i\omega_*\delta_*} \quad \ldots [8.1]$$

Equating the moduli and the arguments we obtain:

$$\left.\begin{aligned} [(1-n)^2 + \omega_*^2]\,[(1 - JE\omega_*^2)^2 + J^2\omega_*^2] &= \\ (n+P)^2(1 - JE\omega_*^2)^2 + n^2J^2\omega_*^2 & \\ \tan^{-1}\frac{\omega_*}{1-n} + \tan^{-1}\frac{J\omega_*}{1 - JE\omega_*^2} &= \\ \pi + \tan^{-1}\frac{n}{n+P}\frac{J\omega_*}{1 - JE\omega_*^2} - \omega_*\delta_* & \end{aligned}\right\} \quad \ldots [8.2]$$

From the first Equation [8.2] we have

$$1 - JE\omega_*^2 = \mp J\omega_* \sqrt{\frac{\omega_*^2 + (1-n)^2 - n^2}{(n+P)^2 - \omega_*^2 - (1-n)^2}} = \mp J\omega_*\Phi \quad \ldots [8.3]$$

Φ being the same function as in Section 7; replacing in the second Equation [8.2]; and solving for δ_*:

$$\delta_* = \frac{1}{\omega_*}\left[\pi - \tan^{-1}\frac{\omega_*}{1-n} \mp \left(\tan^{-1}\frac{n}{n+P}\frac{1}{\Phi} - \tan^{-1}\frac{1}{\Phi}\right)\right]$$
$$= \frac{1}{\omega_*}\left[\pi - \tan^{-1}\frac{\omega_*}{1-n} \pm \left(\tan^{-1}\frac{n+P}{n}\Phi - \tan^{-1}\Phi\right)\right]$$

which is exactly the same as Equation [7.5]. We conclude that as far as the relation between δ_* and ω_* for given values of n, P is concerned, the system of Fig. 4

with $\xi = 1$ behaves exactly like the system of Fig. 3. The curves of Figs. 5, 6, 7, 8, 9, and 10 represent, therefore, also the present case, abstraction being made from the actual values of E and J. A given point on one of the curves represents the critical condition for a certain system if the relative E, J satisfy to Equation [8.3]. The simplest case when the elasticity is negligible, $E = 0$, gives

$$J_{E=0} = J_0 = \mp \frac{1}{\omega_* \Phi} \quad \text{.....[8.4]}$$

As in this case J_0 represents the essentially positive physical quantity defined by the second Equation [6.12], only the lower sign has a physical meaning, and therefore only the lower portion of the curves (below the $\Phi = \infty$ line) corresponds to a real process. Lines of equal J_0 have been drawn in Figs. 8, 9, and 10. At the point $\Phi = 0$ we have $J_0 = \infty$; and the line $\Phi = \infty$ corresponds to $J_0 = 0$ which coincides therefore with the $E_0 = \infty$ line. For given n, P, small values of J_0 (moderate length of lines) result in a decrease of δ_* and of stability; a further increase of J_0 up to $J_0 = \infty$ results in an increase of δ_* and an improvement of stability. When $n \leq 0.5$ above a certain J_0 the combustion is always stable; but if $n > 0.5$ even when $J_0 = \infty$, δ_* is finite and the combustion can be unstable. An increase of $\Delta p/\bar{p}$ at constant J_0 results generally in an increase of δ_* and an improvement of stability, but the combustion will remain unstable even with $\Delta p = \infty$ when the rocket is intrinsically unstable.

The general case $E \neq 0$ can be easily discussed observing that Equation [8.3] can be written

$$\frac{1}{J} = \frac{1}{J_0} + E\omega_*^2$$

where positive or negative values of J_0 are possible, since J_0 now loses its physical meaning and is only the mathematical expression of Equation [8.4]; we see that at $J_0 = 0$, J is always zero; and $J = \infty$ when

$$E = -\frac{1}{J_0 \omega_*^2} = \pm \frac{\Phi}{\omega_*} = E_0$$

E_0 being the function defined by Equation [7.6]. Hence the lines of constant E_0 of Case (a) correspond also to the conditions $E = E_0$, $J = \infty$ of Case (b). (Similarly, the J defined by Equation [7.7] coincides with J_0 defined by Equation [8.4]; so that the $J_0 =$ constant lines of Case (b) represent also the conditions $J = J_0$, $E = \infty$ of Case (a).) It follows that the result of an increase of E is a counterclockwise displacement of the critical point on the corresponding curve of the figures, with a resulting increase or decrease of δ_*, depending on the location of the critical point. If this point is in the most probable region of J (that is, between $\delta_{*\min}$ and $\delta_{*\max}$) the added elasticity will produce an increase in δ_* with beneficial effects on the stability. For given n, P and for every J there exists an optimum value of the elasticity E which renders δ_* maximum.

9 Effect of the Nonuniformity of the Time Lag

In Section 3 we made the explicit assumption that the time lag is the same for all the particles. Let us now assume more generally that different fractions of propellant injected at the same time have different time lags, so that this time lag is not only a function of the pressure, but also of the location of the considered fraction in the jet. The mathematical formulation of this assumption can be derived simply in the following way. Suppose that we inject the propellant through N distinct injectors, each one having a uniform time lag, different from the time lag of the other injectors. If τ_h is the time lag of the hth injector ($h = 1, 2, \ldots, N$), and we assume a relation analogous to Equation [3.1] with the same exponent n for all the injectors, we deduce the equation similar to Equation [4.8]:

$$1 - \frac{d\tau_h}{dt} \cong 1 + n(\varphi - \varphi^{(\tau_h)})$$

Now the burning rate from this injector, at time t, is related to the injection rate at the time $t - \tau_h$ by the equation similar to Equation [4.2]:

$$\dot{m}_{h_b} = \dot{m}_{h_i}^{(\tau_h)} \left(1 - \frac{d\tau_h}{dt}\right)$$

and the total burning rate at time t will be

$$\dot{m}_b = \sum \dot{m}_{h_b} = \sum \dot{m}_{h_i}^{(\tau_h)} \left(1 - \frac{d\tau_h}{dt}\right) = \sum \dot{m}_{h_i}^{(\tau_h)} [1 + n(\varphi - \varphi^{(\tau_h)})]$$

If we pass to the limit of an infinite number of injectors and we replace $\dot{m}_{h_i}^{(\tau_h)}$ with $\dot{m}_i^{(\tau(f))}\, df$ where: f, variable between 0 and 1, represents the location of the fraction we are considering in the jet, τ is now a function of f, and $\dot{m}_i^{(\tau(f))}$ represents the total injection rate at the time $t - \tau(f)$; and if instead of the summation we perform an integration, we can write:

$$\dot{m}_b = \int_0^1 \dot{m}_i^{(\tau(f))} [1 + n(\varphi - \varphi^{(\tau(f))})]\, df$$

Let us now introduce the fractional variations of the burning and of the injection rate defined by Equations [4.4]; we have, neglecting the terms of higher order (products of μ and φ):

$$\mu_b = \int_0^1 [\mu^{(\delta(f))} + n(\varphi - \varphi^{(\delta(f))})]\, df$$
$$= n\varphi + \int_0^1 [\mu^{(\delta(f))} - n\varphi^{(\delta(f))}]\, df \quad \text{.....[9.1]}$$

where we have already replaced the time lag with the (nonuniform) reduced time lag $\delta(f)$ (Equation [4.7]). Introducing Equation [9.1] in the first two members of Equation [4.5], we arrive at the equation of the combustion chamber:

$$\frac{d\varphi}{dz} + (1 - n)\varphi = \int_0^1 [\mu^{(\delta(f))} - n\varphi^{(\delta(f))}]\, df$$

which for uniform $\delta(f)$ becomes Equation [4.9].

If we try on this equation a solution of the type of Equation [7.1] we find, cancelling the common factor $\exp(\alpha z)$:

$$A(\alpha + 1 - n) = (B - nA)\int_0^1 e^{-\alpha\delta(f)}\, df \ldots\ldots [9.2]$$

Equation [9.2] replaces, in the case of nonuniform time lag, the analogous equation derived from Equation [4.9] and used in Sections 7 and 8. We see that from the equations developed there we can obtain those relative to the nonuniform time lag case by simply replacing everywhere $\exp(-\alpha\delta)$ with the integral

$$I(\alpha) = \int_0^1 e^{-\alpha\delta(f)}\, df \ldots\ldots\ldots\ldots\ldots [9.3]$$

which depends, of course, not only on α but also on the distribution function $\delta(f)$ of the time lag.

To discuss in some simple cases the effects of this substitution, let us define an average value of the reduced time lag

$$\delta_m = \int_0^1 \delta(f)\, df$$

and the variation from the average

$$\epsilon(f) = \delta(f) - \delta_m; \int_0^1 \epsilon(f)\, df = 0 \ldots\ldots\ldots [9.4]$$

The integral [9.3] then becomes

$$I(\alpha) = e^{-\alpha\delta_m}\int_0^1 e^{-\alpha\epsilon(f)}\, df = \beta e^{-\alpha\delta_m} \ldots\ldots [9.5]$$

where the coefficient $\beta(\alpha)$ defined in this way will now contain all the effects of the nonuniformity of the time lag when we compare cases with the same δ_m, and is unity for uniform $\delta = \delta_m$.

If we are interested in finding the limit of stability of a given system we can replace $\alpha = i\omega_*$ and obtain

$$\beta = \int_0^1 \cos(\omega_*\epsilon)\, df - i\int_0^1 \sin(\omega_*\epsilon)\, df \ldots\ldots [9.6]$$

Suppose now that f is arranged in such a way that $\delta(f)$, and therefore $\epsilon(f)$, increase monotonically with f. Then, due to Equation [9.4], from a certain negative value ϵ_0 at $f = 0$, ϵ increases to a positive value ϵ_1 at $f = 1$. If this curve is distributed in an antisymmetrical way with respect to $f = 0.5$, that is, if $\epsilon(f) = -\epsilon(1 - f)$, then the second integral of Equation [9.6] is zero, and β is real and smaller than one. If the curve is not antisymmetrical there will be an imaginary part of β, but probably for plausible $\epsilon(f)$ it will be small with respect to the real part, still < 1. The actual computation of β requires the knowledge of $\epsilon(f)$. Of course this function depends on the particular injection system and on the type or combination of propellants; but it is probable that the variation of δ and ϵ is not uniformly distributed with f (linear variation), and that a larger fraction of propellant has δ-values close to δ_m, or ϵ-values close to zero, and a smaller fraction has ϵ-values close to the two extremes ϵ_0, ϵ_1. In order to evaluate numerical examples, let us assume two different $\epsilon(f)$, both with an antisymmetrical variation so that $\epsilon_0 = -\epsilon_1$:

$$\text{I: } \epsilon = \epsilon_1(2f - 1); \quad \text{II: } \epsilon = \frac{2\epsilon_1}{\pi}\sin^{-1}(2f - 1);$$

the second assumption being a simple example of the distributions just discussed. The value of β can be readily evaluated in both cases and is

$$\text{I: } \beta = \frac{\sin\omega_*\epsilon_1}{\omega_*\epsilon_1}; \quad \text{II: } \beta = \frac{\cos\omega_*\epsilon_1}{1 - \left(\frac{2}{\pi}\omega_*\epsilon_1\right)^2} \ldots [9.7]$$

where $\epsilon_1 = (\delta_1 - \delta_0)/2$ is half the total excursion of the reduced time lag. It is again checked that β is < 1. The minimum value is obtained when ϵ_1 is maximum, that is, when $\delta_0 = 0$ and $\epsilon_1 = \delta_1/2 = \delta_m$, so that

$$\text{I: } \beta_{\min} = \frac{\sin\omega_*\delta_m}{\omega_*\delta_m}; \quad \text{II: } \beta_{\min} = \frac{\cos\omega_*\delta_m}{1 - \left(\frac{2}{\pi}\omega_*\delta_m\right)^2} \ldots [9.8]$$

We can use these formulas in the simplest case of the intrinsic instability (constant rate of injection). The corresponding equations are obtained from Equation [5.3] by introducing δ_m instead of δ, and $\beta\exp(-\lambda\delta_m)$ instead of $\exp(-\lambda\delta)$ and finally putting $\lambda = 0$. We obtain

$$\beta\cos\omega_*\delta_{m*} = -\frac{1 - n}{n}; \qquad \beta\sin\omega_*\delta_{m*} = \frac{\omega_*}{n}$$

If $n = 1$ the first always gives $\omega_*\delta_{m*} = \pi/2$, and the second $\omega_* = \beta$, so that

$$\delta_{m*} = \frac{\pi}{2\beta} > \frac{\pi}{2}$$

and the critical time lag (average) is increased with respect to the case of uniform δ. The amount of the increase depends on the value of β. If we take the minimum possible values of Equations [9.8] ($\epsilon_1 = \delta_m$), we have

$$\text{I: } \beta_{\min} = \frac{2}{\pi} = 0.637; \quad \text{II: } \beta_{\min} = \frac{\pi}{4} = 0.786$$

and the corresponding increases of δ_{m*} are of 57 per cent and of 27 per cent.

The value of $\epsilon_1 = \delta_m$ just used is probably larger than the values likely to appear in practice. As a rough estimate, we can say that if the total residence time of the propellants is computed from Equation [4.6] with the average value of $\bar{\tau}$, the total reduced residence time is

$$\frac{\theta_l}{\theta_g} = \delta_m + 1;$$

on the other hand, with $\epsilon_1 = \delta_m$, the maximum reduced time lag is $2\delta_m$ which, with $\delta_m = \pi/2\beta$, is larger than the total reduced residence time, and the corresponding fractions of propellant would not have the time necessary to burn; that is, a loss in combustion efficiency would result. If we assume a more conservative value, $\epsilon_1 = \delta_m/2$, which does not produce the effect just discussed, we have from Equation [9.7]:

$$\text{I: } \beta = \frac{2\sqrt{2}}{\pi} = 0.9; \quad \text{II: } \beta = \frac{2\sqrt{2}}{3} = 0.943$$

and the increases of δ_{m*} are of 11 per cent and 6 per cent.

We conclude that the effect of the nonuniformity of the time lag is in this case an improvement of the stability, and that the improvement for distributions of the more probable type II and not too extreme excursions of the time lag is only of a few per cent.

Analogous conclusions can be reached for other values of n. For instance, the minimum value of n for the existence of intrinsic instability is raised with respect to the uniform case.

From these simple computations, and from others that we exclude for brevity, it seems possible to conclude that the nonuniformity of time lag has always a favorable, though not too important, effect on stability.

References

1 "Stability of Flow in a Rocket Motor," by D. F. Gunder and D. R. Friant, *Journal of Applied Mechanics*, vol. 17, no. 3, 1950, pp. 327–333.

2 "Discussion of the Paper of Reference 1," by M. Yachter, *Journal of Applied Mechanics*, vol. 18, no. 1, 1951, pp. 114–116.

3 "A Theory of Unstable Combustion in Liquid Propellant Rocket Systems," by M. Summerfield (presented at the Heat Transfer and Fluid Mechanics Institute at Stanford University on June 20–22, 1951), *Journal of the American Rocket Society*, vol. 21, no. 5, 1951, pp. 108–114.

4 "Measurement of the Burning Rate of Liquid Propellants," by B. W. Tait, A. G. Whittaker, and H. Williams, *Journal of the American Rocket Society* vol. 21, no. 85, June, 1951, pp. 83–88.

5 "Rocket Applications of the Cavitating Venturi," by L. N. Randall, presented at the joint ASME and ARS Mid-Season Session, Toronto, Canada, July, 1951.

6 "Self-Excited Oscillations in Dynamical Systems Possessing Retarded Actions," by N. Minorsky, *Journal of Applied Mechanics*, vol. 9, no. 2, 1942, pp. 67–71.

(*To be continued in the next issue*)

Special Refractories by CARBORUNDUM

Special silicon carbide refractories made by The Carborundum Company have proved to be the best available materials for ceramic linings in uncooled rocket motors.

Address inquiries to:

The Carborundum Company
Refractories Division
Perth Amboy, New Jersey

Chemical Kinetics and Rocket Nozzle Design

By F. J. KRIEGER[1]

The Rand Corporation, Santa Monica, Calif.

The effect of chemical kinetics on rocket nozzle design was investigated for the particular case of hydrogen gas flowing adiabatically through a typical rocket nozzle having a chamber-to-throat-area ratio of 2 to 1. For comparative purposes the following types of flow were considered: (*a*) Constant composition (frozen equilibrium), (*b*) instantaneous chemical equilibrium (shifting equilibrium), and (*c*) kinetic chemical equilibrium. A stepwise iteration process was employed to perform the integration of the differential equation in case (*c*). In each case the gas entered the nozzle at a temperature of 3500 K and a pressure of 20 atm and was allowed to expand isentropically to an exhaust pressure of 1 atm. The results for a mass flow rate of 1000 gm sec^{-1} are presented in Figs. 2 through 6. The instantaneous equilibrium flow assumption not only gives a higher specific impulse, but also requires a larger nozzle than either the kinetic or the constant composition flow assumption. The kinetic equilibrium flow results are intermediate between those for instantaneous equilibrium flow and those for constant composition flow, the relative position depending on the magnitude of the reaction rate which governs the kinetic equilibrium.

IT HAS been standard practice in the field of rocketry to compute the specific impulse (i.e., the jet velocity divided by the acceleration of gravity) of a propellant system on the basis of either of two fundamental assumptions, namely, that the adiabatic flow of propellant gases from the combustion chamber through the nozzle is such that either (*a*) constant composition or (*b*) instantaneous chemical equilibrium is maintained. For an adiabatic process, assumption (*a*), which says that the inherent reaction rate is zero, gives a minimum value for the specific impulse, whereas assumption (*b*), which says that the inherent reaction rate is infinite, gives a maximum value for the specific impulse. The introduction of reaction rate equations into the computation of specific impulse so complicates the problem that heretofore investigators have, perforce, been generally satisfied with a knowledge of the limiting values obtained on the basis of the above assumptions.

Aside from the computational difficulties which it entails, the kinetic approach, because it requires close adherence to physical reality, tends not only to establish the true specific impulse for a propellant system, but also to give some insight into the design of the nozzle for that system. In general, specific impulse values computed under assumptions (*a*) and (*b*) are made without regard to nozzle configuration and with the added simplifying assumption that the chamber gases enter the nozzle with zero velocity. Since this latter assumption has no physical justification and is erroneous, it leads to spurious values of the specific impulse. In order to obviate this condition it is necessary at the outset to determine the chamber velocity at the entrance to the nozzle for the type of gas flow under consideration. This may be done only by consideration of nozzle configuration.

The nozzle generally accepted by rocket designers is the convergent-divergent De Laval type, which is formed from two intersecting right circular cones. The half angle of the convergent cone is usually 30° and that of the divergent cone, 15°. To prevent discontinuity of flow, the throat section is rounded off with a radius of curvature which is equal to the throat diameter $2r_t$. Such a nozzle was considered by Altman and Penner (1), (2).[2] The nozzle considered in this study is shown in Fig. 1. It differs from the Altman and Penner nozzle in two respects. First, according to current design practice, the entrance area A_e is twice the throat area A_t. This restriction permits one to establish, among other things, the origin of a rectangular coordinate system at the entrance to the nozzle. Secondly, the convergent cone is replaced with a sphere of radius r_c. The sphere is tangent to the rounded throat section at a point where the slope makes an angle of 28° 31′ with the nozzle axis. The use of a spherical section instead of a convergent cone insures continuity of flow from the combustion chamber into the nozzle entrance.

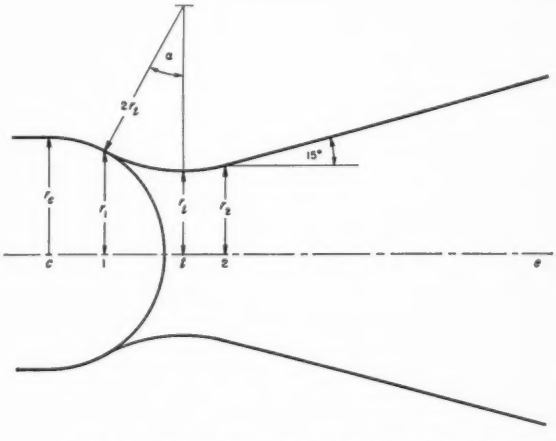

FIG. 1 CROSS SECTION THROUGH ROCKET NOZZLE

Received Sept. 20, 1951.

[1] Physical Scientist, Missiles Division.

[2] Numbers in parentheses refer to Bibliography at end of paper.

The propellant system in this study is pure hydrogen having a chamber temperature of 3500 K and a chamber pressure of 20 atm. Its history prior to its arrival at the entrance to the nozzle is irrelevant. From the basic nozzle design parameters and mass flow rate considerations, the following properties may be computed: (1) Chamber velocity v_c; (2) nozzle throat area A_t; (3) nozzle length L; and (4) jet velocity v_e or equivalent specific impulse I. In this study, the foregoing properties are determined not only for (*a*) constant composition flow and (*b*) instantaneous chemical equilibrium flow, but also for (*c*) kinetic chemical equilibrium flow. Case (*c*) makes use of the expression for the rate of recombination of hydrogen atoms during the adiabatic expansion process of the propellant gas as it flows through the nozzle.

General Thermodynamic Equations

Several basic equations may be derived from a thermodynamic consideration of the propellant gas mixture. For the association reaction

$$2H = H_2$$

the equilibrium constant K_p is given by the expression

$$K_p = N_{H_2}/N_H{}^2P \quad [1]$$

where N_{H_2} and N_H are the mole fractions of H_2 and H, respectively, and P is the total pressure in atmospheres. The mole fractions satisfy the obvious relation

$$N_{H_2} + N_H = 1 \quad [2]$$

The molecular weight of the gas mixture is given by the relationship

$$M = \sum N_i M_i \quad (i = 1, 2) \quad [3]$$

where N_i and M_i are the mole fraction and the molecular weight, respectively, of component i.

The expansion of the propellant gas is assumed to be isentropic. The specific entropy of the gas mixture is given by the expression

$$s = \frac{1}{M}\left(\sum N_i S_i{}^0 - R\sum N_i \ln N_i - R \ln P\right) \quad [4]$$

where s is the entropy in calories per degree per gram, M is the molecular weight of the gas mixture, $S_i{}^0$ is the entropy per mole of component i at one atmosphere and at a given temperature, N_i is the mole fraction of component i, R is the gas constant, and P is the given pressure in atmospheres.

The specific enthalpy of the gas mixture at any point in the expansion process is given by the expression

$$h = \frac{1}{M}\left[\sum N_i \left(\Delta H_{f_i} + \Delta H^T{}_{298.16,\,i}\right)\right] \quad [5]$$

where h is the enthalpy in calories per gram, M is the molecular weight of the gas mixture, and N_i, ΔH_{f_i}, and $\Delta H^T{}_{298.16,\,i}$ are the mole fraction, the heat of formation, and the sensible heat content, respectively, of component i.

By equating the change in kinetic energy of the expanding gas to its change in enthalpy, the velocity at any point in the expansion is found to be

$$v = [v_c{}^2 + 2J(h_c - h)]^{1/2} \quad [6]$$

where v is the velocity in centimeters per second, h is the specific enthalpy in calories per gram, J is the mechanical equivalent of heat, and the subscript c refers to the chamber conditions.

Specific impulse and velocity are related by means of the simple expression

$$I = v/g \quad [7]$$

where I is the specific impulse in seconds, v is the velocity in centimeters per second, and g is the acceleration of gravity. This concept of specific impulse assumes complete or perfect expansion of the propellant gas.

Mass Flow Equations

A fundamental relationship between nozzle configuration and propellant gas mass flow may be derived from the following considerations. The time rate of mass flow μ in grams per second may be defined by the expression

$$\mu = \rho A v \quad [8]$$

where ρ is the density of the gas in grams per cubic centimeter, A is the cross-sectional area of the nozzle in square centimeters, and v is the velocity in centimeters per second. The ideal gas equation may be written in the form

$$P = \frac{\rho}{M} RT \quad [9]$$

where P is the absolute pressure in atmospheres, ρ is the density of the gas in grams per cubic centimeter, M is the molecular weight of the gas, R is the gas constant, and T is the absolute temperature in degrees Kelvin. Equations [8] and [9] may be combined to give the expression

$$A = \frac{\mu RT}{PMv} \quad [10]$$

for the area associated with a given mass flow rate at any point in the nozzle. The corresponding cross-sectional radius is given by the expression

$$r = \left[\frac{\mu RT}{\pi PMv}\right]^{1/2} \quad [11]$$

From the equation

$$x^2 + y^2 = r_c{}^2 \quad [12]$$

which defines the spherical section of the nozzle depicted in Fig. 1, and the fact that $y = r$, the following expression is obtained for the distance downstream from the nozzle entrance through the spherical section

$$x = (r_c{}^2 - r^2)^{1/2} \quad [13]$$

An expression for the distance downstream through the rounded throat section may be derived from the

equation which defines the shape of the throat. In terms of an x, y co-ordinate system having its origin at the center of the nozzle entrance, the equation of such a defining circle is simply

$$(x - x_t)^2 + (y - y_t)^2 = 2r_c^2 \quad [14]$$

where x_t and y_t are the co-ordinates of the center of the circle whose radius is $2r_t$ or $2^{1/2}r_c$. Reference to Fig. 1 shows that

$$y_t = 3r_c/2^{1/2} \quad [15]$$

and that

$$x_t = x_1 + r_c/2^{1/2} \quad [16]$$

where x_1 is the abscissa of the point at station 1 where the circles defined by Equations [12] and [14] are tangent. By combining Equations [14] and [15] and remembering that $y = r$, the following expression for the distance downstream through the throat section is obtained:

$$x = x_t \mp [2r_c^2 - (r - 3r_c/2^{1/2})^2]^{1/2} \quad [17]$$

In Equation [17] the minus sign is valid in the convergent section of the nozzle and the positive sign in the divergent.

Inspection of Fig. 1 shows that the expression for the distance downstream from station 2 is given by the relation

$$x = (r - r_2) \cot \theta \quad [18]$$

where r_2 is the radius of the throat at station 2 where the divergent cone of half angle θ is tangent to the circle which defines the shape of the throat.

Further inspection of Fig. 1 indicates the following particular relations. The angle α, associated with the point of tangency at station 1, is given by the equation

$$\cos \alpha = \frac{3(2^{1/2})}{2(1 + 2^{1/2})} = 0.87868 \quad [19]$$

so that $\alpha = 28.516°$. Thus at station 1

$$r_1 = r_c \cos \alpha = 0.87868 r_c \quad [20]$$

and

$$x_1 = r_c \sin \alpha = 0.47741 r_c \quad [21]$$

At the throat

$$r_t = r_c/2^{1/2} = 0.70711 r_c \quad [22]$$

and

$$x_t = x_1 + 2^{1/2} r_c \sin \alpha = 1.1526 r_c \quad [23]$$

At station 2

$$r_2 = (3 - 2 \cos 15°) r_t = 0.75529 r_c \quad [24]$$

and

$$x_2 = x_t + 2^{1/2} \sin 15° r_c = 1.5186 r_c \quad [25]$$

Kinetic Equations

The recombination of hydrogen atoms to form hydrogen molecules may be represented by the triple-body collision reaction equation

$$Z + 2H \underset{k_b}{\overset{k_f}{\rightleftharpoons}} H_2 + Z \quad [26]$$

where k_f and k_b are the forward and backward reaction rate constants, respectively, and Z is any third body.[3] If $[H]$ denotes the concentration of H in moles per cubic centimeter, then the time rate of change of $[H]$ for a process in which the volume V is changing is given by the expression

$$-\frac{1}{2}\frac{d[H]}{dt} = k_f[H]^2[Z] - k_b[H_2][Z] + \frac{1}{2}\frac{[H]}{V}\frac{dV}{dt} \quad [27]$$

The validity of the third term on the right-hand side of Equation [27] may be easily verified by a consideration of the identity $[H] = n_H/V$, where n_H is the number of moles of H in the volume V of expanding gas.

In this study it is more convenient to deal with the concept of mole fraction N_H than with that of molar concentration $[H]$. By making use of the identities

$$[H] = N_H P/RT \quad [28]$$

and

$$[Z] = P/RT \quad [29]$$

Equation [27] may be written in the form

$$-\frac{dN_H}{dt} = 2\left[k_f N_H^2 (P/RT)^2 - k_b N_{H_2} (P/RT)\right] + N_H \frac{d}{dt} \ln (PV/RT) \quad [30]$$

For a mass of m grams of gas the ideal gas law may be written in the form

$$PV = mRT/M \quad [31]$$

so that

$$\frac{d}{dt} \ln (PV/T) = \frac{d}{dt} \ln (mR/M) = -\frac{1}{M}\frac{dM}{dt} \quad [32]$$

Hence, Equation [30] becomes

$$-\frac{dN_H}{dt} = 2\left[k_f N_H^2 (P/RT)^2 - k_b N_{H_2} (P/RT)\right] - \frac{N_H}{M}\frac{dM}{dt} \quad [33]$$

By using Equations [2] and [3] and the value 1.008 for the atomic weight of hydrogen, the expression for the molecular weight of the gas mixture becomes

$$M = 1.008 (2 - N_H) \quad [34]$$

Equation [33] thus reduces to the following:

$$-\frac{dN_H}{dt} = (2 - N_H)\left[k_f N_H^2 (P/RT)^2 - k_b N_{H_2} (P/RT)\right] \quad [35]$$

Since the equilibrium constant K_p defined by Equation [1] and the rate constants in Equation [26] are related by the expression

$$K_p RT = k_f/k_b \quad [36]$$

Equation [35] may be written in the form

$$-\frac{dN_H}{dt} = \frac{k_f(2 - N_H)}{(RT)^2}(N_H^2 P^2 - N_{H_2} P/K_p) \quad [37]$$

Finally, since the velocity v at any distance x downstream is given by the relation

[3] Compare this treatment with that of Penner (3).

$$v = dx/dt \quad [38]$$

the rate of change of N_H with distance is given by the expression

$$-\frac{dN_H}{dx} = \frac{k_f(2 - N_H)}{v(RT)^2}(N_H{}^2P^2 - N_{H_2}P/K_p) \quad [39]$$

Basic Data

The pertinent thermodynamic data used in this study were taken from the National Bureau of Standards (4). They include the total enthalpy above the reference temperature 298.16 K and the absolute entropy for the chemical species H and H_2 and the logarithms of the equilibrium constants for the reaction $2H = H_2$ at temperatures from 1600 to 3500 K. The heats of formation for H and H_2 at 298.16 K are 52,089 and 0 cal mol^{-1}, respectively.

The pertinent physical constants have the following values: the acceleration of gravity $g = 980.665$ cm sec^{-2}; the gas constant $R = 82.0567$ cm^3 atm deg^{-1} mol^{-1}; the mechanical equivalent of heat $J = 4.1840$ abs joules cal^{-1}.

The forward reaction rate constant k_f in Equation [26] is assumed to have the value 10^{16} cm^6 mol^{-2} sec^{-1} over the entire range of temperatures and pressures covered by this investigation. This assumption is made (*a*) because the chemical literature is singularly lacking in kinetic data for the hydrogen recombination reaction[4] and (*b*) because the primary purpose of this study is to show how a rate equation may be dealt with in a propellant gas expansion problem.

Computational Procedure

In general, the composition of the expanding gas may be determined at any temperature and pressure by the simultaneous solution of Equations [1] and [2]. The entropy of the system, the expansion of which is assumed to be isentropic, may be determined from the initial chamber conditions by means of Equation [4]. Once the value of the entropy has been established, Equation [4] may be used to determine the pressure at any temperature and composition. The velocity of the expanding gas at any point may be computed by means of Equation [6]. The chamber velocity may be determined from the following considerations.

If, for a given mass flow rate μ, a plot of area A versus temperature T is made for various temperatures between T_c and T_e, a smooth curve having a well-defined minimum is obtained. This point of minimum area corresponds to the throat of the nozzle. The chamber velocity may, therefore, be computed from Equation [10] when the design condition

$$A_c = 2\,A_t \quad [40]$$

is satisfied.

Since A_t cannot be computed explicitly, a tentative value for A_c must be assumed on the basis of some nonzero chamber velocity. Then values of A may be computed for various values of T. From a plot of these data a throat area corresponding to the assumed chamber area may be determined. If this process is repeated for several values of A_c and if a plot of A_c/A_t versus A_c is made, then, by interpolation, values of A_c and A_t may be obtained which satisfy Equation [40]. This procedure for determining A_c, A_t, and v_c is perfectly general and is independent of the type of flow considered.

The length of the nozzle may be computed from a knowledge of end conditions only by means of Equations [13], [17], and [18] for constant composition flow and for instantaneous chemical equilibrium flow. The kinetic case, however, requires a stepwise procedure which involves the integration of Equation [39] as well as the use of Equations [13], [17], and [18]. For this purpose it is convenient to use temperature as a parameter and to perform the integration over temperature intervals which are small enough to insure a degree of accuracy consistent with the data used. The two regions where particular care must be exercised are (*a*) at the very entrance to the nozzle, where the temperature gradient is a maximum, and (*b*) at the throat, where the parameters must be determined precisely in order to satisfy the design conditions.

The integration of Equation [39] may be accomplished by writing it in the form

$$dN_H/dT = \frac{dN_H/dL}{dL/dT} \quad [41]$$

where L denotes the length of the nozzle, and by subjecting it to an iterative process which makes use of the methods and equations of the numerical calculus for equal intervals of the argument T. A list of such equations is given by Milne (7). For the present, the following four-point integration formula is satisfactory

$$N_2 = N_0 + (3h/8)\,(N_0' + 3N_1' + 3N_2' + N_3') \quad [42]$$

In this equation h is the temperature interval and the primed quantities are the first derivatives with respect to temperature of the function N at four consecutive temperatures.

In order to carry out the integration process effectively, it is expedient to construct tables of dN_H/dL and L values for a judicious spread of N_H values at the various temperatures considered. Starting values of N_H may be obtained by reference to those calculated for the instantaneous equilibrium case.

Once a set of values of N_H is obtained for the temperature range from T_c to some arbitrary T_e, corresponding values of dN_H/dL and of L may be obtained from the previously constructed tables by interpolation. Values of dL/dT may be derived from a plot of L versus T or by means of an appropriate differentiation formula as given in (7). Equation [42] may then be used to correct the original rough values of N_H as often as necessary to achieve convergence.

[4] In this connection, see (5) and (6).

Results and Discussion

The mole fraction composition of the gas entering the nozzle at a temperature of 3500 K and a pressure of 20 atm is 0.1235 H and 0.8765 H_2, and its specific entropy is 22.918 cal deg^{-1} gm^{-1}. With these data as initial conditions, a mass flow rate of 1000 gm sec^{-1}, the nozzle configuration of Fig. 1, and a 2-to-1 chamber-to-throat-area ratio, the adiabatic flow of hydrogen to an exhaust pressure of 1 atm was studied, assuming first, constant composition flow, then instantaneous chemical equilibrium flow, and finally, kinetic chemical equilibrium flow. The results are presented graphically in Figs. 2 through 6.

Inspection shows that the shape of the kinetic flow nozzle is identical with that of the instantaneous flow nozzle. This is due to the fact that, since the magnitude 10^{16} of the forward rate constant k_f is for all practical purposes infinite, the chamber parameters are numerically equal (as far as significant figures are concerned) for the kinetic and the instantaneous equilibrium flow cases. Since the chamber parameters determine the geometry of the nozzle, it follows that the shape of the nozzles must be identical.

As was to be expected, the kinetic results are for the most part intermediate between the constant composition and the instantaneous equilibrium flow results. This fact was invaluable in estimating starting values

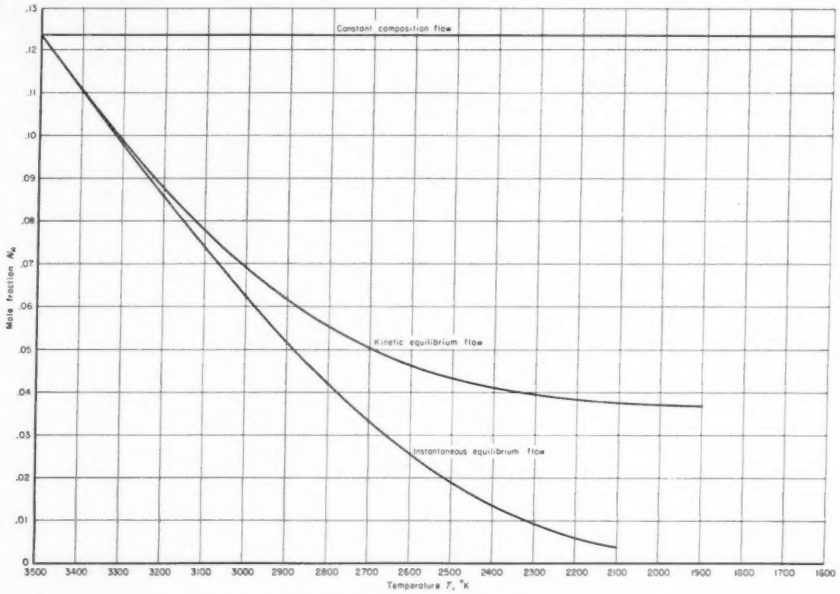

FIG. 2 COMPOSITION VERSUS TEMPERATURE FOR THE ADIABATIC EXPANSION OF HYDROGEN THROUGH A ROCKET NOZZLE

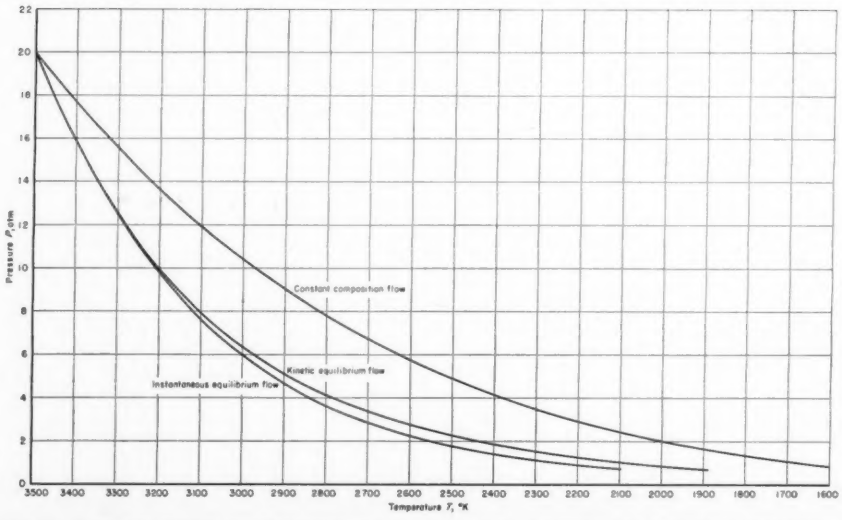

FIG. 3 PRESSURE VERSUS TEMPERATURE FOR THE ADIABATIC EXPANSION OF HYDROGEN THROUGH A ROCKET NOZZLE

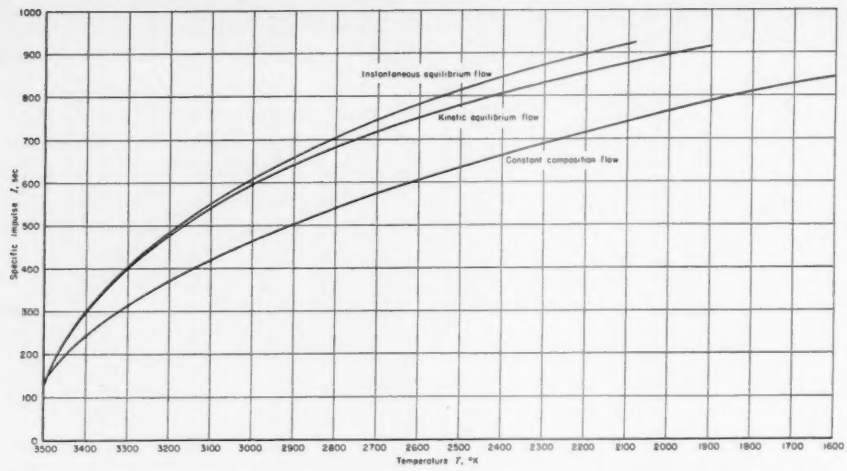

FIG. 4 SPECIFIC IMPULSE VERSUS TEMPERATURE FOR THE ADIABATIC EXPANSION OF HYDROGEN THROUGH A ROCKET NOZZLE

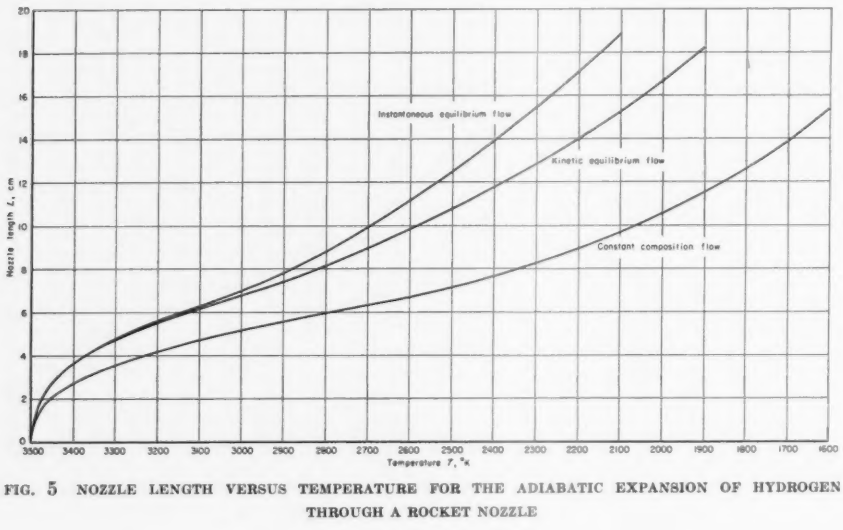

FIG. 5 NOZZLE LENGTH VERSUS TEMPERATURE FOR THE ADIABATIC EXPANSION OF HYDROGEN THROUGH A ROCKET NOZZLE

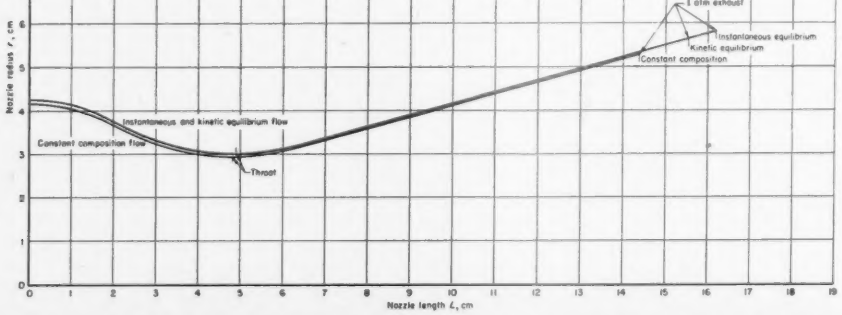

FIG. 6 NOZZLE RADIUS VERSUS NOZZLE LENGTH FOR THE ADIABATIC EXPANSION OF HYDROGEN THROUGH A ROCKET NOZZLE

for the iteration process used to integrate Equation [39]. A temperature interval of 50 K was employed throughout the integration process. A smaller interval might have given smoother results, but the increased labor would have been greater than the accuracy of either the initial data or the final results would warrant.

Fig. 6 depicts the nozzle configuration for the three types of flow investigated. It is interesting to note (*a*) that instantaneous equilibrium flow requires a longer (and larger) nozzle than does constant composition flow, and (*b*) that for kinetic equilibrium flow the nozzle is slightly shorter than for instantaneous equilibrium flow.

It may also be noted that nozzle design affects specific impulse in the following manner. The specification of a 2-to-1 chamber-to-throat-area ratio results in a chamber specific impulse of 141.4 sec for the constant composition flow nozzle and 136.0 sec for both the instantaneous and the kinetic equilibrium flow nozzles. It is obvious from Equation [10] that a zero chamber velocity would require an infinite chamber area, a factor which is not feasible in practice. Furthermore, a zero chamber velocity would yield, at an exhaust pressure of 1 atm, a specific impulse of 823.2 sec instead of 835.4 for constant composition flow, and 873.8 sec instead of 884.3 for instantaneous equilibrium flow. It is thus evident that nozzle configuration, specifically chamber-to-throat-area ratio, has a definite effect on the magnitude of specific impulse or jet velocity.

In the present example the effect of chemical kinetics, i.e., the rate of recombination of hydrogen atoms, on specific impulse is not very pronounced, as the figures 884.3 and 879.6 at an exhaust pressure of 1 atm for instantaneous and kinetic equilibrium flow, respectively, indicate. This is due, of course, to the magnitude of the forward reaction rate constant k_f and to the nature of the chemical species. In other expanding propellant gases, in which the rate constants associated with the pertinent chemical reactions are numerically smaller than the hydrogen rate constant and the chemical species themselves are less active than hydrogen, the general effect would be to displace the kinetic results toward the constant composition flow values. In such cases, even if several differential equations similar to Equation [39] are involved, the method of integration indicated in this paper would be valid, but the computation would best be performed on automatic equipment.

Conclusions

The following conclusions may be drawn from the foregoing study:

1 The effect of chemical kinetics on rocket propellant gases expanding through a nozzle has been determined by the simultaneous solution of three sets of equations based on thermodynamic, nozzle configuration, and chemical reaction rate considerations.

2 The fundamental design calculational requirement, aside from the mass flow rate, is the specification of a finite chamber-to-throat-area ratio.

3 Nozzles designed on the basis of chemical kinetics for perfect expansion are somewhat smaller than instantaneous equilibrium flow nozzles but are larger than constant composition flow nozzles, the difference depending on the magnitude of the reaction rates involved.

4 The method of stepwise integration described may be applied to propellant systems which involve several differential equations with, of course, a corresponding increase in computational labor.

Bibliography

1 "Adiabatic Flow of Hydrogen Gas through a Rocket Nozzle with and without Composition Change," by S. S. Penner and D. Altman, *Journal of the Franklin Institute*, vol. 245, 1948, pp. 421–432.

2 "Chemical Reaction During Adiabatic Flow through a Rocket Nozzle," by D. Altman and S. S. Penner, *Journal of Chemical Physics*, vol. 17, 1949, pp. 56–61.

3 "Maintenance of Near Equilibrium during Isentropic Expansions through a Nozzle," by S. S. Penner, *Journal of the American Chemical Society*, vol. 71, 1949, pp. 788–791.

4 "Selected Values of Chemical Thermodynamic Properties," Series III, National Bureau of Standards, Washington, D. C., June 30, 1948.

5 "The Kinetics of Homogeneous Gas Reactions," by L. S. Kassel, The Chemical Catalog Company, Inc., New York, 1932, pp. 177–180.

6 "Study of the Recombination Reaction of Free Atoms by the Thermal Analysis of the Budde Effect. I. The Recombination of Hydrogen Atoms," by Shoji Shida, Proceedings of the Imperial Academy (Tokyo), vol. 17, 1941, pp. 495–500.

7 "Numerical Calculus," by W. E. Milne, Princeton University Press, Princeton, N. J., 1949, Chapter 4.

Letters to the Editor

This section of the Journal is open to letters not exceeding 600 words in length (or one and one-half columns) devoted to brief research reports or technical discussions of papers previously published. Such letters are published without editorial review, usually within two months of the date of receipt. The style and manner of submission of letters are the same as for regular contributions. (See inside back cover.)

Jet Propulsion News

By C. F. WARNER, Purdue University, *Associate Editor*

Missiles

THE U. S. Navy's Martin *Viking* high-altitude research rocket set a new world's record of 135 miles for single-stage rockets on Aug. 7, 1951. The *Viking* reached a top speed of 4100 mph. Previous record for high altitude rockets was 114 miles reached by the German V-2. The *Viking*'s liquid oxygen and ethyl alcohol rocket engine burned for 75 sec and in that time it had reached an altitude of 25 miles from which point it coasted the rest of the way. The maximum altitude was reached in 4 min and 23 sec. The *Viking*, 48 feet long weighing $5^1/_2$ tons, was the seventh of 10 to be built by the Glenn L. Martin Company for the Naval Research Laboratory.

✦ ✦ ✦

THE U. S. Air Force will activate the 1st Pilotless Bomber Squadron (Light) at the U.S.A.F. Missile Test Center, Cocoa, Fla., on Oct. 1, 1951.

It will be the first operational unit of its kind in the Air Force. The unit will be equipped initially with the *Matador* B-61 pilotless bomber, Fig. 3, now in production by The Glenn L. Martin Company, Baltimore, Md.

The squadron will be supervised in its initial training by an already established training unit, the 6555th Guided Missile Wing, a part of the Air Research and Development Command. Later, it will be made combat-ready by extensive unit training under the supervision of the Tactical Air Command.

✦ ✦ ✦

THE Hycon Manufacturing Company and the Oederkerk & Ludwig Company of Pasadena, Calif., have a joint multimillion-dollar Navy contract for the manufacture of an air-to-air rocket-type missile developed by the personnel of the Navy Ordnance Test Station in Pasadena. The missile, designed to be carried in quantity by high speed jet planes, is powerful enough to destroy any known aircraft with one direct hit.

Aircraft

A U. S. Navy *Skyrocket*, Fig. 4, piloted by Douglas test pilot Bill Bridgeman, has broken its own and all existing altitude records. The exact altitude reached by the supersonic plane in a flight over Muroc Dry Lake, Calif., on August 15, 1951, has not been revealed, al-

FIG. 1. *Viking* JUST BEFORE FIRING

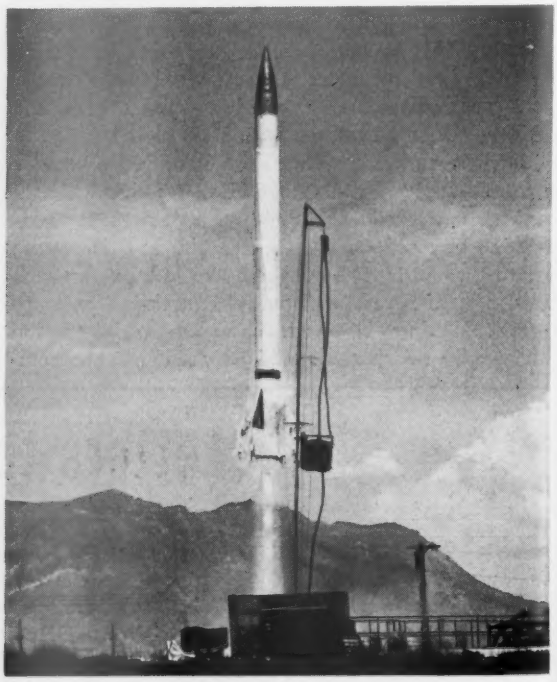

FIG. 2. *Viking* JUST AFTER FIRING

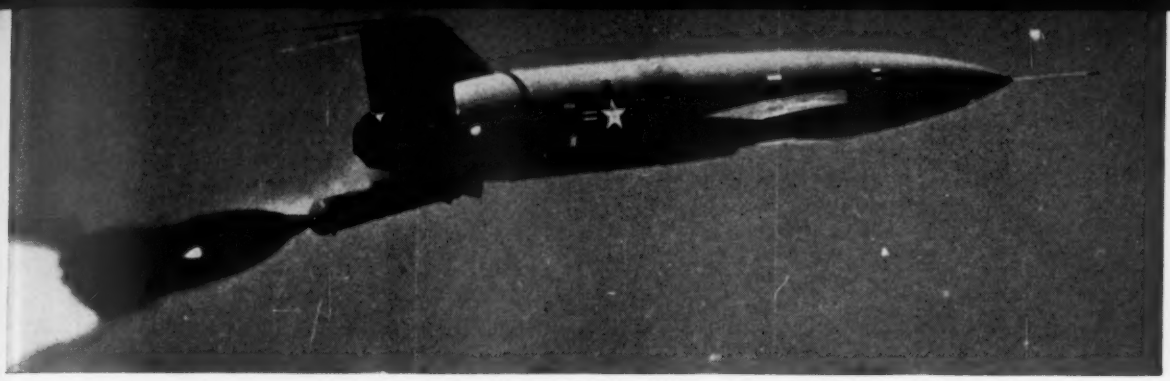

FIG. 3. U. S. AIR FORCE B-61 MARTIN *Matador* PILOTLESS BOMBER

though the officially recognized record is 72,394 ft, established in 1935 by a man-carrying balloon.

The Navy said this latest flight by Mr. Bridgeman in the 45-foot rocket-powered plane successfully concludes the first phase of a research and development program three years old.

The three *Skyrocket* planes used in the tests will be turned over to the National Advisory Committee for Aeronautics for the next phase of a planned research program, Rear Admiral T. F. Combs, chief of the Navy Bureau of Aeronautics, said.

The Navy said that the latest flight was made on a clear bright day. The *Skyrocket*, which is powered by an assembly of four rocket motors, was air-launched from a modified bomber at an altitude of 35,000 ft. Within ten sec the plane had exceeded sonic speed and was climbing away from the earth at a speed of about 1000 mph. Almost immediately, the plane was pulled into a steeper angle of climb to save fuel for climb rather than speed.

The turbojet engine had been removed to make available space for additional rocket motor propellants. During powered flight a ton of propellants per minute is expended.

The Douglas Aircraft Company designed and built the *Skyrocket* to meet the special requirements for high speed and extreme altitude research established by the Navy Bureau of Aeronautics and the National Advisory Committee for Aeronautics to enable procurement of much needed aerodynamic information in the transonic and supersonic speed ranges. The plane was equipped with four hundred openings on the wing and tail surfaces for air pressure determinations, and over 25 miles of electrical wiring were used to connect the electrical instruments.

✦ ✦ ✦

McDONNELL Aircraft Corporation has announced that its new Navy fighter, the XF3H-1 *Demon* jet aircraft has been flight tested for a period of 24 minutes.

✦ ✦ ✦

THE Glenn L. Martin Company has just received an English Electric Canberra light bomber from England. This plane will be built in substantial quantities by the Martin Company for the U. S. Air Force. Kaiser Metal Products, Inc., of Bristol, Pa., is a subcontractor of the Martin Company in connection with this program.

Rocket Engines

THE Curtiss-Wright Corporation's XLR-25 rocket engine, the first rocket power plant capable of being throttled from full thrust to 25 per cent full thrust to be built in this country, has passed reliability tests at the corporation's Propeller Division Plant in Caldwell, N. J. The motor should be ready for acceptance tests by the Air Force soon. This motor is designed for use in the Bell Aircraft Corporation's X-2.

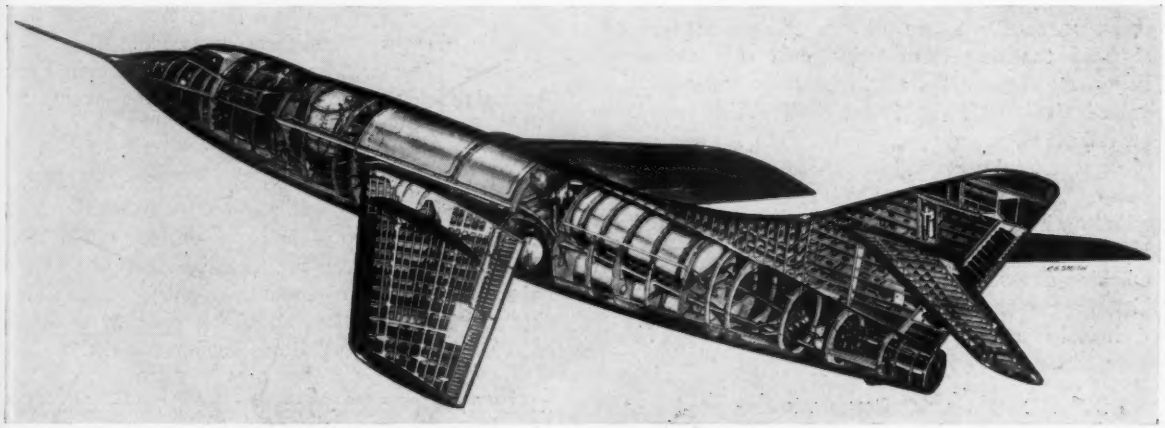

FIG. 4. NAVY'S RESEARCH AIRPLANE D-558-2 *Skyrocket*

Turbojet Engines

THE Pratt & Whitney Aircraft J-42 Turbo-Wasp has become the first jet aircraft engine to reach an officially authorized service life of 1000 hours between major overhauls, it was announced recently by Willam P. Gwinn, general manager. The new 1000-hour overhaul interval for the J-42 brings this Pratt & Whitney jet engine to a level of operational reliability and durability comparable to piston engines. The J-42 is a centrifugal flow type jet engine developed by Pratt & Whitney Aircraft, under auspices of the Navy's Bureau of Aeronautics, from an original design of Rolls-Royce, Ltd. It is rated at 5000 lb static thrust dry and 5750 lb using water injection.

New Facilities

THE U. S. Navy's Bureau of Yards and Docks is completing an aeronautical turbine laboratory at Trenton, N. J. Incorporating designs of the York Corporation, the laboratory will consist of five testing areas composed of two altitude "strato-chambers," two test cells, and one turboprop cell. The world's largest liquid rheostats, to help test full size jet engines, guided missiles, wing sections, and fuselages, are to be built by the Westinghouse Electric Corporation.

✦ ✦ ✦

PRESIDENT Harry Truman recently dedicated the Arnold Engineering Development Center at Tullahoma, Tenn. The $1,575,000,000 institution, to be operated by a private corporation, Aro, Inc., will begin test operations early next year. The facilities will include turbojet and ramjet test units, gas dynamics facilities for testing models at speeds above the Mach 5 range, and propulsion wind tunnels with transonic and supersonic test sections.

✦ ✦ ✦

THE recently established National Bureau of Standards laboratory at Corona, Calif., will be devoted primarily to Defense Department research projects. R. D. Huntoon, who has been named associate director to head the new laboratories, said that the most important activity there will be the development of guided missiles. Every phase of guided missile development from basic and applied research to the fabrication of experimental parts will be carried on. An analogue computer which will compute trajectories of proposed missiles will be installed. Other facilities at the former Navy installation will include electronic laboratories, machine shops, a wind tunnel, jet engine test cells, altitude chamber, a missile assembly section, and a technical library.

✦ ✦ ✦

LOCKHEED Aircraft Corporation reported that it will construct a $12,615,000 aircraft assembly plant for the U. S. Air Force at Palmdale Airport, 65 miles northeast of Los Angeles, Calif. The plant will employ several thousand persons in the assembly of jet aircraft.

Air Research and Development Command

FUTURE plans for guided missiles, supersonic planes, and other technological advancements are being prepared at the Baltimore headquarters of the new Air Research and Development Command. The new unit, known as ARDC for brevity, is dedicated to maintaining continuous United States air supremacy by exploring the unlimited boundaries of scientific knowledge. ARDC headquarters will direct operations at proving grounds throughout the nation. ARDC will eventually have assigned to it all research and development activities of the Air Force.

The new command is the outgrowth of the findings of a committee headed by Dr. Louis N. Ridenour, the dean of the University of Illinois graduate school. In 1949, General Hoyt S. Vandenberg, Chief of Staff, requested that such a committee conduct an intensive survey of Air Force research and development organization, procedures, policies, and facilities. The Ridenour committee recommended that a new command be formed to be responsible for all Air Force research and development.

It was announced on May 23 that Lt. General Earle E. Partridge is to succeed General Schlatter as ARDC commanding general. With the initial phase of the new command's development nearing its close, General Schlatter has been assigned as Commanding General of the Allied Air Forces in Southern Europe. Brigadier General Donald J. Keirn is director of research, and Brigadier General John W. Sessums, Jr., is director of operations. Dr. Mervin J. Kelly and Donald A. Quarles, top-ranking civilian scientists are serving as part-time advisers to General Schlatter and will continue in that capacity.

Personalities

COL. KENNETH E. FIELDS has been appointed director of the Division of Military Application, U. S. Atomic Energy Commission, succeeding Brig. Gen. James McCormack, Jr., who has been assigned as a special assistant to deputy chief of staff for development in U. S. Air Force headquarters.

✦ ✦ ✦

REAR ADM. THOMAS SELBY COMBS, U.S.N., took over the duties of chief of the Bureau of Aeronautics, Department of the Navy, on May 1, 1951, for a four-year term. Prior to this assignment, he was chief of staff and aide to commander-in-chief, Atlantic Fleet. He had been with Bureau of Aeronautics previously, serving from 1946 to 1948 as its deputy chief.

✦ ✦ ✦

D. R. SHOULTS, currently the director of engineering for Aro, Inc., St. Louis, Mo., has been appointed director of the General Electric Company's Aircraft

Nuclear Propulsion Project for the Air Force and Atomic Energy Commission, C. W. Lapierre, manager of the company's Aircraft Gas Turbine Division, announced recently. The project is engaged in the further development of an atomic-powered engine for airplanes. Headquarters of the project will be at the company's Lockland, Ohio, turbojet research, engineering, and manufacturing center.

✦ ✦ ✦

ELMER E. NELSON moved to his new quarters in Sacramento, Calif., to assume his new duties as resident manager of the Aerojet Sacramento Division. The new rocket plant, located 16 miles northeast of Sacramento, was constructed for the purpose of augmenting the present Azusa, Calif., facilities in the production of solid propellant rocket motors.

✦ ✦ ✦

C. D. PERRINE, JR., former specialist in missile homing guidance systems, has been named assistant chief engineer in charge of electronics at Convair, San Diego.

✦ ✦ ✦

JOINT announcement has been made by Harry F. Guggenheim, president of the Daniel and Florence Guggenheim Foundation, Harold W. Dodds, president, Princeton University, and Lee A. DuBridge, president, California Institute of Technology, of the appointment of seven new Daniel and Florence Guggenheim Jet Propulsion fellows. The fellows, selected on the basis of their technical ability, deep interest in rockets and jet propulsion, and demonstrated leadership qualities, will carry out programs of advanced study and pioneering research at the Daniel and Florence Guggenheim Jet Propulsion Centers established by the Foundation at Princeton and Caltech late in 1948.

Recipients of the grants for study at Princeton are: Arnold Goldburg, Mahwah, N. J., a graduate student at Massachusetts Institute of Technology; Marcus P. Knowlton, II, Auburndale, Mass., now studying at Princeton University; Lt. D. M. Saunders, Takoma Park, Md., at present attending the U. S. Naval Postgraduate School at Annapolis, Md.; and Marcel Vinokur, Long Island City, N. Y., a senior at Cornell University.

The fellowships at the Caltech Center are awarded to: George E. Hlavaka, Racine, Wis., now studying toward a Ph.D. degree at Caltech; Robert C. Evans, Pittsburgh, Pa., at present a student in jet propulsion at Caltech; and Herman Carl Thorman, Berea, Ohio, a graduate student in the School of Aeronautics, Purdue University.

The fellowships carry a stipend of $2000 annually, and are normally awarded for one year, but may be renewed for an additional year. All the Princeton fellows appointed last year have had their grants renewed. These are Major Dale D. Davis, U.S.A.F., Effingham, Ill.; Clarence B. Cohen, Mt. Vernon, N. Y.; John E. Scott, Jr., Portsmouth, Va.; and David H. Ross, Chicago, Ill. Caltech fellows who have had their grants renewed are: Thomas C. Adamson, Jr., Lagrange, Ill.; Eldon L. Knuth, Launa, Iowa; and Edward E. Zukoski, Birmingham, Ala.

✦ ✦ ✦

THE Rocket Physics Department of the Aerojet Engineering Corp., as of July 18, 1951, is no longer a separate department. A consolidation has been effected between this department of the Research Division and the Liquid Engine and Proving Grounds Departments. The over-all supervision of the Liquid Engine Department remains in the hands of C. C. Ross, chief engineer, with R. B. Young as assistant chief engineer.

✦ ✦ ✦

RECENT changes in the executive staff of Reaction Motors, Inc., were announced by Charles W. Newhall, Jr., Executive Vice President. R. W. Young, formerly Vice President in charge of Engineering at Wright Aeronautical Corporation, has been elected President of R.M.I., replacing Lovell Lawrence, Jr., who resigned. H. B. Horne, Jr., has been appointed Manager of Engineering, and W. P. Munger, Chief Engineer, replacing H. R. Moles who resigned.

✦ ✦ ✦

ERNEST J. VOGT

One of the purposeful young men of rocketry, Ernest J. Vogt, passed on to his Creator during the early hours of September 27, 1951, at the age of forty. Although ill for many months, his mental faculties were unimpaired until he died, and to his great and constant satisfaction he was able to work on special development projects until the end.

Mr. Vogt began his technical career as a communications engineer, and had already achieved wide recognition for his contributions in this field when he was induced to join the starting nucleus of the Aerojet Engineering Corporation in 1942, thus launching a new career in rocket development. He was quickly promoted to Assistant Chief Engineer, but he later found that the most satisfactory means of expressing his high creative abilities was in the field of heading up self-contained special projects. Of the many important projects that he carried out, there is one that is sufficient in itself to earn him a permanent place on the honor roll of rocketry. He was the Aerojet engineer in charge of designing, building, and finally flight testing the power plant for the XP-79, the first United States airplane powered solely by rocket motors and actually flown. This was in the fall of 1943.

His interest in the broad aspects of rocket propulsion was always keen and imaginative, and he was a constant source of stimulation and enthusiasm to those who were fortunate to be his colleagues. It is reported by Mr. Andrew G. Haley, executor of Mr. Vogt's estate, that among the personal effects by his bedside when he died was an unfinished manuscript on the technical problems of space travel.

He leaves his two children, Andrew John, eight years of age, and Mary Michaela, aged six, and a great many personal friends in the American Rocket Society and elsewhere who mourn his passing.

American Rocket Society News

By A. F. BOCHENEK, *Associate Editor*

Record American Rocket Society Program for 1951 National Convention

THE record program of the 1951 National Convention to be held at the Chalfonte-Haddon Hall Hotel, Atlantic City, N. J., November 28–30, 1951, is ample evidence that the American Rocket Society provides an acknowledged national forum for men who are contributing to the field of jet propulsion and rocket technology.

The three-day program—consisting of five technical sessions at which 17 papers will be presented, an annual meeting of members, and a social program—is expected to attract many of the key figures in the rocket industry and in jet propulsion.

Because the ARS is an affiliate of The American Society of Mechanical Engineers, ARS members will be able to attend without paying any registration fee, the 1951 annual meeting of the ASME which is being held concurrently in the same hotel. The diversified ASME program touching on many engineering problems offers much of common interest to ARS members.

Annual Meeting

The ARS annual meeting will be held on Wednesday, at 9:30 a.m. President H. R. J. Grosch will open the meeting with a report of the Board of Directors. He will be followed by G. Edward Pendray, ARS treasurer, who will report on Society finances. A progress report on the year's activities in membership development will be presented by R. W. Porter, chairman of the Membership Committee.

Following election of a president, vice-president, directors and nominating committee for 1952, the meeting will hear an account of the Second International Congress on Astronautics held recently in London, England, from Lt. Comdr. F. C. Durant III, who was an official ARS delegate to the Congress.

ARS Section Luncheon

At the ARS Section Luncheon at noon Wednesday, important administrative and organizational problems will come under discussion. The luncheon is open to Section officers and official delegates of the individual sections. President Grosch will preside. He will report briefly on 1951 activities and will introduce official representatives of the following ARS Sections, who will report on local activities: New York, Indiana, Southern California, and New Mexico-West Texas.

The rapid growth of the rocket industry and the large number of engineers that are being enlisted to attack various rocket problems have created a need for more ARS Sections to serve the technical needs of these widely scattered centers of rocket interest. This problem will be discussed by R. W. Porter, chairman of the Membership Committee. The advisability of assigning the entire membership on a geographical basis to Sections already organized will be introduced for comment from the floor.

Of immediate interest to all members will be the comments of Martin Summerfield, Editor-in-Chief, on development of the new ARS Journal.

The luncheon program will end with a general discussion of future activities, especially the advisability of planning similar luncheons at future national conventions of the Society.

Honors Night

The high light of the convention will be the banquet and honors night on Thursday when the Society will pay tribute to creative engineers and scientists who by their work have advanced the technology of rocket and jet propulsion.

The main speaker will be the Honorable A. S. Alexander, Under-Secretary of the Army, who will discuss "Matters Relating to National Defense."

In a special ceremony awards will be presented as follows:

1. Goddard Memorial Lecture Award to Comdr. Robert C. Truax, U.S. Navy.
2. C. N. Hickman Award to Dr. William H. Avery, Supervisor, Propulsion Group, Applied Physics Laboratory, Johns Hopkins University, Silver Spring, Md.
3. G. Edward Pendray Award to George P. Sutton, consultant, North American Aviation, Los Angeles, Calif.
4. ARS Student Award to David Elliott and Leo Rosenthal.

Fellow memberships in the Society, acknowledging eminence in the field of rocket and jet propulsion engineering, will be bestowed on:

Chandler C. Ross, Aerojet Engineering Corporation, Azusa, Calif.

Benjamin F. Coffman, Jr., Ship Installations Division, Bureau of Aeronautics, Navy Dept., Washington, D. C.

E. H. Hull, General Electric Company, Schenectady, N. Y.

Charles E. Bartley, Jet Propulsion Laboratory, California Institute of Technology, Pasadena, Calif.

Col. H. N. Toftoy, chief, Rocket Branch, Research and Development Division, Office of Chief of Ordnance, Washington, D. C.

Technical Program

The tentative program follows:

3:00 p.m., Wednesday, November 28

Chairman: C. C. Ross, chief engineer, liquid engine department, Aerojet Engineering Corporation, Azusa, Calif.

Vice-Chairman: Powel Brown, rocket test engineer, special projects department, M. W. Kellogg Company, Jersey City, N. J.

Attitude Stabilization for Supersonic Vehicles, by C. W. Besserer, supervisor of engineering, and A. J. Bell, staff engineer, Applied Physics Laboratory, The Johns Hopkins University, Silver Spring, Md.

Some Experimental Dynamic Launching Techniques for Testing Aircraft Rockets, by A. W. Nelson, Naval Ordnance Test Station, Inyokern, Calif.

Unusual Applications of the Momentum Principle, by T. F. Reinhardt, U. S. Naval Air Rocket Test Station, Lake Denmark, Dover, N. J.

9:30 a.m. Thursday, November 29

Chairmen: J. H. Sheets, chief rocket design engineer, Curtiss-Wright Corporation, Propeller Division, Caldwell, N.J.

Vice-Chairman: M. Meyer, supervising project engineer, Curtiss-Wright Corporation, Propeller Division, Caldwell, N. J.

Installation of Rocket Engines in Airplanes, by F. A. Coss, Reaction Motors, Inc., Rockaway, N. J.

Description of the NOTS Aeroballistics Laboratory, by I. E. Highberg, Naval Ordnance Test Station, Inyokern, Calif.

The United States Air Force Experimental Rocket Engine Test Station, Edwards, Calif., by Lt. Richard A. Schmidt, chief, test engineering section,

Rocket Branch, and Donald L. Dynes, rocket engine test engineer, Rocket Branch, Edwards Air Force Base, Muroc, Calif.

2:30 p.m. Thursday, November 29

Chairman: Col. N. C. Appold, U. S. Air Force, chief, Power Plant Laboratory, Aeronautics Division, Wright Air Development Center, Dayton, Ohio.

Vice-Chairman: Lt. Col. E. N. Hall, U. S. Air Force, assistant chief, nonrotating engine branch, Power Plant Laboratory, Wright Air Development Center, Dayton, Ohio.

Isothermal Combustion Under Flow Conditions, by Capt. J. A. Bierlein and K. Scheller, power plant research engineers, Wright Air Development Center, Wright-Patterson Air Force Base, Dayton, Ohio.

Porous, Sweat and Film Cooling With Reactable Coolants, by Luigi Crocco, Robert H. Goddard Professor, The Daniel and Florence Guggenheim Jet Propulsion Center, Princeton University, Princeton, N. J.

High Flux Heat Transfer and Coke Deposition of JP-3, by J. B. Hatcher and D. R. Dartz, Jet Propulsion Laboratory, California Institute of Technology, Pasadena, Calif.

The Principle of the Concentric Nozzle, by W. F. Kaufman and B. N. Abramson, U. S. Naval Air Rocket Test Station, Lake Denmark, Dover, N. J.

9:30 a.m. Friday, November 30

Chairman: C. M. Hudson, technical assistant to the chief, Rocket Branch, Research & Development Division, Office of Chief of Ordnance, Washington, D. C.

Vice-Chairman: H. F. Calcote, Experiment, Inc., Richmond, Va.

Combustion Studies with a Rocket Motor Having a Full Length Observation Window, by Kurt Berman and Stanley E. Logan, General Electric Company, Malta Test Station, Ballston Spa, N. Y.

Photographic Techniques Applied to Combustion Studies — Two-Dimensional Transparent Thrust Chamber, by J. D. Thackrey and John H. Altseimer, development engineer, Aerojet Engineering Corporation, Azusa, Calif.

Experimental Problems in High Pressure Combustion, by R. L. Wehrli, chief physicist, Reaction Motors, Inc., Rockaway, N. J.

2:30 p.m. Friday, November 30

Chairman: George P. Sutton, supervisor, Aerophysics Laboratory, North American Aviation, Inc., Downey, Calif.

Vice-Chairman: O. K. Doyle, specialist, Aerophysics Laboratory, North American Aviation, Inc., Downey, Calif.

Flow Stability in Small Orifices by R. P. Northrup, General Electric Company, Malta Test Station, Ballston Spa, N. Y.

Injector Spray and Hydraulic Methods of Rocket Motor Analysis, by Kurt R. Stehling, rocket research engineer, Bell Aircraft Corporation, Buffalo, N. Y.

Fluctuations in a Spray Formed by Two Impinging Jets, by Marcus F. Heidmann, aeronautical research scientist, and Jack C. Humphrey, NACA Flight Propulsion Laboratory, Cleveland, Ohio.

Some Interactions of Circular Liquid Jets, by K. Dexter Miller, Jr., project engineer, special projects department, The M. W. Kellogg Company, Jersey City, N. J.

R. W. Porter Reviews V-2 Launching Program at New York Chapter Meeting

The work horse of high altitude research—the German-designed V-2—came in for some well-earned plaudits recently from Dr. R. W. Porter who is in charge of the U. S. Army's Guided Missile Project for the General Electric Company. With vehicles capable of carrying payloads as large as 4000 lb, the V-2 program made it possible for the personnel of two rocket proving grounds, 15 university research groups, and many government and industrial designers to "cut their teeth" in the relatively new art of building and launching rockets.

Dr. Porter spoke before 100 ARS members and guests of the New York Chapter of the American Rocket Society at its monthly meeting on October 19, 1951. While his topic was "V-2 Troubles" he made it abundantly clear that even from the launching failures valuable lessons were learned.

With the aid of German engineers and technicians, who eagerly turned over to American engineers available parts and records of the German V-2 program, the Army was able to launch successfully 45 V-2's out of 68 firings. Of these, 32 were perfect launchings with no malfunctioning of any of the components. The remaining 13 showed minor erratic behavior after take-off, although not serious enough to interfere with the research purposes of the firings.

This record, Dr. Porter said, was considerably better than that originally predicted by the German eng neers. Because of better workmanship in some of the American-produced components, the V-2's reached higher altitudes and carried heavier payloads than the V-2's fired in Germany, although the units were of exactly the same design.

In justifying the cost of the program, Dr.

(*Left to right:* L. D. White, director of Hermes Project, White Sands Proving Grounds, and director of ARS New Mexico Section. C. W. Chillson, consulting engineer, Curtiss Wright Corporation, and vice-president of ARS. R. W. Porter, division engineer, General Electric Company, Schenectady, N. Y., and director of ARS. Lee J. Bregenzer, design engineer, Port of New York Authority, New York, N. Y., and director of ARS New York Section. Roy Healy, division head, operating division, M. W. Kellogg Company, Jersey City, N. J., and past president of ARS.)

Porter pointed out that the firings saved the nation time and money in training research personnel, firing crews, and industrial designers, and produced some interesting and useful upper atmosphere data which could be obtained in no other way than by full-scale tests on actual rockets of the size of the V-2.

Dr. Porter praised the aid given the Government by the 15 American universities who voluntarily organized an Upper Atmosphere Research Panel to advise on the use of the V-2's. Government agencies gladly accepted the aid of the panel and turned over to it the responsibility of allocating payloads of successive V-2's to various research projects.

Eight of the firings were of the two-stage type, using a V-2 to launch a smaller Wac Corporal. The perfection of a multiple staging technique is considered one of the most significant results of the program. But the record of achievement, made possible by the large V-2 payloads and the ingenuity of the co-operating research teams, contained a long list of aerodynamic, heat-transfer, and component-design data.

In the rundown of the firing failures, Dr. Porter attributed 22 to poor design, wearout, and poor workmanship of components, 8 to inexperience in launching technique, 4 to special experiments conducted in connection with the firings, 1 to personnel laxity, and 1 to a random cause. Dr. Porter expressed confidence that in a like number of future firings no more than 5 failures would occur.

The evening ended with a short film on V-2 operations and a discussion period followed by refreshments.

ARS Joins International Astronautical Federation

By Lt. Comdr. F. C. Durant III (U.S.N.)

ON September 3–8, 1951, the Second International Astronautical Congress was held in London, England. Host for the week-long convention was the British Interplanetary Society. The purpose of this Congress was to establish an International Astronautical Federation and to present technical papers on the problems of realizing earth satellite vehicles and interplanetary travel. Presiding at the Congress was Provisional President Dr. Eugen Sänger who was elected as first President of the International Astronautical Federation. Dr. G. Loeser (G.f.W.) and Andrew G. Haley (ARS) were elected Vice-Presidents for matters relating to Europe and the United States, respectively. Also attending the Congress were Prof. Herman Oberth and Dr. Irene Bredt.

In addition to the United States and Great Britain, authorized delegates were present from societies in France, Sweden, Germany (British and U. S. Zones), Austria, Switzerland, Italy, Spain, and Argentina. Representing the American Rocket Society, Andrew G. Haley, as General Counsel, was principal delegate on parliamentary matters, and Lt. Comdr. Frederick C. Durant III (U.S.N.) acted as principal delegate on technical matters.

Lt. Comdr. Durant presented a paper for ARS member Dr. Wernher von Braun, entitled "The Importance of Satellite Vehicles in Interplanetary Flight." The subject of this paper was the keynote of the Congress. The importance of the artificial satellite as a take-off point for interplanetary travel received complete acceptance by the assembled delegates. Dr. von Braun's paper was actually a synopsis of a book, entitled "Mars Project," to be published shortly. The scientific appendix of this work presents data and calculations showing that the artificial satellite and subsequent circumplanetary flight are technically feasible today if money, personnel, material, and technical direction were made available. This realization that the manned, artificial satellite is a logical and expected step beyond current rocket-powered missiles has never before been so universally accepted by professional engineers and scientists.

The Detroit Rocket Society, Pacific Rocket Society, and Reaction Research Society were represented by E. V. Sawyer and David Elliott.

Steps were taken to standardize nomenclature and symbols relating to rocket propulsion and astronautics. In addition, a home address in Switzerland is being obtained. An international archive has been established to provide reference material on subjects relating to astronautics. Ing. Josef Stemmer of Baden will coordinate this effort. Vice-Presidents Loeser and Haley were directed to prepare a draft constitution, which will be circulated to the member societies prior to the next meeting. The next meeting of the Federation will be in 1952 at Stuttgart.

PRINCIPAL DELEGATES PRESENT AT SECOND INTERNATIONAL ASTRONAUTICAL CONGRESS

Country	Society	Location	Principal Delegates
Great Britain	British Interplanetary Society	London	Arthur C. Clarke A. V. Cleaver
Germany	Gesellschaft für Weltraumforschung	Stuttgart	Dr. G. Loeser Heinz H. Kölle
	Nordwestdeutsche G.f.W.	Frankfurt	Albert Stemmer F. K. Jungclaas
Austria	Osterreichische G.f.W.	Innsbruck	Friedrich Hecht
France	Groupement Astronautique Français	Paris	A. Ananoff
Sweden	S.I.S.	Stockholm	Ing. Åke Hjerstrand
Switzerland	A.S. für Weltraumforschung	Baden	Ing. Josef A. Stemmer
Italy	A.I.R.	Bologna	Dr. Giovanni Casiraghi Prof. Eula Capt. F. Partel
Spain	A.E.A.	Madrid	Tomas Mūr
Argentina	Sociedad Argentina Interplanetaria	Buenos Aires	Prof. Teofilo M. Tabanera

Butterfly POWER...
• MICROTORQUE Variable Resistors and Potentiometers require as little as .003 in. oz. torque to operate. This unique feature makes the MICROTORQUE invaluable for applications where the position of instrument pointers, gyroscopes, and delicate instruments in general must be recorded, transmitted or indicated at a distance, and Giannini are the sole makers of MICROTORQUE Potentiometers.
A variety of resistance values and circuits available.
Write for booklet.
G. M. Giannini & Co., Inc.
Pasadena 1, California
giannini

Technical Literature Digest

By H. S. SEIFERT, California Institute of Technology, *Associate Editor*

CONTRIBUTORS: D. Altman, D. I. Baker, R. B. Canright, F. C. Gunther, S. S. Penner, H. S. Seifert

EDITOR'S NOTE:

The following collection of references is not intended to be comprehensive, but is rather a selection of the most significant and stimulating papers which have come to the attention of the contributors. The reader will understand that a considerable body of literature is unavailable because of security restrictions. We invite contributions to this department of references which have not come to our attention, as well as comment on how the department may better serve its function of providing leads to the jet propulsion applications of many diverse fields of knowledge.

Book Reviews

ROCKETS, MISSILES AND SPACE TRAVEL, by Willy Ley, The Viking Press, New York, 1951, xii + 436 pp. $5.95.

Reviewed by H. S. SEIFERT

THE popular appeal of the subject of rockets and space travel is demonstrated by the fact that this volume of Mr. Ley's is essentially a sixth edition of "Rockets," first published in 1944. Spanish, Italian, and German editions also exist.

"Rockets, Missiles and Space Travel" is a history of rocketry, compiled in roughly chronological order, which describes the efforts and hardships of the early visionaries and rocket experimentalists, and which shows how their dreams have been in part fulfilled. It is written with great sympathy and insight into the lives and thoughts of these men, and is well garnished with incidents calculated to emphasize the human and dramatic aspects of their lives. Mr. Ley is in an advantageous position to do this since he himself was a charter member and officer of the original German rocket society, the VfR (Verein für Raumschiffahrt).

The book contains chapters on the early classical period of the concept of space flight, the Jules Verne or fantasy era, the first weapon rockets, and the Russian, French, German, and American pioneers. This material is followed by three chapters new to this edition: One on weapon rockets, one on the German rocket development center at Peenemunde, and the last on the corresponding American center at White Sands Proving Ground in New Mexico. The concluding chapters on orbital rockets, the space ship, and the space terminal are largely discussions of the dynamics of long-range flight, with little emphasis on the speculative subjects of vehicle design or pilot physiology.

The 90 pages of appendixes contain an interesting assortment of relatively new information, including a discussion of rocket airplanes, the characteristics of various missiles, and tables relating to space travel such as meteorite and other astronomical data. There is a reasonably complete bibliography of rocket literature, including a section on imaginative literature!

The book is popular rather than technical in content, written with emphasis on the dramatic, and in a discursive and at times even rambling style. Nevertheless, it will interest serious workers in rocketry for the wealth of incidental information and anecdote which it supplies. Physical concepts are accurately and soundly discussed, and illustrations are plentiful. The reviewer is impressed by the author's evident enthusiasm and the breadth of his information. While this volume cannot be considered to be a textbook of rocket principles, it nevertheless should be available in every jet propulsion library as a historical source book.

THE STRUCTURE AND MECHANICAL PROPERTIES OF METALS, by Bruce Chalmers, John Wiley & Sons, Inc., New York, N. Y., 1951, ix + 132 pp. $3.50.

Reviewed by LAWRENCE J. HULL

THE object of the author in "The Structure and Mechanical Properties of Metals" is to provide a simple, easily understood picture of the structure of metals and the relation of the structure to the mechanical properties. Dr. Chalmers has accomplished this objective to a high degree without resort to mathematical considerations. He explains the theory of structure of pure metals, then enlarges the picture to include alloys. This is supplemented by chapters describing the effects of distortion and heat treatment on structure. A short chapter is included on the general determination of structure, followed by an excellent treatment of mechanical properties and their dependence on structure. This chapter should be quite useful for the engineer who desires an easily understood and well presented source of information on what mechanical properties are and what they mean.

The book adheres to the material described by the title and is not a work on general metallurgy nor a reference handbook. Inaccuracies may be noted by the careful reader, some of which appear in the tabular data. It is assumed that the reader has a general background in physics and chemistry and that many common engineering terms will be understood. The book is recommended to the engineer who does not have a general knowledge of the subject and who is seeking a readable account of it. It is recommended to the practicing metallurgical or mechanical engineer only for review.

Books

Introduction to the Transfer of Heat and Mass, by E. R. G. Eckert, McGraw-Hill Book Co., Inc., New York, N. Y., 1950.

The Handbook of Measurement and Control, by M. F. Behar, The Instruments Publishing Co., Inc., Pittsburgh, Pa., 1951.

Flow Measurement with Orifice Meters, by R. F. Stearns and others, D. Van Nostrand Co., Inc., New York, N. Y., 1951.

Guided Missiles: Rockets and Torpedoes, by Frank Ross, Lothrop, Lee and Shepard Co., Inc., New York, N. Y., 1951, 186 pp.

The Physics of Powder Metallurgy (a symposium), by Walter E. Kingston, McGraw-Hill Book Co., Inc., New York, N. Y., 1951, 404 pp., $8.50.

Handbook of Supersonic Aerodynamics, NAVORD Report 1488, The Johns Hopkins Univ., APL, Silver Spring, Md., July 15, 1951.

Jet Propulsion Engines

Investigations of Axial Flow Compressors, by J. T. Bowen, R. H. Sabersky, and W. D. Rannie, *Transactions of The American Society of Mechanical Engineers*, vol. 73, January, 1951, pp. 1–15.

U. S. Research Project SQUID: Rocket, Ramjet and Pulse-Jet, by Hugh Harvey, *Shell Aviation News*, August, 1950, pp. 16–18.

Burners for Supersonic Ramjets, by J. B. Fenn, H. B. Forney, and R. C. Garmon, *Industrial and Engineering Chemistry*, vol. 43, July, 1951, pp. 1663–1672.

The Solid Fuel Ramjet, by E. F. Chandler, *Aero Digest*, vol. 61, September 1950, pp. 19, 86, 87.

Air Inlets, by Robert McLarren, *Aero Digest*, vol. 62, April, 1951, pp. 75–85.

An Analysis of Helicopter Propulsion Systems, by J. A. Johnson, *Transactions of The American Society of Mechanical Engineers*, vol. 73, July, 1951, p. 519.

The Generalized Approach to the Selection of Propulsion Systems for Aircraft, by L. R. Woodworth and C. C. Kelber, Institute of the Aeronautical Sciences, Preprint No. 345, 1951.

On the Theory of the Stationary and Pulsating Ramjet Engine (in German), by E. Sänger, *Schweiz. Arch.*, vol. 16, November-December, 1950, pp. 11, 341-352, 369–378.

Rocket Propulsion Engines

Determination of Rocket-Motor Heat-Transfer Coefficients by the Transient Method, by Stanley Greenfield, *Journal of the Aeronautical Sciences*, vol. 18, August, 1951, p. 512.

Heat Transfer in Rocket Motors and the Application of Film and Sweat Cooling, by R. H. Boden, *Transactions of The American Society of Mechanical Engineers*, vol. 73, May, 1951, pp. 385–390.

Rocket Linings, by W. H. Duckworth, *Aviation Week*, vol. 54, June 25, 1951, p. 31.

Survey of Development of Liquid Rockets in Germany and Their Future Prospects, by W. von Braun, *Journal of the British Interplanetary Society*, vol. 10, March, 1951, pp. 75–80.

The Effect of Solid Particles in Rocket Exhausts, by N. J. Bowman, *Journal of Space Flight*, vol. 3, June, 1951, pp. 1–15.

The Use of Auxiliary Rockets in High-Speed Aircraft, by Zb. Plaskowski, *Aircraft Engineering*, vol. 23, March, 1951, pp. 72–75.

Heat Transfer and Fluid Flow

Heat Transfer to a Fluid Flowing Turbulently in a Smooth Pipe With Walls at Constant Temperature, by R. A. Seban and T. T. Shimazaki, *Transactions of The American Society of Mechanical Engineers*, August, 1951, pp. 803–809.

A Study of the Mechanism of Boiling Heat Transfer, by W. M. Rohsenow, *Transactions of The American Society of Mechanical Engineers*, vol. 73, July, 1951, p. 609.

A Summary of Viscosity and Heat-Conduction Data for He, A, H_2, O_2, CO, CO_2, H_2O and Air, by F. G. Keyes, *Transactions of The American Society of Mechanical Engineers*, vol. 73, July, 1951, p. 597.

Investigation of Turbulent Flow and Heat Transfer in Smooth Tubes, Including the Effects of Variable Fluid Properties, by R. G. Deissler, *Transactions of The American Society of Mechanical Engineers*, vol. 73, February, 1951, pp. 101–107.

Fluid Flow through Porous Metals, by Leon Green, Jr., and Pol Duwez, *Journal of Applied Mechanics*, vol. 18, March, 1951, pp. 39–45.

Flow of Gases in Porous Media, by by L. H. Wilson, W. L. Sibbitt, and M. Jakob, *Journal of Applied Physics*, vol. 22, August, 1951, pp. 1027–1030.

Vaporization Rates and Heat Transfer Coefficients for Pure Liquid Drops, by Robert D. Ingebo, NACA Technical Note 2368, July, 1951.

The Rate of Evaporation of Droplets. V. Evaporation Characteristics of Some Branched-Chain Hydrocarbons and a Straight-Chain Fluorocarbon, by R. S. Bradley and G. C. S. Waghorn, *Proceedings of the Royal Society of London, Series A*, vol. 206, March 22, 1951, pp. 65–72.

Some Kinematic Properties of Munroe Jets, by W. M. Evans, *Research*, vol. 3, August, 1950, pp. 376–378.

Aerodynamic Heating at High Speeds, by T. Nonweiler, *Journal of the British Interplanetary Society*, vol. 10, July, 1951, pp. 160–176.

Boundary Layers and Skin Friction in High-Speed Flow, by A. D. Young, *Journal of the Royal Aeronautical Society*, vol. 55, May, 1951, pp. 285–301.

Investigations Concerning Flow Conditions in a Centrifugal Pump, and the Effect of Blade Loading on Head Slip, by J. F. Peck, *The Institution of Mechanical Engineers*, vol. 164, 1951, p. 1.

Solution of Certain Unsteady Heat Flow Problems by Relaxation Methods, by A. Gilmour, *British Journal of Applied Physics*, vol. 2, July, 1951, pp. 199–204.

An Air-Flow Analogy for the Solution of Transient Heat Conduction Problems, by M. B. Coyle, *British Journal of Applied Physics*, vol. 2, January, 1951, pp. 12–18.

Compressible Flows, by J. D. Kelley, *American Journal of Physics*, vol. 19, April, 1951, pp. 237–243.

Note on Desirability of Completely Expanded Nozzles, by C. B. Cohen and P. J. Evans, Jr., *Journal of the Aeronautical Sciences*, vol. 17, December, 1950, pp. 811–812.

Combustion

Net Heat of Combustion of AN-F-58 Aircraft Fuels, by S. Rothberg and R. S. Jessup, *Industrial & Engineering Chemistry*, vol. 43, April, 1951, pp. 981–985.

Method for Determining Distribution of Luminous Emitters in the Cone of a Laminar Bunsen Flame, by T. P. Clark, NACA Technical Note 2246, 1951, 28 pp.

Method of Calculating the Combustion Temperature of Gas Mixtures, by H. Wolff, *Zeitschrift für Elektrochemie*, vol. 54, 1950, pp. 556–560.

Explosive Sensitivity of Ammonium Nitrate-Hydrocarbon Mixtures, by M. A. Cook and E. L. Talbot, *Industrial and Engineering Chemistry*, vol. 43, May, 1951, pp. 1098–1102.

Thermodynamics and Chemical Kinetics of One-Dimensional Nonviscous Flow Through a Laval Nozzle, by S. S. Penner, *Journal of Chemical Physics*, vol. 19, 1951, pp. 877–881.

Detonation of Secondary Explosives by an Electric Spark (in French), by R. Schall, *Comptes rendus*, vol. 233, 1951, pp. 706–708.

Elementary Processes Occurring in the Boudouard-Reaction (i.e., $2CO = CO_2 + C_{solid} + 41K$ cals) and Burning of Coal at Elevated Temperatures (in German), by H. Behrens, *Naturwissenschaften*, vol. 8, 1951, p. 187.

Chemiionization in Flames (Ionization induced by excessive concentrations of free radicals) (in German), by H. Behrens, *Naturwissenschaften*, vol. 8, 1951, pp. 187–188.

On the Kinetics of Establishing of Equilibrium in Flames (in German), by H. Behrens, *Zeitschrift für Physikalische Chemie*, vol. 195, 1951, pp. 329–336.

On the Structure and Combustion Kinetics of Diffusion Flames (in German), by H. Behrens, *Zeitschrift für Physikalische Chemie*, vol. 197, 1951, pp. 1–5.

Self-Excitation of Flame Oscillations in Cylindrical Tubes (in German), by H. Behrens, *Zeitschrift für Physikalische Chemie*, vol. 197, 1951, pp. 6–16.

Initiatium of Explosions in Liquids. Measurement of the Transient Pressures During Impact, by P. Gay, *Transactions of the Faraday Society*, vol. 46, pp. 848–852.

The Theory of Flame Propagation II, by J. O. Hirschfelder and C. F. Curtiss, *The Journal of Physical and Colloid Chemistry*, vol. 55, 1951, pp. 774–788.

Physicochemical Aspects of the Combustion of Solid Fuels, by J. R. Arthur and J. R. Bowring, *Industrial and Engineering Chemistry*, vol. 43, 1951, pp. 528-533.

Burning Velocities of Propane-Air Mixtures, by F. H. Garner, R. Long, and G. K. Ashforth, *Fuel*, vol. 30, 1951, pp. 63–66.

A Comparison of Quenching Distance and Inflammability Limit Data for Propane-Air Flames, by Dorothy Martin Simon, *Journal of Applied Physics*, vol. 22, 1951, p. 103.

Pre-Combustion Chemical Reactions in Engines, by O. Widmaier, *Brennstaff-Chemie*, vol. 32, 1951, pp. 104–110.

Ignition of Methane-Air Mixtures by Rapid Compression, by A. C. Edgerton, N. P. W. Moore, and W. T. Lyn, *Nature*, vol. 167, 1951, pp. 191–192.

Study of the Flame-Stability Characteristics of Different Vaporized Fuels in a Small-Scale Combustion Chamber, by R. J. Wakelin, R. Heran, and R. R. Baldwin, *Fuel*, vol. 30, 1951, pp. 82–91.

Flame Speeds in Hydrazine Vapour and in Mixtures of Hydrazine and Ammonia with Oxygen, by R. C. Murray, *Transactions of the Faraday Society*, vol. 47, July, 1951, pp. 743–751.

The Oxidation, Decomposition, Ignition, and Detonation of Fuel Vapors and Gases, by R. O. King, *Canadian Journal of Technology*, vol. 29, August, 1951, pp. 382–390.

A Discussion on Detonation, by W. G. Penney and others, *Proceedings of the Royal Society of London, Series A*, vol. 203, November, 1950, pp. 1–33.

The Cool Flame of Methyl Ethyl Ketone, by J. Bardwell and Sir Cyril Hinshelwood, *Proceedings of the Royal Society of London, Series A*, vol. 205, February 22, 1951, pp. 375–390.

Spectroscopic Studies of Low-Pressure Flames V. Evidence for Abnormally High Electronic Excitation, by A. G. Gaydon and H. G. Wolfhard, *Proceedings of the Royal Society of London, Series S*, vol. 205, January 22, 1951, pp. 118–134.

Flame Spectra of Systems with NO^2 Groups (in German), by H. Behrens and F. Rössler, *Zeitschrift für Naturforschung*, vol. 6a, 1951, pp. 154–160.

Spectra and Kinetics of NO-Containng Flames (in German), by H. Behrens, *Zeitschrift für Elektrochemie und Angewandte Physikalische Chemie*, vol. 54, 1950, pp. 535–538.

The Emission of Flame Spectra, by A. G. Gaydon, *Quarterly Reviews of the Chemical Society of London*, vol. 4, 1950, pp. 1–19.

Kinetics of OH Radicals From Flame Emission Spectra III. Total Transition Probabilities and the Energetic Distribution of $OH(^2\Sigma^+)$ and $O_2(^3\Sigma_u^-)$ in the Oxy-Hydrogen Flame, by K. E. Shuler, *Journal of Chemical Physics*, vol. 19, July, 1951, pp. 888–894.

Elementary Reaction in the Gas Phase Involving Excited Electronic States, by K. J. Laidler and K. E. Shuler, *Chemical Reviews*, vol. 48, April, 1951, pp. 153–224.

Fuels, Propellants, and Materials

Kinetics of the Polymorphic Changes in NH_4NO_3 General Character of the Kinetics of the IV–III Conversion, by B. V. Erofeev and N. I. Mitskevich, *Zhur. Fiz. Khim.*, vol. 24, 1950, pp. 1235–1251.

Stabilizer for Hydrogen Peroxide, by J. Isemura and S. Nakamura, *Science (Japan)*, vol. 19, 1949, pp. 379–380.

Force Constants, Frequency Assignments, and Thermodynamic Properties of Ozone, by M. J. Klein, F. T. Cleveland, and A. G. Meister, *Journal of Chemical Physics*, vol. 19, August, 1951, p. 1068.

The Freezing-Point Diagram of the Hydrazine-Water System, by T. C. H. Hill and J. F. Sumner, *Journal of Chemical Society*, March, 1951, pp. 838–40.

The Heat of Dissociation of Fluorine, by R. N. Doescher, *Journal of Chemical Physics*, vol. 19, August, 1951, p. 1070.

Autoxidation of Hydrazine, by L. F. Audrieth and P. H. Mohr, *Industrial and Engineering Chemistry*, vol. 43, August, 1951, p. 1774.

Ignition Temperatures of Magnesium and Magnesium Alloys, by W. M. Fassell, *Journal of Metals*, vol. 3, July, 1951, p. 522.

The Manufacture of Sintered Alumina Ware, by R. Scott, *Metallurgia*, vol. 43, July, 1951, pp. 50–52.

The Preparation of Alumina Bodies by the Slip-Casting Method, by W. Watt and J. P. Roberts, *Metallurgia*, vol. 43, June, 1951, pp. 307–308.

Engineering Materials in Ordnance Equipment, by B. S. Mesick, *Materials and Methods*, vol. 33, May, 1951, p. 59.

Titanium and Its Alloys, by Anderson Ashburn, *American Machinist*, vol. 95, June 11, 1951, p. 146.

Linear Thermal Expansion of Artificial Graphites to 1,370 C., by M. D. Burdick, *Journal of Research*, vol. 47, July, 1951, pp. 35–40.

Some Mechanical Properties of Graphite at Elevated Temperatures, by C. Malmstrom, R. Keen, and L. Green, Jr., *Journal of Applied Physics*, vol. 22, May, 1951, pp. 593–600.

An Introduction to Arc-Cast Molybdenum and Its Alloys, by J. L. Ham, *Transactions of The American Society of Mechanical Engineers*, vol. 73, August, 1951, pp. 723–732.

SCINTILLA MAGNETO DIVISION

BENDIX AVIATION CORPORATION

SIDNEY, NEW YORK

Manufacturers of Ignition Systems for Jet, Turbine and Piston Power Plants, Fuel Injection Equipment for Railway, Marine and Industrial Diesel Engines, Electrical Connectors, Ignition Analyzers, Moldings and Special Components.

High Temperature Steels and Alloys for Gas Turbines, by T. Bishop, *Metal Progress*, vol. 59, May, 1951, pp. 653–656, 690–696.

Some Properties of Beryllium Oxide and Beryllium Oxide-Niobium Ceramals, by C. F. Robards and J. J. Gangler, NACA Research Memo E50G21, March, 1951, 18 pp.

Physical-Chemical Topics

Availability and Irreversibility in Thermodynamics, by Joseph H. Keenan, *British Journal of Applied Physics*, vol. 2, July, 1951, pp. 183–192.

Irreversibility and Generalized Noise, by H. B. Calhn and T. A. Welton, *Physicals Review*, vol. 83, 1951, pp. 34–40.

Viscosity Behavior of Gases, by L. A. Bromley and C. R. Wilke, *Industrial and Engineering Chemistry*, vol. 43, July, 1951, pp. 1641–1648.

Symposium on Anomalies in Reaction Kinetics—Four Sessions, *Journal of Physical and Colloid Chemistry*, vol. 55, June, 1951.

Air Condensation in Hypersonic Flow, by P. Wegener, S. Reed, Jr., E. Stollenwerk, and G. Lundquist, *Journal of Applied Physics*, vol. 22, August, 1951, pp. 1077–1085.

Recent Theories of Transport Processes in Liquids, by R. Eisenschitz, *Nature*, vol. 167, February, 1951, pp. 216–220.

Instrumentation and Experimental Techniques

A Method for Correcting Orifice-Meter Measurements for Flow Pulsations, by E. V. Hardway, Jr., *Instruments*, vol. 24, July, 1951, pp. 763–765.

A New Flash Illumination Unit for Ballistic Photography, by H. F. Quinn and O. J. Bourque, *Review of Scientific Instruments*, vol. 22, February, 1951, pp. 101–105.

A Study of Head Loss in Venturi-Meter Diffuser Sections, by Joel Warren, *Transactions of The American Society of Mechanical Engineers*, vol. 73, May, 1951, pp. 399–402.

An Analog Computer for Flame Gas Composition, by W. S. McEwan and S. Skolnik, *Review of Scientific Instruments*, vol. 22, March 1951, pp. 125–133.

An Electromagnetic Flowmeter for Transient Flow Studies, by J. S. Arnold, *Review of Scientific Instruments*, vol. 22, January, 1951, pp. 43–47.

Discharge Measurements by Means of Venturi Tubes, by A. L. Jorissen, *Transactions of The American Society of Mechanical Engineers*, vol. 73, May, 1951, pp. 403–411.

Measurement of Velocity and Pressure of Gases in Rocket Flames by Spectroscopic Methods, by F. P. Bundy, H. M. Strong, and A. B. Gregg, *Journal of Applied Physics*, vol. 22, August, 1951, pp. 1069–1077.

High-Speed Sampling Techniques, by B. R. Shepard, *Electronics*, vol. 24, August, 1951, pp. 112–115.

REACHING NEW HORIZONS

HISTORIC EVENTS IN
REACTION MOTORS' DECADE OF ROCKET DEVELOPMENT

The Navy's Douglas Skyrocket has attained "the highest speeds and altitudes ever recorded by a piloted aircraft," proving the routine practicality of flying far beyond the speed of sound. As in the Air Force's historic X-1, the Skyrocket's successful rocket engine was designed and built by REACTION MOTORS.

The broadest background of research and development in the field have produced an incomparable record of rocketry achievements for Reaction Motors, Inc. . . . progress so continuous that yesterday's rocket engines already are obsolete. If you haven't talked with RMI *today*, you do not know the newest developments in rocket power for piloted aircraft, guided missiles and many other applications.

RMI

SINCE 1941—THE FIRST NAME IN ROCKETRY

PERMANENT POSITIONS FOR TOP MEN—unmatched opportunity to do original research with the longest established organization in this field of the future. Design and layout draftsmen—stress analysts—electronic instrumentation engineers — mechanical engineers — are needed by our expansion program. Send resume or telephone Personnel Director.

REACTION MOTORS, INC., Rockaway, New Jersey

Induction Method for Measuring Fluid Flow, by A. J. Morris, *Electrical Engineering*, vol. 70, June, 1951, p. 529.

Instruments for Upper Atmosphere and Interplanetary Navigation, by J. C. Bellamy, *Navigation*, vol. 2, December, 1950, pp. 272–275.

Kerr Cell Photography of High Speed Phenomena, by E. M. Pugh, R. v. Heine-Geldern, S. Foner, and E. C. Mutschler, *Journal of Applied Physics*, vol. 22, April, 1951, pp. 487–493.

Power Unit for High-Intensity Light Source, by A. E. Young, S. McCullough, and R. L. Smith, NACA Research Memo E50K27, July 9, 1951.

Solar Furnace for High Temperature Research, by W. M. Conn, *American Ceramic Society Bulletin*, vol. 30, 1951, pp. 163–164.

Step Multiplier in Guided Missile Computer, by Edwin A. Goldberg, *Electronics*, vol. 24, August, 1951, pp. 120–124.

Study of Linear-Resistance Flowmeters, by F. W. Fleming, *Transactions of The American Society of Mechanical Engineers*, vol. 73, July, 1951, p. 621.

The Long Range Proving Ground, by Robert D. Hullihan, *Ordnance*, vol. 36, July–August, 1951, pp. 158–160.

The Trajectograph ONERA (in French), by I. Podiasky, *La Recherche Aéronautique*, Nov.–Dec., 1950, pp. 35–43.

Use of Image Converter Tube for High-Speed Shutter Action, by A. W. Hogan, *Proceedings of the Institute of Radio Engineers*, vol. 39, March, 1951, pp. 268–270.

Woomera; Post-War Progress with British Guided Missiles; The Australian Rocket Range, *Flight*, vol. 59, April 13, 1951, pp. 429–431.

Flight, Ballistics, and Vehicle Development

Research with High-Speed (Rocket-Powered) Models, Anonymous. *Aeroplane*, vol. 81, August 17, 1951, pp. 190–192.

Fundamental Dynamics of Reaction-Powered Space Vehicles, by L. N. Thompson, *Aircraft Engineer*, vol. 23, August, 1951, p. 228.

The Evasion of Hazardous Objects in Space, by Wayne Proell, *Journal of Space Flight*, vol. 3, May, 1951, pp. 1–9.

Meteors and Space Travel, by Michael W. Ovenden, *Journal of the British Interplanetary Society*, vol. 10, July, 1951, pp. 176–180.

Evolution of the Guided Missile, by K. W. Gatland, (Series beginning May 4th) *Flight*, vol. 60, August 3, 1951, pp. 140–143

Motion Relative to the Surface of the Rotating Earth, by R. H. Bacon, *American Journal of Physics*, vol. 19, January, 1951, pp. 52–56.

On the Accuracy of Long-Range Ballistic Rockets, by W. E. Frye, *Journal of Applied Physics*, vol. 22, May, 1951, pp. 585–589.

What Will Space Flight Require? Eugen Sänger, *Rocketscience*, vol. 5, June, 1951, pp. 26–33.

The Lunar Base, by G. V. E. Thompson, *Journal of the British Interplanetary Society*, vol. 10, March, 1951, pp. 49–70.

Long-Distance Rocket Flight, Anonymous, *Mechanical Engineering*, vol. 73, August, 1951, p. 656.

Orbital Rockets: I Some Preliminary Considerations, by Kenneth W. Gatland; II The Rocket Structure with Special Reference to Expendable Construction, by Alan E. Dixon; III Conception of an Instrument-Carrying Orbital Rocket,

SILENCE
Jet Engine
Roar!

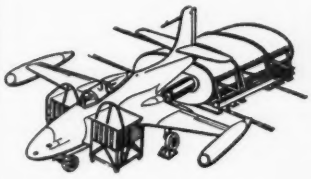

with the
Industrial Sound Control
PORTABLE
JET TEST MUFFLER
• Dampens Noise Efficiently
• Deflects hot gases safely
• Easily moved anywhere

Bring the test cell to the plane with this revolutionary portable jet test muffler. Jet engines with or without after-burners can be tested right in the plane.

Foreign: Cementation (Mufflite) Limited London
Licencées: Les Travaux Souterrains Paris

Industrial Sound Control, Inc.
45 GRANBY STREET
HARTFORD, CONN.
2119 SEPULVEDA BLVD. LOS ANGELES, CALIF.

TRACK SHOCKPROOF
MOBILE RECORDER
FOR INDUSTRY & SCIENCE

Ampex specializes in designing and manufacturing custom-built recording equipment to meet your requirements. A few of the many proven applications are illustrated.

AX-49

PRECISION & PERFORMANCE

AMPEX
Magnetic Tape RECORDERS
AMPEX ELECTRIC CORPORATION
Redwood City . . . . California

Unrivalled for AUDIO & INSTRUMENTATION Recording

AMPEX
Performance Includes . . .
• STANDARD MODELS to 80,000 cps
• CUSTOM BUILT MODELS to 100,000 cps
• LOW FLUTTER MODELS less than 0.1% PEAK-TO-PEAK
• LOW FREQUENCY MODELS 0 to 5,000 cps (FM System)

AMPEX RECORDERS are available with 1 to 14 tracks using ¼" to 1" tape.

by Anthony M. Kunesch, *Journal of the British Interplanetary Society*, vol. 10, May, 1951, pp. 97–115.

Other Classifications

(Meteorology, Astrophysics, etc.)

A Preliminary Study of a Physical Basis of Bird Navigation, by H. L. Yeagley, *Journal of Applied Physics*, vol. 22, June, 1951, pp. 746–760.

The Effects of Time and Temperature Upon Tolerance to Positive Acceleration, by Erneste Martin and James P. Henry, *Technical Data Digest*, vol. 16, June, 1951, pp. 19–23.

Physics and Psychophysics of Weightlessness, by H. Haber, *Journal of Aviation Medicine*, June, 1951, p. 180.

Influence of Certain Anti-Motion-Sickness Drugs on Psychomotor and Mental Performance, by R. A. MacKay, *Journal of Aviation Medicine*, June, 1951, p. 194.

Biological Problems of Space Flight, by J. B. Haldane, *Journal of the British Interplanetary Society*, vol. 10, July, 1951, pp. 154–158.

Physiological Endurance in Jet Missiles (in Italian), by G. A. Crocco, *Termotecnica*, vol. 5, February, 1951, pp. 55–59.

Radiation Effects on Man in Space, by Conrad Buettner, *American Meteor Society Bulletiin*, May, 1951, p. 183.

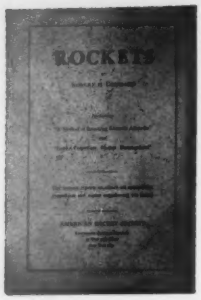

ROCKETS

by

Dr. R. H. Goddard

A theoretical and experimental classic by the rocket pioneer. Includes "A Method of Reaching Extreme Altitudes" and "Liquid Rocket Propellant Development." 1946, 111 pages. Price $3.50. Order from the American Rocket Society, 29 West 39th Street, R-719, New York 18, N. Y.

GROVE

SELF-ACTUATED

CONTROLS AND REGULATORS

for

High pressure liquids and gases

•

Pressure Reducing
Back Pressure
Relief and By-Pass
Manual Valves

•

Special light weight units
for air-borne service.

•

Special materials for corrosive
or low-temperature applications.

•

GROVE REGULATOR COMPANY

Oakland
Los Angeles
Houston
New York

C. B. KAUPP & SONS

SPINNINGS

IN FLIGHT

Close Tolerance
Sheet Metal Fabrication

Complete Tool Shop

Deep Drawing - Press Work

Welding

Experimental Work
With All Types of Metals

Metal Spinning Since 1900

32 NEWARK WAY
MAPLEWOOD, N. J.

PIERCING THE UNKNOWN

This IBM electronic tube assembly cuts through the unknown like a rocket through the stratosphere.

It probes the mysteries of the atom's core; predicts critical wing flutter of fast aircraft; traces paths of light through a lens system; calculates trajectories of guided missiles; plots the course of planets for the navigator.

It calculates payrolls, inventories, costs; points out savings of time and money.

These compact, pluggable units are the heart of IBM Electronic Calculators.

INTERNATIONAL BUSINESS MACHINES

IBM

IBM Electronic Business Machines are vital defense weapons in the hands of our nation's industrial engineers and scientists.

MPB

"Suppliers to the World's Foremost Instrument Manufacturers"

For vital requirements, aviation instrument makers and diversified manufacturers of precision equipment choose MPB miniature ball bearings as standard.

Available to critical tolerances in over 70 different types and sizes from .100" to 5/16" O.D.

A Few Examples of Typical Stock Sizes:

Complete and competent engineering assistance for your applications is promptly available. Comprehensive catalog on request.

MINIATURE *Precision* BEARINGS
INCORPORATED
KEENE, NEW HAMPSHIRE

CURRAN ENGINEERING CO.

Manufacturer of

MECHANICAL COMPONENTS
from
METALS, CERAMICS, AND PHENOLICS

Consultants and Specialists of
ROCKET IGNITER ASSEMBLIES
and
LONGITUDAL SHAPED CHARGE CUTTERS

"CENCO" Process for
HIGH TEMPERATURE-HIGH DIELECTRIC INSULATING OF METALLIC ASSEMBLIES

7614 Santa Monica Blvd.
Los Angeles 46 California.

TAC does what no other tool can do!

AT LAST! AN OPEN-END RATCHET WRENCH — the world's first true *universal* wrench. A patented design for connections on tubing, rods, piping, conduit, studs, etc. Sixty-four socket sizes from ¾" to 4". Smallest effective ratcheting arc yet — 5° to 7½°. TAC will also do every job any ordinary ratchet wrench will do: one TAC set replaces literally dozens of single-purpose hand tools.

makers of advanced tools for industry

TAC

TAC is the registered trademark of

TUBING APPLIANCE CO.
7112 South Victoria • 10321 Anza Ave. • Los Angeles, Calif.

Get the Facts about your Future with

Martin
AIRCRAFT
Builders of Dependable Aircraft Since 1909

Discover the greater opportunities offered engineers by the greatest diversity of projects of any aircraft company in the East! Write today for fact-packed brochure.

SEND FOR ENGINEERING BROCHURE

THE GLENN L. MARTIN COMPANY
Personnel Dept. • Section A • Baltimore 3, Md.

Please send me your brochure describing engineering opportunities at Martin.

My name _____

My address _____

My city and state _____

My engineering field _____

Finishing School for
GUIDED MISSILES

The Air Force Missile Test Center, used by all our military services as a long-range proving ground, stretches thousands of miles from Florida, out over the Bahamas, into the South Atlantic.

A pilotless bomber roars away from its launching stand, picks up speed, zooms into the blue. Setting its course for a far-off target in the ocean, it rockets over a chain of tiny islands where men and machines check its flight, its behavior, the operation of its guidance and control systems. It's a vital part of our air power of the future—aeronautical research and development laying the foundation for continued U. S. air supremacy!

Operated by the USAF's Air Research and Development Command, the Missile Test Center is geared up to test the wide variety of missiles, rockets and pilotless aircraft vital to modern air power. It reached its full stature with the recent completion of down-range observation stations. And the dramatic B-61 pilotless bomber, the Matador, designed and produced by Martin as part of its diversified missiles program, was the first to use the completed range. THE GLENN L. MARTIN COMPANY, Baltimore 3, Maryland.

Martin AIRCRAFT

Builders of Dependable Aircraft Since 1909

Illustration is artist's conception of Air Force B-61 Matador pilotless bomber.

DEVELOPERS AND MANUFACTURERS OF: Navy P5M-1 Marlin seaplanes • Air Force B-57A Canberra night intruder bombers • Air Force B-61 Matador pilotless bombers • Navy P4M-1 Mercator patrol planes • Navy KDM-1 Plover target drones • Navy Viking high-altitude research rockets • Air Force XB-51 developmental tactical bomber • Martin airliners • Guided missiles • Electronic fire control & radar systems • **LEADERS IN** Building Air Power to Guard the Peace, Air Transport to Serve It.

Brainwork for defense

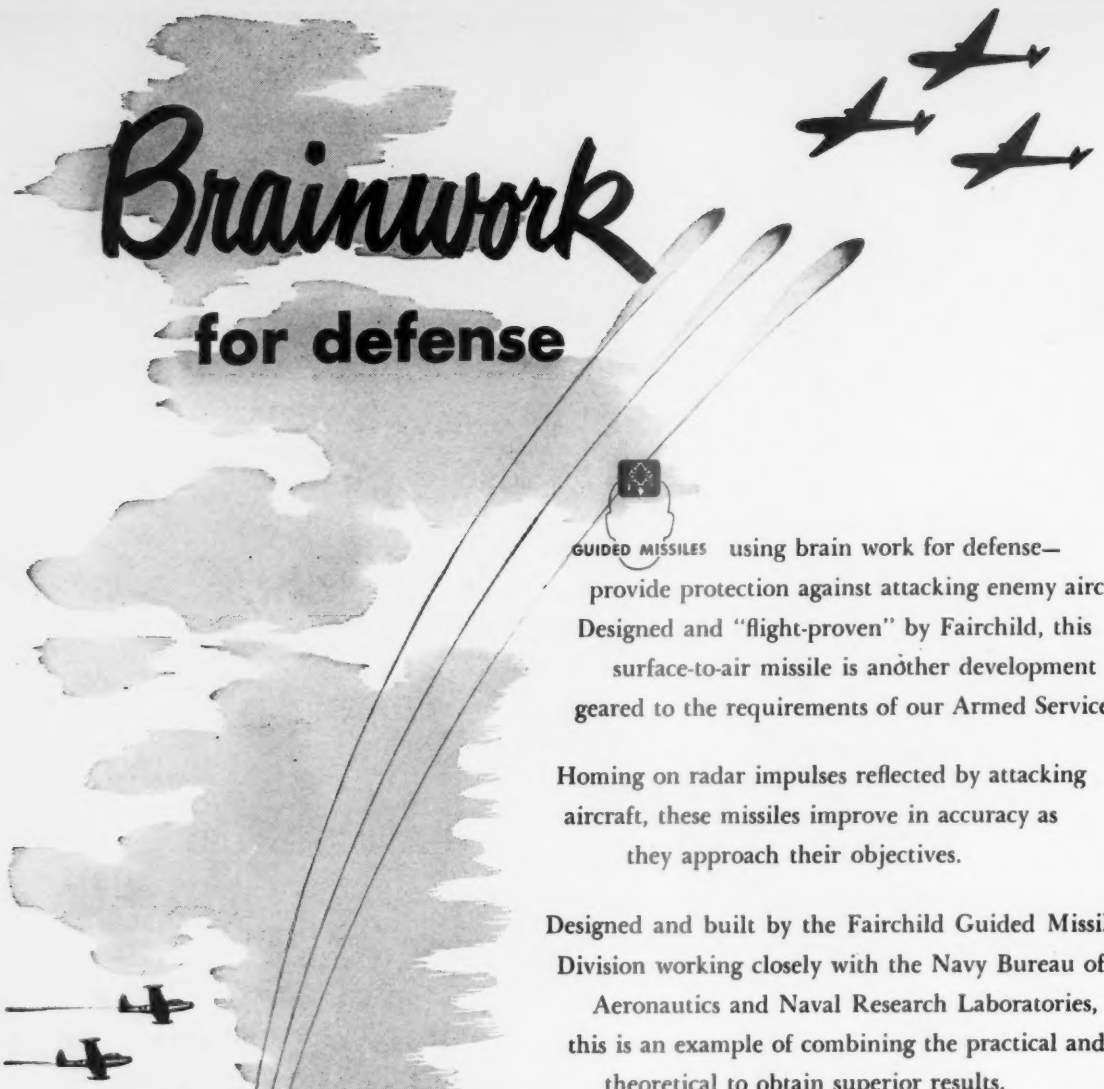

GUIDED MISSILES using brain work for defense—provide protection against attacking enemy aircraft. Designed and "flight-proven" by Fairchild, this surface-to-air missile is another development geared to the requirements of our Armed Services.

Homing on radar impulses reflected by attacking aircraft, these missiles improve in accuracy as they approach their objectives.

Designed and built by the Fairchild Guided Missiles Division working closely with the Navy Bureau of Aeronautics and Naval Research Laboratories, this is an example of combining the practical and theoretical to obtain superior results.

ENGINE AND AIRPLANE CORPORATION

FAIRCHILD

Guided Missiles Division

FARMINGDALE, N. Y.

Other Divisions: **Fairchild Aircraft Division,** Hagerstown, Md., Chicago, Ill.
Fairchild Engine Division and **Stratos Division,** Farmingdale, N. Y.

NITRIC ACID

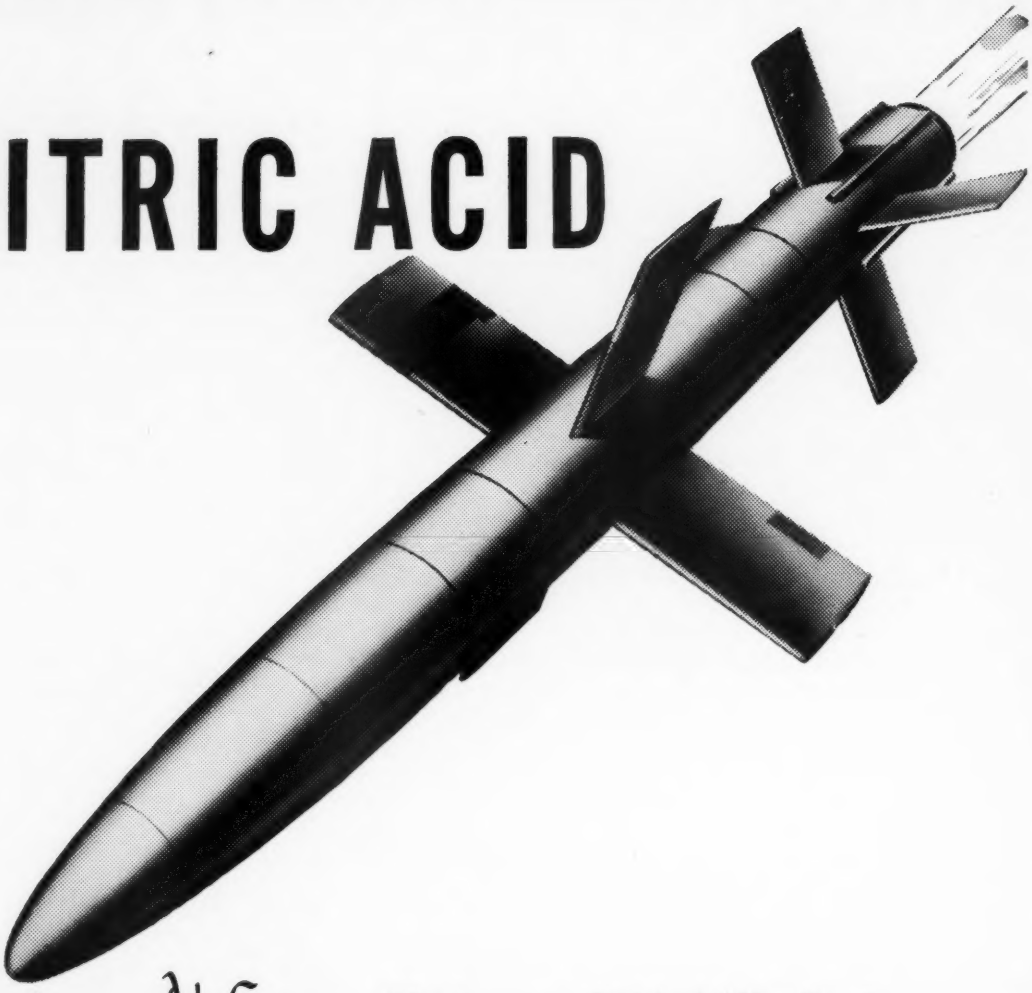

Ancient as Alchemy ...Modern as Guided Missiles!

Known for fourteen centuries—yet required for propelling the most advanced aircraft and guided missiles! That's the story of Nitric Acid, the ageless chemical.

Alone, or as a component of mixed acid, Nitric has long had a host of important industrial uses. In today's broad defense program, its role is more vital than ever.

As a primary producer for over 50 years, General Chemical is known for the uniformity and high quality of its Nitric Acid—in any desired strength and grade—for any need. Thorough knowledge of the product and its properties recently led to General's development of the first Anhydrous Nitric Acid, as well as special fuming forms for urgent military and industrial programs.

For your Nitric needs, consult General Chemical first. Further information on any of the grades and strengths listed here may be obtained from the nearest General Chemical office.

Grades of General Chemical Nitric Acid include:

Standard
36°, 38°, 40° and 42° Baume

Diamond*
36°, 38°, 40° and 42° Baume

Photo Engravers
36°, 38°, 40° and 42° Baume

Nitric Acid 95%
(48.5° Be), Diamond and Standard

Reagent, A.C.S.
Sp. Gr. 1.42

White Fuming
Reagent, A.C.S. and Technical, Sp. Gr. 1.49-1.50

Red Fuming
Reagent, and Technical, Sp. Gr. 1.59-1.60

Anhydrous
Total acidity 99.8% min.

*Highest Commercial Quality

BASIC CHEMICALS

FOR AMERICAN INDUSTRY

GENERAL CHEMICAL DIVISION
ALLIED CHEMICAL & DYE CORPORATION
40 Rector Street, New York 6, N. Y.

Offices: Albany • Atlanta • Baltimore • Birmingham • Boston • Bridgeport Buffalo • Charlotte • Chicago • Cleveland • Denver • Detroit • Greenville (Miss.) Houston • Jacksonville • Kalamazoo • Los Angeles • Minneapolis • New York Philadelphia • Pittsburgh • Providence • St. Louis • San Francisco • Seattle Yakima (Wash.)

In Wisconsin: General Chemical Company, Inc., Milwaukee, Wis.
In Canada: The Nichols Chemical Company, Limited • Montreal • Toronto • Vancouver

ARS Reprints and Preprints

PRICE PER COPY: 25 cents to members; 50 cents to nonmembers.

Code No.	*Title and Author*
28T-51	"Rocket Applications of the Cavitating Venturi," by L. N. Randall
29T-51	"Equipment for Handling High Strength Hydrogen Peroxide," by Noah S. Davis, Jr.
30T-51	"Optical Methods of Rocket Motor Evaluation," by Kurt Stehling
31T-51	"Materials for Use in Uncooled Liquid Propellant Rocket Motors," by W. R. Sheridan
32T-51	"Successful Engineering of Ceramic Lined Rocket Motors," by H. Z. Schofield and W. H. Duckworth
33T-51	"Silicon Carbide Linings for Uncooled Rocket Motors," by K. C. Nicholson
15-50	"A General Method for the Calculation of Theoretical Performance of Rocket Engines," by V. N. Huff
16-50	"Stability of Liquid Films for Cooling Rocket Motors," by M. J. Zucrow, C. M. Beighley and E. L. Knuth
17-50	"Notes on the Behavior of Supersonic Gases in Overexpanded Nozzles," by K. Scheller and J. A. Bierlein
18-50	"Optimum Thrust Programming for a Sounding Rocket," by H. S. Tsien and Robert C. Evans
19-50	"Heat Recovery and Maximum Thermodynamic Efficiency in a Rocket," by J. J. Ward and J. W. Clegg
20-50	"Naval Air Rocket Test Station—Purpose and Progress," by Lt. Comdr. F. C. Durant, III
21-50	"Operations with the High Altitude Sounding Rocket Viking," by J. P. Layton
22-50	"Rocket Engine Flight Testing," by R. F. Gompertz
23-50	"Micro-Scale Rocket Studies," by Bradford Darling and Saul Wolf
24-50	"Some Measurements of the Burning Rates of Mixed Liquid Bi-Propellants," by C. W. Tait, A. G. Whittaker and H. Williams
25-50 A	"Tasks We Face," by F. Zwicky
26-50	"Throttling Thrust Chamber Control," by M. Meyer
27-50	"Expellant Bags for Rocket Propellant Tanks," by W. R. Sheridan
1-49	"A Survey of Injector Designs for Use in Liquid Propellant Rocket Motors," by B. N. Abramson
2-49	"Instruction and Research in Jet Propulsion," by Luigi Crocco
3-49	"An Investigation of Some of the Parameters Affecting Overall Rocket Performance," by C. H. Harry
4-49	"Rocket Engine Developments," by Roy Healy
5-49 A	"Instruction and Research at the Daniel and Florence Guggenheim Jet Propulsion Center," by Hsue-Shen Tsien
7-49	"The Air Force Experimental Rocket Engine Test Station," by K. F. Mundt
8-49	"Handling of Liquid Oxygen," by G. E. Simpson
9-49	"Nitrogen Tetroxide as an Oxidizer in Rocket Propulsion," by Douglas H. Ross
41L-51	"The Importance of Satellite Vehicles in Interplanetary Flight," by Dr. Wernher von Braun

American Rocket Society
29 W. 39th Street, New York 18, N. Y.

Please send me the reprints checked below:

☐ 28T-51	☐ 32T-51	☐ 17-50	☐ 21-50	☐ 25-50 A	☐ 2-49	☐ 7-49
☐ 29T-51	☐ 33T-51	☐ 18-50	☐ 22-50	☐ 26-50	☐ 3-49	☐ 8-49
☐ 30T-51	☐ 15-50	☐ 19-50	☐ 23-50	☐ 27-50	☐ 4-49	☐ 9-49
☐ 31T-51	☐ 16-50	☐ 20-50	☐ 24-50	☐ 1-49	☐ 5-49A	☐ 41L-51

My (check) (money order) for $..... is attached.

Signed.....Address.....

.....

THE AMERICAN ROCKET SOCIETY

AIMS The American Rocket Society is a professional engineering and scientific organization devoted to the encouragement of research and development of jet and rocket propulsion devices and their application to problems of transportation and communication. At the present time it is also concerned with the military uses of the reaction principle.

The Society carries out its aims by the following methods:

Represents the jet propulsion profession before the public, promotes interest in jet propulsion and its applications, encourages the formation of regional chapters and student branches where technical conferences may be held.

Publishes and disseminates news, experimental results, and technical information to its members, through the medium of its Journal.

Encourages and aids those actively working in this field by organizing national and regional technical meetings where contributed and invited papers are presented and discussed.

MEMBERSHIP Five types of membership are offered: MEMBER, shall consist of scientists, engineers, persons actively engaged in the field of jet propulsion and rocketry, and others who may be deemed eligible for membership by the Board of Directors; ASSOCIATE, for those interested in the development of jet propulsion and rocketry and who are deemed eligible for such membership by the Board of Directors; STUDENT, for persons not over 25 years of age, interested in the development of jet propulsion and rocketry, who are students of some recognized educational institution. CORPORATE membership shall consist of educational, scientific, industrial, or other corporations or associations interested in the development of jet propulsion and rocketry. Each corporate member shall be entitled to five representatives who shall have the rights and privileges of Members. AFFILIATE CORPORATE membership shall consist of scientific, industrial and other corporations or associations interested in the development of jet propulsion and rocketry to the extent that a part of their activities are directed to that end, directly or indirectly. Each affiliate corporate member shall be entitled to one representative who shall have the rights and privileges of an Associate Member. Furthermore, each affiliate corporate member shall be entitled to four advertisements per year in the Journal in accordance with special advertising rates

The American Rocket Society is an affiliate of The American Society of Mechanical Engineers. Annual dues, including Journal subscriptions, are: Member, $10.00; Associate, $10.00; Student, $5.00 per annum.

OFFICERS

President	H. R. J. Grosch
Vice-President	C. W. Chillson
Secretary	A. C. Slade
Treasurer	G. Edward Pendray
General Counsel	Andrew G. Haley

BOARD OF DIRECTORS

C. W. Chillson	John J. Murphy
F. C. Durant, III	Frank A. Parker, Jr.
Andrew G. Haley	R. W. Porter
Howard R. Moles	C. C. Ross

R. Tom Sawyer

COMMITTEES

Executive Committee	H. R. J. Grosch, *Chairman*
Membership Committee	R. W. Porter, *Chairman*
Finance Committee	Andrew G. Haley, *Chairman*
Program Committee	C. W. Chillson, *Chairman*

SECTIONS

NEW YORK	James Wheeler, *Pres.*
SOUTHERN CALIFORNIA	R. B. Canright, *Pres.*
INDIANA	David McNay, *Pres.*
NEW MEXICO-WEST TEXAS	Herbert L. Karsch, *Pres.*

INFORMATION FOR AUTHORS

Manuscripts must be double spaced on one side of paper only with wide margins to allow for instructions to printer. Submit two copies, original and first carbon. Include a 100–200 word abstract of paper. The title of the paper should be brief to simplify indexing. The author's name should be given without title, degree or honor. A footnote on the first page should indicate the author's position and affiliation. Include only essential illustrations, tables, and mathematics. References should be grouped at the end of the manuscript; footnotes are reserved for comments on the text. Use American Standard symbols and abbreviations published by the American Standards Association. References should be given as follows: For Journal Articles; Title, Authors, Journal, Volume, Year, Page Numbers. For Books: Title, Author, Publisher, City, Edition, Year, Page Numbers. Line drawings must be made with India ink on white paper or tracing cloth. Photographs should be clear, glossy prints. Legends must accompany each illustration submitted, and should be listed in order on a separate sheet of paper.

Send manuscripts to the Editor-in-Chief, Martin Summerfield, Department of Aeronautical Engineering, Princeton University, Princeton, N. J.

Rates for Reprints

For quotations or orders not covered write to the Secretary
Reprints must be ordered when galley proof is returned to the Editor

	4 page	*8 page*	*16 page*
100 copies	$12.00	$20.00	$35.00
200 copies	20.00	33.00	66.00
500 copies	35.00	55.00	108.00

ROCKET POWER FOR DEFENSE

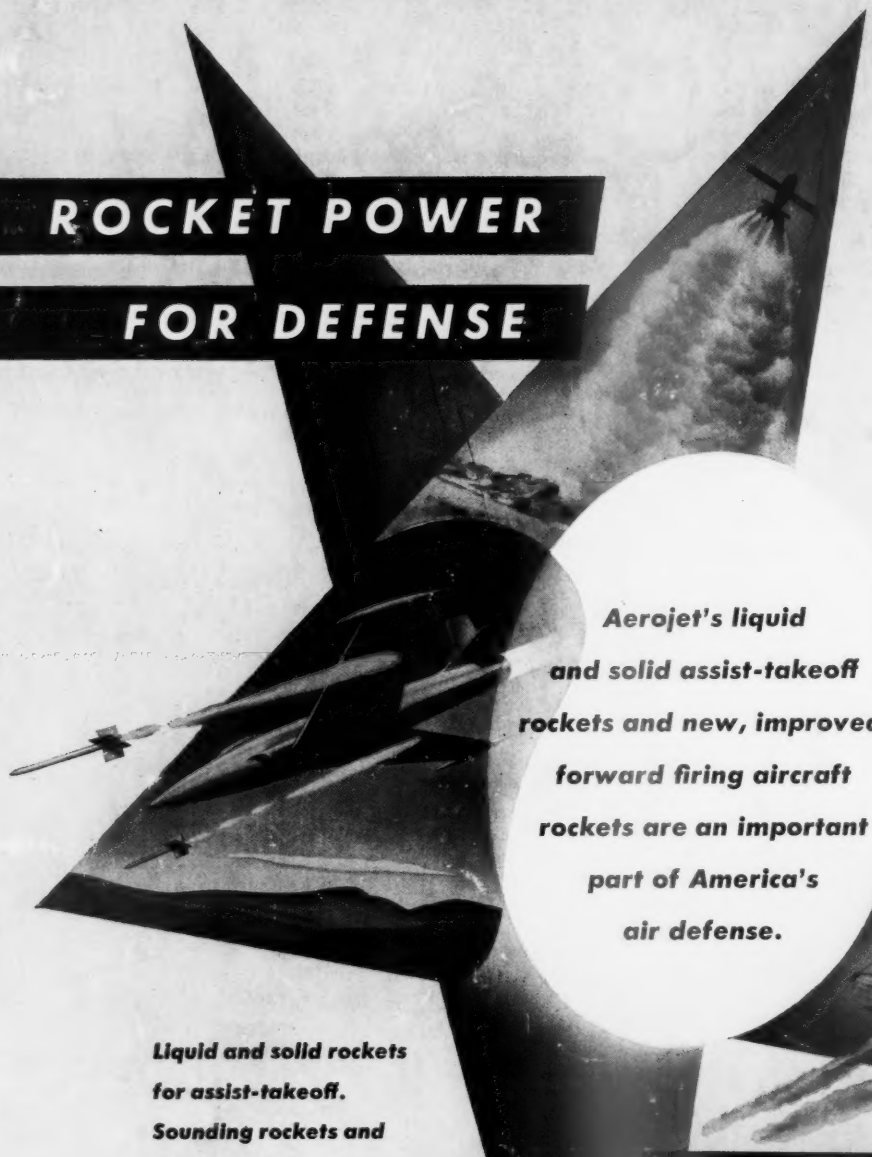

Aerojet's liquid and solid assist-takeoff rockets and new, improved, forward firing aircraft rockets are an important part of America's air defense.

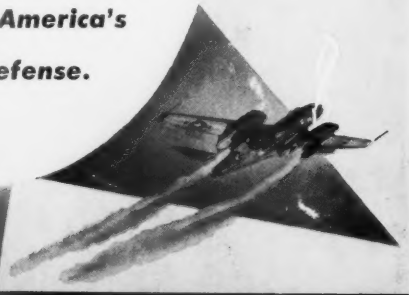

Liquid and solid rockets for assist-takeoff. Sounding rockets and missile boosters. Rocket test installations. Complete research, engineering, and manufacturing facilities.

Aerojet
ENGINEERING CORP.
AZUSA CALIFORNIA

A SUBSIDIARY OF THE GENERAL TIRE & RUBBER CO.